



MASTERARBEIT / MASTER'S THESIS

Titel der Masterarbeit / Title of the Master's Thesis

„Interaction of Immune-Modulating Substances with
Intestinal Epithelial Cells “

verfasst von / submitted by

Sarah Exenberger, BSc

angestrebter akademischer Grad / in partial fulfilment of the requirements for the degree
of

Master of Science (MSc)

Wien, 2016 / Vienna 2016

Studienkennzahl lt. Studienblatt / A 066 830
degree programme code as it appears on
the student record sheet:

Studienrichtung lt. Studienblatt / Masterstudium Molekulare Mikrobiologie, Mikrobielle
degree programme as it appears on Ökologie und Immunbiologie/ Master's degree
the student record sheet: programme Molecular Microbiology, Microbial Ecology
and Immunobiology

Betreut von / Supervisor:

Assoc. Prof. Priv.-Doz. DDr. Eva Untersmayr-
Elsenhuber

Mitbetreut von / Co-Supervisor:



universität
wien

Master's thesis

**„Interaction of Immune-Modulating
Substances with Intestinal Epithelial Cells “**

Sarah Exenberger, BSc

2016

Academic advisor:

Assoc. Prof. DDr. Eva Untersmayr-Eisenhuber
Department of Pathophysiology and Allergy Research
Center of Pathophysiology, Infectiology and Immunology
Medical University of Vienna



The work was carried out at the
Department of Pathophysiology and Allergy Research,
Medical University of Vienna



Part of the thesis was funded by the
Fond zur Förderung der wissenschaftlichen Forschung (FWF).

FWF

Der Wissenschaftsfonds.

Acknowledgements

First and foremost, I would like to express my gratitude to my academic supervisor Assoc. Prof. DDr. Eva Untersmayr-Elsenhuber for her expertise, critical review and patience during the research and completion of the thesis. Without her help, the accomplishment of this work would not have been possible.

My sincere thanks further go to Elisabeth Fürst, Dipl. Biol, PhD for her insightful comments, encouragement and profound knowledge. Her inspiring questions, expertise and encouragement helped me to widen my research in various perspectives.

Besides my advisor, I would like to thank all past and present members of the gastrointestinal immunology group, Denise Heiden, Anna Ondracek MSc and Cornelia Schulz MSc, for their support and companionship.

Last but not least, I would like to thank my family: my parents Anita and Leonhard Exenberger, my sister Corina Exenberger and her companion Verena Tatzer for their immense patience, love and support throughout writing this thesis, my studies and my whole life. A special thank also goes to my friends who pushed me and made me laugh when I was discouraged and desperate. Furthermore, I would like to thank Mag^a. Chistine Tatzer for proofreading this thesis.

Abbreviations

AAL	aleuria aurantia lectin
AAL-MP	AAL coated microparticle
AMP	antimicrobial peptide
APC	antigen presenting cell
CaCo2TC7	human colon adenoma carcinoma cells
DC	dendritic cells
DDW	double distilled water
DMEM	Dulbeco's modified eagle medium
ERK	extracellular signal-regulated kinase
FAA	fatty acid receptor
FBS/FCS	Fetal Bovine Serum
FcγRI	high IgG affinity receptor
FcεRI	high IgE affinity receptor
FcεRII	low IgE affinity receptor
G protein	guanine nucleotide binding protein
GALT	gut associated lymphoid tissue
GI	gastrointestinal tract
GM1	glycosylated monosialoganglioside 1
HDL	high density lipoprotein
IEC	intestinal epithelial cells
IFN	interferon
IgA	immunoglobulin A
IgE	immunoglobulin E
IgG	immunoglobulin G

IL	interleukin
ITS	Insulin Transferrin Selenium
J chain	joining chain
LPS	lipopolysaccharide
MAMP	microbe-associated molecular pattern
M-cells	microfold cells
MHC	major histocompatibility complex
MP	PLGA microparticle
MUC	mucus protein
NA	neuraminidase from <i>vibrio cholerae</i>
NA-MP	NA coated microparticle
OIT	oral immunotherapy
OVA	albumin from chicken egg white
PAMPs	pathogen associated molecular pattern
PI3K	Phosphoinositol 3 kinase
pIgR	poly-Ig-receptor
Plain-MP	uncoated microparticle
PLGA	Poly-(D,L-lactide-co-glycolide)
PP	Peyer's patch
qRT-PCR	quantitative real-time PCR
RT-PCR	reverse transcription PCR
S1P	sphingosine-1-phosphate
S1P1-5	sphingosine-1-phosphate receptor 1-5
SC	secretory component
SGPL	sphingosine-1-phosphate lyase
sIgA	secreted IgA

SMase	sphingomyelinase
SphK1	sphingosine kinase 1
SphK2	sphingosine kinase 2
SPP	sphingosine-1-phosphate phosphatase
SPT	serine palmitoyl transferase
TCR	T cell receptor
TEER	transepithelial electrical resistance
TGF β	tumor growth factor β
Th	T helper cell
TJ	tight junction
TLR	toll like receptor
TNF α	tumor Necrosis Factor α
Tr1	type 1 regulatory T cell
Treg	regulatory T cell
TSLP	thymatic stromal lymphopietin
WGA	wheat germ agglutinin
WGA-MP	WGA coated microparticle
ZO	zonula occludens protein

1. Abstract

In food-allergic patients a dysregulation of the intestinal barrier leads to the enhanced passage of antigen, which results in the formation of Immunoglobulin E (IgE) producing plasma cells and the recruitment of allergy effector cells like mast cells. Upon activation, mast cells produce and release high amounts of allergy mediators, which promote the clinical implications such as vasodilation, increased vascular permeability, contraction of airway smooth muscles as well as increased mucus secretion or anaphylactic shock.

One mast cell mediator, which influences the homeostasis of intestinal epithelial cells, is sphingosine-1-phosphate (S1P). This bioactive lipid is a key mediator for immunological functions by mediating immune cell trafficking. In allergic individuals elevated levels of S1P were found, which are produced and released by activated mast cells. These elevated levels induce allergic reactions like vascular permeability and contraction of smooth muscle cells. This study aimed to explore the interaction of S1P with the intestinal epithelium. The results show that Caco2 cells, a model cell line of intestinal epithelial cells, are able to produce and degrade S1P. Furthermore, they express two specific S1P receptors, S1P2 and S1P3. S1P stimulation of Caco2 cells causes the formation of tight junctions and enhanced transepithelial electrical resistance (TEER) as well as slightly upregulated inflammatory cytokine production. This leads to the assumption that S1P might have a protective function on intestinal barrier integrity.

Since adverse reactions of allergic patients to the allergen can lead to severe clinical symptoms and anaphylactic shock, curative treatment possibilities are urgently needed. Specific immunotherapies aim to re-establish the tolerance against the allergen in the patient. In food allergies, the most prominent treatment option is oral immunotherapy. Through the administration of increasing amounts of allergen, the re-establishment of tolerance is achieved. One possibility to administer the allergen is by loading it into poly-(D, L-lactide-co-glycolide) microparticles (MPs). These structures protect the allergen from digestion and allow specific targeting of intestinal epithelial cells. Our aim was to evaluate the effect of differently coated MPs on intestinal epithelium. The results show that MPs induce cytokines related to a Th1 response while not impairing the barrier integrity. The most promising results were obtained using NA-MPs. From these experiments we can conclude that bound MPs are a novel and promising option for treatment of food allergy.

Table of contents:

Abbreviations	4
1. Abstract	8
2. Introduction	14
2.1 Intestine	14
2.1.1 Outer Barrier	15
2.1.2 Inner Barrier	21
2.1.3 Oral tolerance	22
2.2 Food Allergy	24
2.2.1 Definition	24
2.2.2 Sensitization phase	24
2.2.3 Effector phase	25
2.2.4 Intestinal epithelium in food hypersensitivity	25
2.3 Sphingosine-1-phosphate	27
2.3.1 Metabolism	28
2.3.2 Role of S1P in Immune Regulation	29
2.3.3 Role of S1P in Food Allergy	30
2.4 Oral treatment of food allergy	31
2.4.1 Specific Immunotherapy	31
2.4.2 Poly-(D,L-lactide-co-glycolide) Microparticles	32
2.5 Aim of thesis	35
3. Material and Methods	36
3.1 Material	36
3.1.1 Chemicals	36

3.1.2 Kits	37
3.1.3 Buffers.....	37
3.1.4 Cell Cultivation	39
3.1.5 Antibodies.....	39
3.1.6 qRT-PCR Primers & TaqMan Assays.....	40
3.1.7 SDS Page	42
3.2 Methods	43
3.2.1 Cell Culture	43
3.2.2 Cell Stimulation	44
3.2.3 Analysis of Gene Expression by Real-time PCR	45
3.2.4 Analysis of Protein Expression by Western Blot:	49
3.2.5 Trans-Epithelial Electrical Resistance.....	52
3.2.6 Calcium Mobilization Assay	53
3.3 Statistics	55
4. Results	56
4.1 Influence of Sphingosine-1-Phosphate on Intestinal Epithelial Cells ..	56
4.1.1 Expression of S1P Metabolizing Enzymes in Intestinal Epithelial Cells.....	56
4.1.2 Influence of S1P Signalling on Cytokine and Tight Junction Expression.....	59
4.2 Effect of Poly-(D, L-lactide-co-glycolide) Microparticles on Intestinal Epithelial Cells	64
4.2.1 Influence of Targeted and Coated Microparticle Treatment on Cytokine Expression.....	64
4.2.2 Effect of Particle Stimulation on Tight Junction Formation of Intestinal Epithelial Cells	71

5. Discussion	77
6. References	82
7. Appendix	97
7.1 List of Tables	97
7.2 List of Figures	98
7.3 Zusammenfassung	104

2. Introduction

2.1 Intestine

The human intestine is a part of the gastrointestinal (GI) tract and subdivided into the small intestine and colon. The intestine can reach a length of approximately 7 m with a mucosal surface area of about 200 m². This makes the intestine the largest area of the human body which is exposed to the external environment. The major structure responsible for the protection of the human body against the external environment is a 20µm thick epithelial cell monolayer. Underneath the intestinal epithelium lies a loose connective tissue, lamina propria, which contains blood vessels, the mucosa- associated lymphoid tissue as well as 80% of the entire human lymphocytes ^{1,2}.

The main task of the GI is the sufficient and adequate absorption of dietary nutrients, electrolytes and water. Absorption of nutritional components and minerals takes place in the small intestine whereas the colon is the site of electrolyte and water uptake. The intestinal epithelium is, thus, mainly composed of absorptive cells, enterocytes which are specialized to translocate molecules from the luminal site to the lamina propria where they diffuse into small blood vessels ³. The specific translocation of the nutrients can occur either via transepithelial/transcellular or paracellular transport ⁴⁻⁶. Macromolecules larger than 500 Da, such as amino acids, sugars, electrolytes and short-chain fatty acids are transported through the cells transepithelially/transcellularly ⁷. Enterocytes therefore need two energy- dependent sets of specific transporters: One that translocates the molecule from the lumen into the cell, and one that releases it from the cell into the lamina propria. Molecules and solubilized compounds smaller than 500 Da, such as Na⁺ are passively transported through the intercellular space ⁷. This paracellular translocation occurs along an electrochemical gradient and therefore does not require energy. Furthermore, this transport is tightly regulated by intercellular complexes called tight junctions (TJ) and adherens junctions, which are responsible for the strong and semipermeable character of the intestinal barrier ⁸.

Tight junctions

TJ are located at the apical membrane of the intestinal epithelial cells (IECs) and regulate the transport of molecules. They seal the IECs together, hence they provide a physical barrier for luminal entities. Disruption of TJ by environmental factors can lead to a break in the intestinal epithelium, which is associated with severe diseases like inflammatory bowel disease as well as food allergy ^{2,7,9,10}. In the intestine, TJ consist mainly of protein interaction of two distinct families: occludin and claudin.

Occludin is a ~65 kDa, tetraspanning integral membrane protein which consists of two extracellular loops ¹¹. Its localisation within the TJ as well as the regulation of the paracellular permeability is modulated via phosphorylation of one extracellular loop ¹². The other extracellular loop interacts with further TJ proteins like claudin or JAM ¹³. Occludin is linked to the cytoskeleton via the connectors zonula occludens protein 1 (ZO-1) or ZO-2 ^{14,15}.

The claudin family is formed by proteins of 20-27 kDa size with four hydrophobic transmembrane domains, two extracellular loops, and a cytoplasmic C and N domain ^{16,17}. The two extracellular loops are used for the establishment of homo (claudin-1, 2, 3, 5, 6, 9, 11, 14, and 19) or heterophilic (claudin-3 with either claudin-1, 2 or 5) interactions ¹⁸. The C-terminal interacts with ZO-1, ZO-2 or ZO-3 and is therefore the anchor to the cytoskeleton ¹⁹. Claudin protein interactions directly regulate permeability by forming paracellular pores which transport specific ions ^{16,20}.

Adherens junctions

Adherens junctions are located underneath TJ and are responsible for initiation as well as stabilization of cell adhesions ²¹. The major form of adherens junctions consists of the interaction of cadherin, mainly E-cadherin, with proteins of the catenin family. These proteins are important for the regulation of cytoskeleton organization, cadherin stability and intracellular signalling ²². The interactions are required to control the formation and function of adherens junctions ²³.

Since the intestine is in constant contact with the external environment, it needs a strong barrier function to protect the human body against foreign entities. To successfully form a strong defence against harmful agents while maintaining the main function of nutritional absorbance, two main barrier layers have evolved: the outer and the inner barrier.

2.1.1 Outer Barrier

The major responsibility of the outer or physical barrier is to prevent the adhesion of foreign bacteria as well as to regulate the diffusion of nutritional components. It consists of three distinct parts: intestinal microbiota, mucus layers and IECs.

Microbiota

The intestinal microbiota is composed of 10^{13} - 10^{14} different microorganisms being of distinct composition in each individual ²⁴. The mixture between symbionts and optional pathogens in the intestine changes during life because it is influenced by different factors such as diet, age, medication, illness, stress and life style ²⁵⁻²⁸. By establishing nutritional competition, adhesion and growth of pathogens is prevented ²⁸. Furthermore,

commensals are able to release microbe-associated molecular pattern molecules (MAMPs) into the mucus layers and thereby regulate the toll-like receptor (TLR) expression pattern of IECs ²⁹. Furthermore, microbes are able to prime the innate as well as the adaptive immune system of the intestine by increasing Immunoglobulin A (IgA) levels as well as the release of antimicrobial peptides by Paneth cells and enterocytes into the underlying mucus layers ^{30,31}.

An important mediator for the regulation of the growth and composition of the intestinal microbiota is IgA, which is present in its secretory form (sIgA) in the mucus layers. In the intestine, IgA producing plasma cells secrete IgA dimers, which are covalently bound to a joining (J) chain by disulphide bonds in the Fc region of their heavy chain ^{32,33}. The J-chain of this complex binds to the poly-Ig-receptor (pIgR), found on the basolateral membrane of IECs and induces the active transepithelial transport ^{1,32,33}. At the apical membrane the pIgR-IgA complex is proteolytically cleaved and only the extracellular domain of the pIgR remains bound to the IgA complex ^{1,34,35}. This secretory component (SC) of the pIgR, protects the IgA dimer from proteolysis, increasing its stability and acting as an anchor to the mucus ^{1,32,35}. The sIgA binds specific epitopes on the surface of bacteria with its variable region, thereby preventing the possible interaction of bacteria with IECs ³². Furthermore, through non-specific binding of bacterial glycans to the SC as well as the constant region of the IgA, sIgA is able to limit microbe motility ³⁶. This leads to the specific anchoring of IgA bound bacteria to the apical membrane of IECs, which induces an increased phosphorylation of TJ proteins, a higher pIgR expression as well as higher production of thymic stromal lymphopoietin (TSLP) ^{37,38}. Additionally, sIgA is responsible for the clearance of pathogens as well as viruses and endotoxins from the mucosal barrier and also from the inside of IECs ^{1,32,39,40}. This makes sIgA an important mediator for adaptive immunity and oral tolerance.

Mucus

The mucus forms a strong physical barrier against foreign particles and bacteria and consists of two distinct layers in the colon ⁴¹. The outer loose and unattached mucus layer, which is mainly composed of the proteins, MUC2, MUC5 and MUC6, is degraded by commensal bacteria and has a disorganized appearance ^{1,42,43}. The stratified and dense inner mucus layer consists of MUC1, MUC3A, MUC3B, MUC12, MUC13 and MUC17, being bound to the IECs and prevents bacteria from interacting with the intestinal epithelium ^{1,44}. In the small intestine, however, the mucus is discontinuous and not as well defined as in the colon ⁴¹. The different mucin proteins are constitutively produced and secreted by goblet cells and a full replacement of the mucus layers takes place every 6-12

hours¹. The mucus gel provides a physical protection of the intestinal epithelium, since it traps invading microbes⁴⁵.

In addition to the physical barrier function, the mucus layers also provide a chemical barrier against the interaction of IECs with harmful agents or bacteria. Antimicrobial peptides (AMPs) as well as sIgA are released by the underneath lying IECs into the mucus layers to regulate the bacterial density.

AMPs are peptides with a highly diverse amino acid sequence as well as secondary structure that share the ability to form clusters of hydrophobic and cationic amino acid residues in separated sections (amphipathic design)^{46,47}. Due to this amphipathic property, AMPs are able to specifically target the negatively charged lipopolysaccharides (LPS) on the surface of the outer membrane of bacteria⁴⁷. AMPs bind to the LPS and get inserted into the bacterial membrane by displacement of lipids resulting in an alteration of surface structure as well as a disruption of outer membranes^{48,49}. Since resistance towards AMPs would require membrane restructuring, bacteria are not able to develop a defence mechanism. Therefore AMPs efficiently regulate the growth of commensal and pathogenic bacteria^{47,50}. As a self-protective measurement, AMPs are generated as an inactive precursor in IECs and are activated by proteolytic cleavage after secretion into the mucus layers^{47,51}. In the human body, two major families of AMPs, defensins and cathelicidins, are found.

In addition to their antimicrobial function, AMPs are also chemo-attractants for specific immune cells, thereby bridging the gap between the innate and adaptive immune reaction. Human α -defensins attract immature peripheral T cells as well as immature dendritic cells (DC) which promote the antigen specific immune response⁴⁷. The inducible defensin, β defensin 2, attracts memory T cells as well as immature DCs, which advances a specific adaptive immune reaction⁴⁷. Moreover, the cathelicidin LL-37 enhances the selective migration of peripheral blood monocytes, neutrophils as well as immature T cells to the side of inflammation⁵². Furthermore, LL-37 is found to be an important mediator in tissue repair as it promotes neovascularisation and re-epithelialization^{53,54}.

Intestinal Epithelium

The intestinal epithelium is the major component of the intestine which is responsible for nutritional, electrolyte as well as water absorption. It is formed by a 20 μ m thick cellular monolayer consisting of six distinct cell types¹. In the small intestinal tract the absorptive surface is increased by formation of protuberances into the intestinal lumen, villi, and tubular invaginations into the underlying tissue, called crypts of Lieberkühn⁶⁷ (Fig.1).

The villi of the small intestine are composed of different cell types which have distinct functions like nutritional absorption as well as hormone and mucus secretion. The crypt, which contains pluripotent stem cells, is the centre of proliferation. All cell types along the crypt-villi axis originate from these pluripotent stem cells. Upon differentiation, the cells transit along this axis up to the villus tops, where they undergo spontaneous apoptosis and are shed into the lumen ⁵⁶. Within 4-5 days, the whole intestinal epithelium is renewed, which makes it the strongest self-renewing tissue in adult mammals ⁵⁷.

In every crypt, four to six pluripotent stem cells can be found, which are either actively cycling and situated above Paneth cells or undifferentiated and located in-between Paneth cells ⁵⁸. Most of the time, stem cells divide asymmetrically into one stem cell and one amplifying daughter cell, which will start to differentiate and transit towards the top of the villi after dividing itself 4-5 times ⁵⁷. The stem cell either dies or duplicates itself which leads to the effect that whole crypts are able to either die or repopulate crypts in the intestinal epithelium through crypt fission ⁵⁹.

Differentiated cell types

At the base of the crypts of Lieberkühn the so-called Paneth cells can be found. These specialised secreting cells are specific to the small intestine and absent in the colon ⁶⁰. Every crypt contains between 5 and 16 Paneth cells, which show a turnover rate of about 15 days ^{61,62}. They are the only cells which migrate towards the crypt base. This is facilitated by the expression of the tyrosine kinase guidance receptors EphB 2 and 3. Upon interaction with its ligand, ephrin B, which is highly expressed by villi cells, the receptors generate a repulsive force, which results in the migration towards the crypt base ⁶³. On their intercellular apical surface, the pyramidal-shaped Paneth cell contains cytoplasmic granules, which become more sophisticated towards the crypt base ⁶¹. High amounts of defensins, their activating enzymes and lysozymes that catalyse the hydrolysis of the linkage between the N-acetylmuramic acid and glucosamine of bacterial peptidoglycans damaging microbial cell walls, are stored within these cytoplasmic granules ^{62,64}. Upon microbial challenge, Paneth cells secrete those granules into the mucus layers and thereby regulate the bacterial composition and density (**Mucus**).

Goblet cells are another secretory cell type of the intestinal epithelium, which are located in the crypts as well as in the villi. The amount of goblet cells increases towards the distal end of the intestine with the highest amounts in the colon ⁶¹. During their migration from the crypt base towards the villi, goblet cells fill various storage granules with multiple mucin proteins, which they slowly and constantly release into the lumen through exocytosis ⁶⁵. In the granules, mucin proteins are stored in condensed forms and expand their volume in the lumen through the binding of water ⁴². This and their interaction

with other mucin proteins leads to the formation of the mucus layer with its various function (**Mucus**)⁴⁴. The released mucus moves downwards and hence leaves the villi tips of the small intestine uncovered⁶¹. It is known that upon bacterial stimulation goblet cells release their entire stored granules^{66,67}. However, the controlling mechanism is not fully understood to date.

Enteroendocrine cells are the third secretory cell type of the intestinal epithelium. They can be found throughout the whole crypt-villi axis with the highest abundance in the crypts⁶¹. In the human intestine only 1% are enteroendocrine cells⁶⁸. They form large cytoplasmic granules, which contain more than 20 hormones⁶¹. Secretion of these hormones into the lumen regulates and coordinates the function of the intestine^{57,69}. In the small intestine enteroendocrine cells are activated through the sensing of the intraluminal content by various nutritional receptors, like the fatty acid receptors (FAA2 and FAA3), on their apical surface⁷⁰. Through the secretion of hormones like serotonin (5-HT), cells are able to regulate the digestive function of the intestine, while release into the lamina propria may result in paracellular stimulation of neighbouring cells, distribution via the blood circulation or signalling to the nervous system⁷¹.

The most abundant cell type of the intestinal epithelium are enterocytes. These polarized columnar cells form more than 80% of the intestinal epithelium. Within the small intestine they are located at the upper end of the crypts and throughout the entire villi⁶¹. To efficiently fulfil their main task, the transepithelial absorption of nutritional compounds, enterocytes have a brush border which enhances their surface area on their apical side⁵⁷. This borderline consists of microvilli, which are deformations of the apical membrane with uniform length and appearance, through the polymerisation and bundling of actin filaments⁷². To stabilise the intestinal brush border, actin bundles are anchored to the terminal web, which itself is linked through various proteins, amongst them myosin and ezrin, to the cytoskeleton⁷². The most prominent of those proteins are Myosin-1a, which is found only in the intestinal tract and mediates the crosslinking of the actin chore to the membrane⁷². Upon bacterial stimulation, enterocytes produce and secrete AMPs into the lumen and thereby contribute to the chemical barrier function of the mucus (**Mucus**). One of those secreted AMPs is the intestinal alkaline phosphatase, which dephosphorylates bacterial lipopolysaccharides as well as regulates the interaction of epithelial cells and microbes through the formation of clusters on the surface of commensals⁷³. Thereby it renders the bound bacteria less stimulatory and inhibits inflammation⁷⁴.

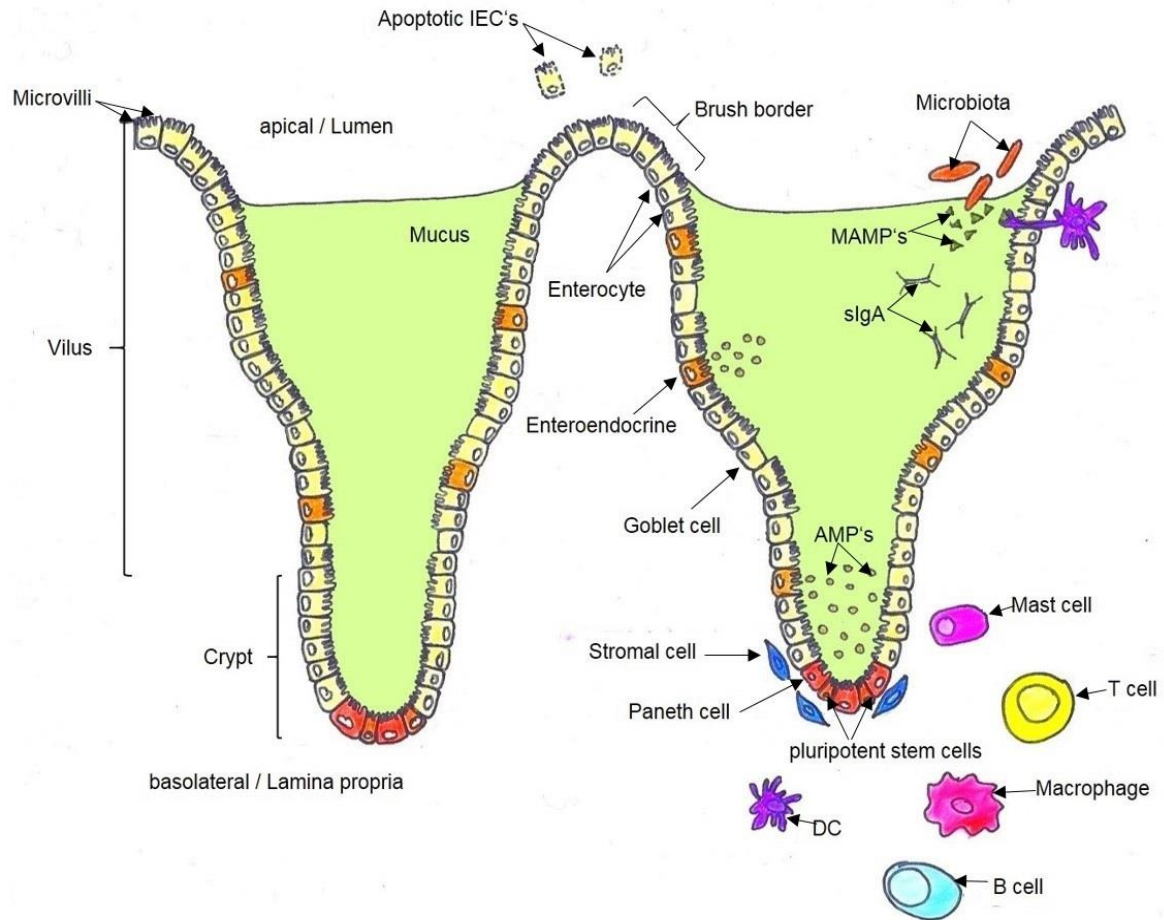


Figure 1: Schematic picture of the intestinal epithelium and involved intestinal epithelial cells. The intestinal epithelium is structured into villi and crypts to enhance its surface area and covers those with mucus to protect itself against harmful agents. To further enhance its surface area, the intestinal epithelial cells (IECs) form microvilli towards the apical located lumen, also called brush border, where they absorb the nutrient components and release them into the basolateral located lamina propria (left side). The IECs consist of various cell types which are located at different positions along the crypt-villus axis. The cells are constantly renewed by pluripotent stem cells, influenced by stromal cell released factors, and move along the crypt-villus axis towards the villi tops where they are shed into the lumen and undergo apoptosis (middle). Various factors protect the intestinal epithelium from harmful agents and pathogens. The overlying microbiota releases microbe associated molecular patterns (MAMP's) - if stimulated by certain factors - into the underlying mucus layers. These MAMP's and other foreign antigens, are recognised by secreted Immunoglobulin A (sIgA) and antimicrobial peptides (AMP's). Furthermore, antigens within the lamina propria or sampled by dendritic cells (DCs) through the IECs, are processed by macrophages as well as DCs and presented to lymphocytes (B and T cells) which further shape the immunologic response by releasing antibodies, cytokines and chemokines which recruit further cells, like mast cells (right side).

2.1.2 Inner Barrier

The inner or functional barrier is on the one hand responsible for the specific immune response against harmful foreign entities such as pathogens, and on the other hand associated with immune tolerance towards nutritional components and commensal bacteria. The gut associated lymphoid tissue (GALT) is the largest lymphoid organ containing up to 80% of lymphocytes of the human body ¹.

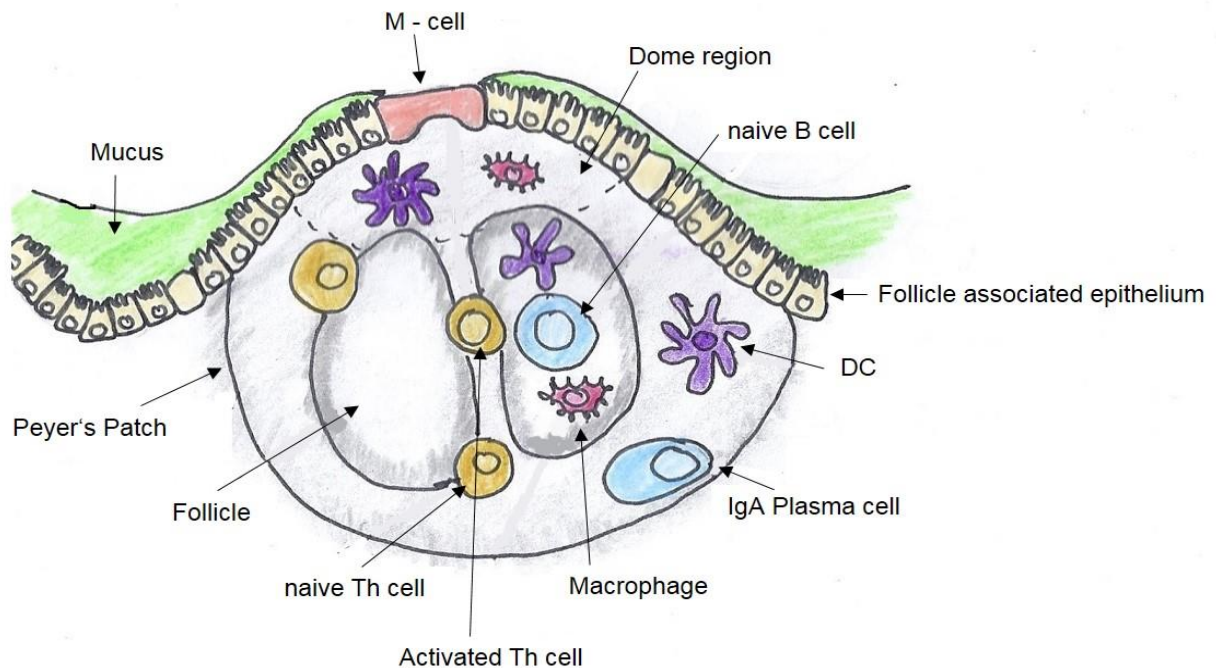
As part of the functional barrier, enterocytes efficiently transport IgA through the intestinal barrier and release sIgA into the lumen (**Microbiota**). Additionally, expression of the low affinity IgE receptor (FcεRII) and high affinity receptor (FcεRI), indicate the importance of IECs in IgE mediated diseases ^{75,76}. Furthermore, they are capable of releasing immune modulatory cytokines and chemokines upon activation of pattern recognition receptor signalling, which mainly induces immune tolerance. Enterocytes are nonprofessional antigen-presenting cells (APCs) expressing both major histocompatibility complex (MHC)-I and MHC-II ^{77,78}. After presentation of MHC bound antigens to differentiated T cells, residing in the lamina propria, enterocytes produce cytokines like TSLP, tumour growth factor β (TGFβ) and retinoic acid, which control oral tolerance ³⁸.

Another epithelial cell type, which is involved in the presentation process of luminal antigen to immune cells, are Microfold (M) cells. These specialized cells are located within the follicle-associated epithelium and display a reduced glycocalyx, irregular brush border and reduced microvilli ⁶¹. Compared to all other cell types, M-cells are specialised for the internalization and transport of antigens to the underlying Peyer's patches (PP) ⁶¹. The antigen transport via phagocytosis or fluid-phase endocytosis, allows the shuttling of structurally intact antigens ⁷⁹. On their basolateral side, M-cells release these antigens via exocytosis ¹. Moreover, M-cells were found to possess specific IgA receptors and promote the uptake as well as transport of IgA bound antigens ⁸⁰.

PPs are structured like lymphoid follicles into the follicular and inter-follicular areas. In the germinal centers of the follicular area high amounts of B lymphocytes, DCs and macrophages are found, whereas in the inter-follicular area high amounts of T-cells as well as DCs are located ⁸¹. The area below the intestinal epithelium and above the follicular structures is called the dome region where numerous macrophages, DCs as well as B and T lymphocytes reside (Fig.2) ¹. PPs are connected with mesenteric lymph nodes through lymphatic vessels ⁸². Within these lymphatic structures, processing of antigens as well as antigen presentation to naïve B and T cells takes place ⁸².

In the lamina propria several distinct subtypes of DCs, macrophages, mast cells, T cells and B cells are found, which are able to interact with antigens presented by IECs and

mediate immune response. In addition, high amounts of various intraepithelial lymphocytes are found within the epithelium. These cells are mainly CD8⁺ $\gamma\delta$ T cells mediating intestinal epithelial homeostasis as well as adoptive and innate immune



response⁸³.

Figure 2: Schematic drawing of M-cell with beneath lying Peyer patch. Antigens are able to pass the intestinal epithelium through microfold (M) cells, which are embedded in the surrounding follicle associated epithelium and barely covered with mucus. Entering the beneath lying dome region of the Peyer's Patch, the antigen is processed by dendritic cells (DCs) and macrophages which present them to naïve B cells in the follicle areas or naïve T helper (Th) cells in the inter-follicular areas of the PP's. Through the presentation, the lymphocytes get activated and differentiate into specific effector cells, like IgA plasma cells, before they either move to the connected mesenteric lymph nodes or are released into the lamina propria.

2.1.3 Oral tolerance

Oral tolerance is defined as the active suppression of cellular or humoral immune responses towards orally administered antigens⁸⁴. This tolerance is mediated by regulatory T cells (Treg), impaired T cell proliferation, decreased inflammatory cytokine production and reduced systemic hypersensitivity⁸⁵. Many different factors contribute to the establishment of oral tolerance, for example the amount of encountered antigen, the genetic background of the host, and the time point of antigen exposure.

The most important factor is the differentiation of naïve T cells towards a Treg phenotype after repeated ingestion of low allergen doses⁸⁵. During ingestion, foreign antigens are processed by gastric acid as well as enzymes of the GI and thereby reduce

their immunogenicity. The remaining molecules interact with the IECs and are transported to the lamina propria through different pathways: Either through the selective absorption and transport via M-cells, or through endocytosis by enterocytes and presented on MHC-II on their basolateral side. Additionally, CD11c⁺ DCs are able to sample luminal antigen by intercalating with IECs while not impairing TJ formation ⁸⁶. In the lamina propria as well as PPs, a specific subtype of DCs characterised by the surface integrin CD103, take up the antigens and process them further ⁸⁷. Subsequently these DCs migrate to mesenteric lymph nodes ⁸⁸ or PPs where they present the antigen epitope on surface receptors to immature B and T cells ^{89,90}. Presentation of allergen to an immature B cell results into somatic hypermutation and recombinant class switch towards an IgA producing B-cell. These cells migrate into the lamina propria where they further differentiate into IgA plasma cells, which produce high amounts of IgA if activated ^{91,92}. An important activation factor is TGF β being produced and released by various T helper (Th) cells as well as IECs. Th cells undergo activation in the lamina propria or in mesenteric lymph nodes as well as in PPs in response to antigen presentation ¹. Like IgA producing B cells, Th cells also express gut homing receptors on their surface which are upregulated through the production of retinoic acid by the CD103⁺DCs during their activation ^{93,94}. The produced retinoic acid additionally shifts the immature Th cell towards the FoxP3 expressing Treg phenotype ⁹⁵. Activated Treg cells produce high amounts of TGF β as well as interleukin (IL)-10 and suppress the formation of effector T cells by inducing their apoptosis ⁹⁶. Furthermore, Treg derived TGF β contributes to the activation of IgA producing plasma cells ⁹⁶. Other cells mediating oral tolerance beside Tregs, are Th3 and type 1 regulatory T cells (Tr1) cells which do not express FoxP3 ¹. Upon activation Th3 cells produce TGF β and IL-4 as well as IL-10 ⁹⁷. IL-10 drives the generation of Tr1 cells. These cells produce IL-10 and suppress antigen specific immune responses ⁹⁸. In turn, TGF β binds to FoxP3 expressing Treg cells ⁹⁹⁻¹⁰¹ and block a Th1 or Th2 dominated immune response and thereby mediate tolerance towards the food antigen ¹⁰².

In contrast to this, single exposure to high amounts of antigen induce lymphocyte anergy through inactivation and deletion of specific T cell clones ⁸⁴. The inactivation in mesenteric lymph nodes and PPs is mediated by T cell receptor (TCR) ligation without co-stimulation, leading to the specific induction of apoptosis ¹⁰³.

The breakdown of oral tolerance is associated with strong and adverse immune reactions. Even though environmental and genetic factors seem to play an important role; the exact mechanism is not yet fully understood. Diseases like inflammatory bowel disease are associated with the absence of oral tolerance towards commensal bacteria.

Another hypersensitivity reaction associated with the breakdown of oral tolerance towards dietary compounds is food allergy.

2.2 Food Allergy

2.2.1 Definition

Food allergy is an abnormal immunologic response to food that occurs immediately after contact with food antigens and reoccurs at every exposure. Depending on the immune mediator of the adverse reactions, food allergy is divided into IgE-mediated and non-IgE-mediated reactions ¹⁰⁴. In recent years, the numbers of food-allergic patients have steadily increased in western countries, IgE mediated reactions being the most common ones ¹⁰⁵. In this thesis I will therefore focus on this type of food allergic reactions.

2.2.2 Sensitization phase

During the encounter of the antigen in susceptible hosts, the allergen is able to reach the intestinal epithelium with its full allergenic potential ^{106–108}. In combination with other factors, such as antigen character, genetic predispositions, amount of allergen exposure, environmental factors, or the age at which the allergen is encountered, internalisation and processing of the allergen prime the DCs towards an allergenic phenotype ⁷. Recognition of the presented allergen by the TCR and binding of the co-stimulators CD80 as well as CD86 on DCs with CD28 on T cell surfaces in the presence of an allergy specific milieu, results in Th2 differentiation ¹⁰⁹. It is hypothesized that factors released by the microbiota induce pro-inflammatory TSLP production, which stimulates basophiles to produce the early IL-4 milieu ¹¹⁰. However, the exact mechanism how this initial allergy specific milieu is created is not yet fully known. The differentiated effector Th2 cells enhance the formation of a Th2 response by clonal expansion and production of IL-4, IL-5 and IL-13 in high quantities ¹⁰⁹. While most of the produced Th2 cells die, some of the Th2 cells further differentiate into Th2 memory cells, which sustain the allergic reaction ¹⁰⁹.

In comparison to T cells, B-cells are able to directly bind an allergen via surface bound immunoglobulin ¹. Interaction of Th2 cells with allergen bound B-cells induces an IgE class switch recombination in the B-cell ¹¹¹. This is mediated through the Th2 associated cytokines IL-4 and IL-13 which are released upon interaction of Th2 and immature B cell. The cytokines induce the translocation of STAT6 into the nucleus of the B cells, which in turn results in binding to the promotor region of genes encoding for the constant region of IgE. Through interaction of CD40 ligand on activated Th2 cells with CD40 receptor on B cells, the class switch recombination is mediated by the translocation of NFκB into the nucleus ¹¹¹. The activated and matured B cell in turn produces and releases high amounts

of allergen specific IgE. These antibodies bind to their high affinity receptor FcεRI on mast cells, basophils, eosinophils, Langerhans cells and APCs, IECs, or to the low affinity receptor FcεRII on enterocytes, macrophages, monocytes, follicular DCs, mature B cells and platelets ¹¹². This interaction arms the cells to mediate an allergic reaction upon re-encounter of the specific allergen. The production of IgE by activated B cells upon allergen encounter, without clinical symptoms, defines the sensitisation phase ¹⁰⁹.

2.2.3 Effector phase

During the elicitation phase of allergic patients, re-encounter of the allergen leads to the binding of antigen to the IgE bound to their specific FcεRI on mast cells as well as basophils and additionally induces the fast production of specific IgE by either immature B cells or memory B cells. Crosslinking of receptors results in activation and rapid degranulation of mast cells ¹¹³. High amounts of allergy mediator proteins like histamine, platelet activating factor, triptase, carboxypeptidase, chymase and heparin are released into the surrounding area ¹¹⁴. These mediators are responsible for the clinical symptoms during an allergic response. They induce vasodilation, increased vascular permeability, contraction of airway smooth muscles, as well as increased mucus secretion if released locally ¹¹³. Additionally, rapid and systemic release of basophil and mast cell mediators lead to an anaphylactic reaction ¹¹⁵.

Besides allergy mediators, mast cells also produce Th2 associated cytokines such as IL-4, IL-5 and IL-13 which promote the migration of eosinophils as well as other immune cells towards the site of mast cell degranulation ¹⁰⁵. This in turn leads to the enhanced formation of inflammation and chronification of allergic reactions in patients.

2.2.4 Intestinal epithelium in food hypersensitivity

One of the key players in the establishment and severity of food allergic reactions is the integrity of the intestinal epithelium. Alteration of the intestinal permeability allows increased antigen transport and, therefore, higher interaction with DCs and antigen presentation. Accordingly, an evaluation of the intestinal permeability index, measured by the recovery rate of Lactulose/Mannitol in urine, reported enhanced ratios in unchallenged food allergic patients compared to healthy control individuals ¹¹⁶. Additionally, after antigen challenge, food allergic patients showed further enhanced ratios in accordance with the severity of their clinical symptoms ^{116,117}. This provides evidence that the intestinal permeability is disrupted in food allergy even without allergen encounter.

Investigations of the enhanced permeability showed that in sensitised rats, allergen specific transcytosis of intact proteins across the intestinal epithelium is increased prior to mast cell activation ^{118,119}. This uptake of allergen was mediated by the low affinity

receptor FcεRII, which is expressed on IEC surfaces and upregulated by IL-4¹¹⁹. After sensitisation, allergen-specific IgE binds to FcεRII and the complex is translocated to the apical membrane, where it binds the specific allergen and mediates the enhanced antigen transcytosis¹²⁰. Experiments with human cell cultures confirmed the presence of the low affinity receptor on human enterocytes as well as its function to induce enhanced allergen uptake prior to mast cell activation¹²¹. Furthermore, recent studies provide evidence that IECs also express the high affinity receptor (FcεRI), which might also contribute to the enhanced allergen uptake and the resulting severe allergic reactions⁷⁵.

Additionally to the upregulation of FcεRII on IEC membranes, the allergy-associated Th2 cytokine, IL-4, increases the intestinal permeability by inhibiting the epithelial Na⁺/K⁺-ATPase¹²². IL-4 thereby enhances the selective apical to basolateral transport of antigens through the transcellular and paracellular way, while impairing the transepithelial resistance¹²³. Furthermore, in combination with interferon (IFN)γ, the presence of IL-4 induces the expression of pore-forming TJ protein claudin-2 in epithelial cells¹²⁴. Exposure of IEC to IL-13, another allergy-associated Th2 cytokine, leads to a similar decrease in transepithelial resistance, which is mediated by an enhanced apoptosis rate as well as the increased induction of claudin-2 expression^{125,126}. Since oral allergen challenge of sensitised mice did not induce allergy-related diarrhoea in the absence of mast cells, enhanced intestinal permeability is also associated with mast cell degranulation¹²⁷. Mast cell released mediators, for example the mast cell released tryptase, were found to impair the epithelial barrier function by relocating ZO-1 and occludin in an extracellular signal-regulated kinase (ERK) dependent way¹²⁸. Furthermore, the major basic protein, which is stored in eosinophils and released upon activation, also reduces the intestinal barrier function by downregulating the expression of occludin in IECs¹²⁹. This data provides evidence that food allergy elicitation alters the intestinal barrier function. However, it is not yet clear whether the intestinal epithelium is disorganized prior to sensitization and therefore allows enhanced antigen passage, or if the disruption of the barrier is caused by allergic reactions.

In asthma-related allergies it is known that the bronchial epithelial barrier is directly disrupted upon the encounter of a major house dust mite allergen, Der p1¹³⁰. Through its enzymatic activity, Der p1 causes the cleavage of occludin and ZO-1, which results in the disruption of TJ formation and thereby contributes to allergy sensitization. However, not much is known about the direct influence of food allergens on the intestinal epithelium. A recent study provided evidence that a major peanut allergen, Ara h2, alters the expression level of several immune modulatory genes in human IECs¹³¹. Direct interaction with Ara h2 thereby leads to induction of NFκB and TSLP expression as well as TLR signalling in

IECs. The heat-treated form of the allergen, as often encountered in roasted peanuts, had a higher binding capacity to the IECs and resulted in the induction of stress-responsive genes. Further investigations of the interaction of peanut allergens with IECs showed that Ara h1, Ara h2 and Ara h6 are able to cross the intestinal barrier without compromising the cell viability ¹³². Thereby IECs showed a concentration-dependent transport for Ara h1, but a consistent transport of Ara h2. Ara h1 and Ara h2 showed a high co-localisation rate with ZO-1, which leads to the disruption of the TJ formation between ZO-1 with claudin-1, JAM-A and occludin, resulting in increased transepithelial permeability and enhanced allergen passage.

This data provides evidence that food allergens directly alter the intestinal permeability and epithelial barrier function thereby promoting their enhanced uptake and transport across the epithelium. Additional studies are needed to investigate the influence of other food allergens, coupled intracellular messengers and other intercellular signalling partners which further influence IECs homeostasis.

2.3 Sphingosine-1-phosphate

One important factor influencing IEC homeostasis is the bioactive sphingolipid sphingosine-1-phosphate (S1P). Through a Phosphoinositol-3-kinase (PI3K) dependent pathway S1P induces phosphorylation of Akt and glycogen synthase kinase 3 (GSK-3), which results in decreasing levels of caspase-3 protein activity and the inhibition of apoptosis ¹³³. Furthermore, S1P promotes the phosphorylation of ERK1 and ERK2, which enhance the expression of the c-Myc gene and thereby induce cell proliferation ^{134,135}. The induction of IEC proliferation is further facilitated through the S1P-driven activation of p38 mitogen-activated protein kinases ¹³⁵.

S1P also influences the intestinal barrier function since the presence of S1P enhances the transepithelial resistance and reduces the paracellular permeability ¹³⁶. This effect is induced through the S1P-driven upregulation of the adherens junction protein E-cadherine, which showed enhanced localisation on the cell-cell contact regions after S1P stimulation. Though the underlying mechanism is not fully known, presence of S1P induced cytoplasmic Ca²⁺ levels which enhanced the transcription of E-cadherine mRNA while not affecting other adherens junction proteins like β -catenin and JAM-1.

Although S1P shows the highest abundance in intestinal tissues, not much is known about its further interactions with IECs and the underlying mechanisms ¹³⁷.

2.3.1 Metabolism

S1P is a product of the sphingolipid metabolism, which is highly active in the intestine. Sphingolipids are present in the small intestinal mucosa cells mainly in the apical membrane of intestinal villi and only scarcely in the basolateral membrane ¹³⁸. Sphingolipids can be formed through de novo synthesis mediated by the condensation of serine and palmitoyl-CoA at the cytosolic face of the endoplasmic reticulum through serine palmitoyl transferase (SPT) to sphinganine. This lipid is further processed to ceramide by ceramide synthase and to sphingosine by ceramidase. S1P is anabolised through the ATP dependent phosphorylation of sphingosine via sphingosine kinase 1 (SphK1) or sphingosine kinase 2 (SphK2). Another mechanism of sphingolipid production is the degradation of sphingomyelin from the plasma membrane by sphingomyelinase (SMase) to ceramide ¹³⁹.

In the small intestine of humans, a SMase with alkaline pH optimum, is found within the brush border of intestinal mucosal cells ¹⁴⁰. The enzyme is located at the apical surface membrane of microvilli, in endosomal structures beneath them, and in Golgi complexes showing the possibility to easily degrade sphingomyelin to ceramide upon activation. Additionally, enriched ceramidase activity is found in small intestinal brush borders, outlining the further processing from ceramide to sphingosine ^{141,142}. Apparently IECs are able to anabolise S1P, since they show SphK1 activity, and its overexpression is associated with cancer formation ^{134,143,144}. Furthermore, IECs are also able to synthesise sphingosine de novo since they show activity of SPT ^{145,146}. However, not much is known about the de novo synthesis in intestinal cells.

Erythrocytes, platelet, endothelial and mast cells also produce S1P through the phosphorylation of sphingosine by SphK ^{147,148}. Vascular endothelial growth factor, tumor necrosis factor (TNF) α , TGF β and IL-1 β , as well as other pro-inflammatory cytokines regulate the activity of SphKs ¹⁴⁹⁻¹⁵¹. The stimuli lead to the activation and translocation of SphK1 from the cytoplasm to the plasma membrane as well as the activation of SphK2 found at the nucleus membrane and at the endoplasmatic reticulum ^{149,152-155}.

The generated S1P may accumulate intracellularly and act as a second messenger which mediates proliferation and apoptosis ¹⁵⁶. However, not much is known about the intracellular function of S1P or its signalling mechanism. Or secreted in the extracellular environment by ABC transporters, as shown for mast cells, where, if released in plasma environment, it can bind to high density lipoprotein (HDL) as well as to albumin and provide a circulating reservoir of S1P in blood ^{157,158}. In tissues, S1P is reversibly dephosphorylated by S1P phosphatases (SPP1 and S1PP2) or irreversibly degraded by S1P lyase (SGPL) ¹⁵⁹⁻¹⁶². The complete absence of these S1P catabolizing enzymes in

erythrocytes, platelets and mast cells lead to a S1P gradient between HDL bound S1P in blood (0.2-0.9 μ M S1P) and S1P deprived tissues (0.5-75pmol/mg).

2.3.2 Role of S1P in Immune Regulation

Through the expression of specific receptors (S1P1-S1P5) by various cell types, S1P is able to act as intercellular signalling molecule and regulate different cellular functions such as cell proliferation, migration, cytoskeletal organisation as well as immunological reactions like lymphocyte egress and trafficking, vascular permeability or adherens junction assembly ¹⁶³. These effects depend on the activated S1P receptor subtype since each one couples with a distinct α subunit of guanine nucleotide-binding (G) proteins and induces different downstream signalling ¹⁶⁴. S1P1, which is widely expressed in adult tissue, particularly on endothelial, brain and heart cells as well as on lymphocytes, exclusively couples with Gi/o and thereby inhibits cAMP production and the various functions mediated by cAMP dependent protein kinase ¹⁶⁵. Activation of S1P1 hence modulates cell proliferation and motility. The ubiquitously expressed receptors S1P2 and S1P3 couple both with Gi/o, Gq and G12/13 and thereby mediate Gq dependent activation of phospholipase C and Ca²⁺ accumulation in cytosol, which modulates several cellular functions ¹⁵⁸. However, activation of S1P2 leads foremost to coupling with G12 which inhibits migration, while activated S1P3 foremost couples with G13, which induces cell migration ^{166,167}. The S1P4 receptor, found on lung and lymphoid cells, as well as S1P5 receptor, found on brain, skin and spleen cells, both couple with Gi/o and G12/13, leading to the induction of cell migration ¹⁶³.

In inflamed tissues, SphK1 is activated by TNF α , pro-inflammatory cytokines as well as sequestered S1P ^{149-151,168}. Encounter of immune stimuli like Immunoglobulin G (IgG) and platelet-activating factor also induce SphK1 activity in platelets, which leads to enhanced S1P production ¹⁶⁹. Moreover, crosslinking of the IgG high affinity receptor, Fc γ RI, as well as mast cell activation by Fc ϵ RI crosslinking and degranulation further induces SphK activation and enhances the S1P concentration in the inflamed tissue ^{159,169}. These elevated tissue S1P levels mediate the recruitment of immune cells which express different S1P receptors.

B and T-lymphocytes regulate their maturation within the lymph node and thymus by regulating the expression of S1P1 on their surface ¹⁶⁹. Encounter of antigen presenting DCs and cell differentiating cytokines, leads to the upregulation of S1P1 expression on lymphocyte surface and allows their egress from the lymph node into lymphatic vessels and blood ¹⁷⁰. Furthermore, S1P1 expression on the lymphocyte surface allows the sensing of the S1P gradient and promotes the recruitment of cells towards the side of inflammation ¹⁷¹. Additionally, S1P1 expression on macrophages promotes their migration

as well as their activation and phenotype switching ¹⁷². Activation of S1P2 on macrophages increases their production and release of inflammatory cytokines ¹⁷³. In contrast to this, migration of mature as well as immature DCs is induced by S1P3 activation which also regulates DC endocytosis ¹⁷⁴. Activated natural killer cells need S1P5 signalling to egress from lymph nodes and bone marrow and S1P1 expression further allows their enhanced recruitment to the side of inflammation ¹⁷⁵. Migration of neutrophils towards the inflamed tissue as well as their activation is dependent on induced S1P4 signalling ¹⁷⁶.

In the intestine, S1P receptor signalling plays an important role in the induction of immune responses by regulating the trafficking of peritoneal B cells to the intestine ¹⁷⁷. Activation of an IgM producing B cell in the PPs leads to the downregulation of S1P1 expression during the IgM to IgA cell differentiation ¹⁷⁸. The surface expression of S1P1 is recovered in the IgA plasma cell and allows the egress from PPs. Furthermore, expression of S1P1 on intraepithelial lymphocytes regulates their location within the intestine, showing high expression of S1P1 on naïve cells in the large intestine and low S1P1 expression on intraepithelial cells in the small intestine ¹⁷¹.

The presence of both S1P receptors and SphKs on mast cells make S1P also an important mediator in allergic reactions. Mast cells are able to sense even low concentrations of S1P and specifically migrate towards it ¹⁶⁸. Elevated S1P levels found in the bronchoalveolar fluid during allergic reactions allow enhanced recruitment of mast cells, which is mediated by expressed S1P1 ¹⁷⁹. Crosslinking of FcεRI after allergen encounter activates mast cell SphK1, which produces high amounts of S1P ¹⁸⁰. The produced S1P is released by mast cells and transactivates S1P2 on mast cell surfaces, leading to mobilization of intracellular calcium and increased allergy mediator production as well as degranulation ^{181,182}. The high amounts of released S1P induce the airway hyperresponsiveness seen in asthmatic reactions ^{183,184}. Interaction of S1P with its specific receptors on airways smooth muscle cells promote their proliferation and cause airway remodelling in asthma ¹⁷⁹. These interactions also lead to calcium mobilisation within the cells and induce airway smooth muscle cell contraction ¹⁸⁵. Activation of S1P2 on vascular epithelial cells additionally promotes increased pulmonary vasoconstriction ¹⁸⁶.

2.3.3 Role of S1P in Food Allergy

Mouse models of food allergy provided evidence that S1P1 signalling is responsible for allergy-mediated diarrhoea ¹⁸⁷. Thereby activation of S1P1 on CD4⁺ T cells, which show high receptor expression in allergic mice, induced their proliferation in PPs as well as their migration into the lamina propria and enhanced IL-4 production ¹⁸⁷. Moreover, S1P signalling induced the migration of IgE bound mast cells, which also express S1P1, into

the lamina propria¹⁸⁷. The hyper-reactive mast cells accumulate and degranulate in an SphK1- dependent way, thereby releasing their various mediators, including high amounts of S1P, in the surrounding tissue¹⁸².

In human intestinal cell cultures, elevated S1P levels promoted enhanced transepithelial transport of allergens via increasing the epithelial permeability in a concentration- dependent manner¹⁸⁸. However, the exact mechanism of how this effect is mediated remained unknown.

Besides the already mentioned functions of S1P in other allergies, not much is known about its specific effect on the intestine or its contribution to the establishment of food allergy and the severity of food allergic reactions.

2.4 Oral treatment of food allergy

Since food allergic patients may suffer from severe adverse reactions upon encounter of the triggering allergen, there is a high need for curative treatment of food allergic reactions. Specific immunotherapies aim to re-establish the oral tolerance reaction in the patient through administration of the allergen.

2.4.1 Specific Immunotherapy

In specific immunotherapy, individuals receive rising doses of allergens under medical control over a specific time. This leads to a change in the immunologic response upon allergen encounter and is associated with desensitisation. Three different routes of immunotherapy application – subcutaneous, sublingual and oral – were shown to be efficient for inhalative allergies¹⁸⁹. However, in food allergies, the administration of allergen by subcutaneous immunotherapy is associated with a high risk for severe systemic reactions^{189,190}. Furthermore, the administration of allergen through a drop of purified allergen under the tongue as in sublingual immunotherapy results in various side effects and is of questionable efficiency¹⁸⁹. Therefore, oral immunotherapy (OIT) is the only viable treatment option for food allergies besides the strict avoidance of allergen and self- injectable epinephrine.

Oral Immunotherapy

During OIT, increasing dosages of specific allergen are orally administered to the patient in three phases. The first induces a rushed desensitization through high dosage administration over 1-2 days with 6-8 doses of allergen. This phase as well as the second phase, which contains weekly allergen dosages over a 6-12- month period, is clinically supervised. The following maintenance phase calls for allergen doses to be administered daily for years without clinical supervision¹⁹¹.

Successful OIT results in increased IgG₄ and TGFβ levels as well as decreased levels of the Th2 related cytokines IL-5 and IL-13¹⁹⁰. Consequently, lower amounts of allergen-specific Th2 cells are activated and the proliferation of Treg cells, which is associated with the induction of oral tolerance towards the encountered allergen, is initiated¹⁹².

Since the allergens need to reach the intestine in a bioavailable and intact form to induce the above mentioned reactions, high amounts of allergens are administered¹⁹³. The allergen ingestion by not yet desensitized patients can lead to multiple side effects reaching from oral pursuits up to anaphylactic shock as is sometimes observed during peanut desensitization¹⁸⁹. Adverse reactions which are not controllable by H₁-antihistamines or sodium cromolyn, like severe urticarial, diarrhoea, vomiting or chronic abdominal pain, lead to the termination of treatment¹⁹⁴. However, in case of controllable side effects like mild urticarial, angioedema or moderate abdominal pain, OIT is continued¹⁹⁴.

2.4.2 Poly-(D,L-lactide-co-glycolide) Microparticles

To enhance the specific delivery of bioavailable allergen to the intestine, allergens are encapsulated into poly-(D,L-lactide-co-glycolide) (PLGA) microparticles (MP).

PLGA is a highly biocompatible and bio-degradable polymer material which deteriorates through terminal chain hydrolysis into lactic and glycolic monomers which are exploited in krebs cycle^{195,196}. Encapsulation of allergen within MPs, via either emulsification or water-in-oil-in-water emulsion results in the protection of the entrapped substance from degradation and efficient delivery¹⁹⁶. Deterioration of MPs releases the enclosed antigen continuously over a period of days, which mimics booster injections of vaccines¹⁹⁹. Due to this and their capacity to enhance immune reactions, MPs are often used as antigen carriers in various vaccines²⁰⁰. The spherical- shaped MPs are stable enough to allow oral application and are therefore available for OIT^{199,200}.

Binding of ingested MPs to the intestinal epithelium is regulated by their surface charge and hydrophilicity. Changing the negative MPs surface charge to positive, allows higher penetration of the negatively charged IECs²⁰¹. In addition, increasing the surface hydrophilicity of MPs by coating them with poloxamer reduced their intestinal uptake, whereas increasing the surface hydrophilicity by chitosan coating induced interactions of MPs with IEC^{202,203}. This effect, however, seems to be mediated by the changed surface charge of MPs after poloxamer coating, which is not affected by chitosan treatment of MPs. The binding and interaction capability of MPs with IECs is further influenced by their size. Smaller MPs (100nm) have a higher interaction rate resulting in an intracellular distribution within IECs, whereas bigger MPs (up to 2 μm) interact in lower numbers and

are bound to the apical membrane of IECs ²⁰⁴. Specific internalisation through M cells, which have the capacity to transcytose particulate structures up to 10 µm, is also regulated through MPs size ²⁰⁵. Thereby endocytosis is highly efficient for MP sizes smaller than 1µm ^{205,206}. Through exocytosis from M cells, MPs are delivered into PPs. This results in systematic distribution if they are smaller than 5µm, or they are trapped within PPs for up to 35 days, if they are bigger than 5µm ²⁰⁷. In PPs, MPs interact with APCs and initiate allergen- specific IgG production by upregulating IFN γ and downregulating IL-4 ^{208–210}.

To enhance the binding as well as transepithelial transport, both enterocytes and M cells are specifically targeted through functionalisation of MPs. This is achieved through coating of MPs with substances which specifically bind to surface molecules of IECs. One of the possibilities are nontoxic plant lectins, contained in diet, which interact with enterocytes through binding of apical expressed oligosaccharides ²¹¹. Lectins thereby exhibit resistance to proteolytic cleavage and different carbohydrate binding preferences.

Wheat germ agglutinin (WGA), a dimeric protein containing two to four carbohydrate-binding sites per subunit, from *Triticum vulgare*, specifically binds to N-acetyl-D-glucosamine containing glycoproteins of IECs ²¹¹. It is further able to specifically bind sialic acid residues on IEC surfaces ²¹². These moieties are highly expressed on enterocytes, allowing their specific targeting by WGA functionalisation of MPs ²¹¹. The interaction of IECs with the lectin leads to its absorption and intracellular accumulation ²¹³. Investigations of WGA- coated MPs (WGA-MPs) in mice showed an enhanced production of specific IgG for the major birch pollen allergen Betv1 compared to uncoated MPs (Plain-MPs) treatment ²¹⁴. However, this effect could not be seen in Betv1- sensitized mice leading to the assumption that WGA-MPs- controlled enterocyte targeting is not enough to induce the desired immune response and other coating lectins are needed ²¹⁵.

Aleuria aurantia lectin (AAL) from the eatable orange peel fungus *Aleuria Aurantia* shows high similarity to neuraminidases of M cell invading pathogens ²¹⁶. Through its specific binding to α -L-fucose motifs, predominantly found on murine M cells, allows targeting of M cells and consequently PPs by AAL coated MPs (AAL-MPs) ²¹⁵. Treatment with AAL-MPs of sensitized mice resulted in the enhanced production of allergen- specific Th1 antibody as well as the upregulation of regulatory cytokines IL-10 and IFN γ . However, elevated IL-4 production was also observed. The induced cytokine levels were higher than after WGA-MPs treatment, revealing AAL-MPs treatment as more efficient. Experiments in cell culture affirmed the binding of AAL to human M cells ²¹⁷. AAL-MPs treatment of PBMCs of allergic patients resulted in enhanced uptake and high induction of IL-2 and IFN γ production whereas Th2 cytokines were not regulated.

Another possibility to enhance the binding and transepithelial transport of MPs through the intestinal epithelium is the usage of neuraminidases from IECs invading pathogens. One investigated option is the neuraminidase (NA) from *Vibrio cholera*, which is structured into a central β -propeller catalytic domain (NA) flanked by two lectin domains^{216,218}. Cells within the GI, especially M cells, exhibit ubiquitous expression of higher gangliosides on their apical surface^{206,219}. The sialidase from *Vibrio cholerae* hydrolyses those gangliosides to glycosylated monosialoganglioside 1 (GM1) by removing sialic acid residues²²⁰. The specific binding of the N-terminal lectin domain to sialic acid residues thereby is responsible for the high affinity binding of NA to gangliosides²²¹. GM1 is the specific receptor for cholera toxin which facilitates the cell penetration and uptake capability of *Vibrio cholerae*²²⁰. A recent study, showed that NA- coated MPs (NA-MPs) bind specifically to α -L-fucose motifs and GM1 of IECs. Compared to AAL-MPs or WGA-MPs stimulated cells, NA-MPs displayed an enhanced binding to and uptake by those IECs [unpublished data].

2.5 Aim of thesis

In this thesis, I focus on food allergic reactions, specifically on the influence of S1P, a mediator known to be involved in various allergic reactions, on IECs, and on novel therapeutic options to treat patients with food allergy.

The first aim of this thesis is to investigate the role of S1P in IECs. S1P is known to play a crucial role in allergies such as asthma, however, there is very limited data on the role of S1P in food allergy. To find out whether or not IECs can respond to S1P, S1P receptor expression as well as S1P signalling was measured. TJ formation and barrier expression as well as cytokine expression was investigated after S1P stimulation to investigate the role of S1P in the establishment of an inflammatory or tolerogenic milieu. In addition, the production or degradation of S1P by IECs in response to inflammatory signals was investigated.

The second aim of this thesis is to evaluate the effect of lectin coated allergen loaded MPs on IECs. Since different coating materials resulted in diverse cell attachment patterns and uptake rates in previous studies, the aim was to investigate if lectin coated MPs stimulation results in impaired TJ formation and therefore enhanced uptake. Furthermore, I explored if lectin coated MPs stimulation leads to altered cytokine expression over time in IECs.

3. Material and Methods

3.1 Material

3.1.1 Chemicals

Name	Manufacturer	Cat. number
AAL	Vector Laboratories	L-1390
10xDPBS	gibco	14200-067
Acetic acid	VWR Chemicals	20104298
Acrylamide	BioRad	161-0148
APS	BioRad	161-0700
Calcium ionophor	SIGMA	C7522-1MG
Chloroform	Sigma-Aldrich	132950-2.5l
Distilled H ₂ O DNase and RNase free	gibco	10977035
Ethanol	VWR Chemicals	20821310
Glycine	Merck Millipore	1041691000
Isopropanol	Merck Millipore	1096342511
ITS	Gibco Lifetechnologies	41400-045
JTE-013	Cayman chemicals, Biomol GmbH	10009458
Methanol	Merck Millipore	1060092500
NA	SIGMA	N7885_1UN
NaCl	Merck Millipore	1064040500
OVA	SIGMA	A5503-10G
Phenolchloroform	amresco	0883-100ml
proteinase inhibitor	SIGMA	P2714-1BTL
S1P d-erythro	ENZO, Life Sciences	SL-140
SDS	Sigma	L5750-500G

TEMED	SIGMA	T9281-25 ml
TNF α (human recombinant TNF α lysophilized 10 μ g)	Gibco, invitrogen	PHC3015
TRIS	Merck Millipore	1083820500
TRIzol Reagent RNA	ambion	15596-018
Trypsin	Gibco, life technologies	25300-054
Tween	Sigma	P1379
WGA	Vector Laboratories	L-1020

3.1.2 Kits

Kit	Manufacturer	Cat. number
DNase Kit	ambion lifetechnologies	AM2239
Fluo-4 Direct™ Calcium Assay Kit	invitrogen	F10471
High Capacity Reverse Transcription Kit	Applied Biosystems, Life Technologies	4368814
MycoAlert mycoplasma detection kit	Lonza	LT07
Pierce BCA Protein Assay Kit	Thermo Scientific	23225
RNeasy Mini Kit	QIAGEN	74104

3.1.3 Buffers

Buffer	Formula	Manufacturer/ Formula	Cat. number
Blocking Buffer	washing buffer		
	5 % Drymilk powder	Fixmilch	MD7774920
Electrophoresis Buffer (2 L)	250 mM TRIS	(60.6 g)	
	1.9 M Glycine	(292 g)	
	35 mM SDS	(20 g)	

	DDW	(2000 ml)
	pH 8.3	
Lysis Buffer (Nonidet-NP40, 15 ml)	150 mM NaCl	(131,49 mg)
	1 % Triton X-100	(150 µl)
	50 mM Tris	(90,85 mg)
	DDW	(15 ml)
	pH 8.0	
Restore PLUS Western Blot Stripping Buffer		Thermo Scientific 46430
Running buffer (450 ml)	1.5 M TRIS	(81.77 g)
	DDW	(450 ml)
	pH 8.0	
Stacking buffer (200 ml)	0.8 M TRIS	(20 g)
	DDW	(200 ml)
	pH 6.8	
Transfer Buffer (1 L)	25 mM TRIS	(3.03 g)
	192 mM Glycine	(14.41 g)
	20 % Methanol	(200 ml)
	DDW	(1000 ml)
	pH 8.3 stored at 4°C	
Washing buffer (1 L)	50 mM TRIS	(6.07 g)
	150 mM NaCl	(8.78 g)
	0.1 % Tween-20	(1 ml)
	DDW	(1000 ml)
	pH 7.4	

3.1.4 Cell Cultivation

Cell cultivation media	Formula	Per 500ml Medium	Manufacturer	Cat. number
<i>cultivation media</i>				
Complete Medium	DMEM high glucose	(500 ml)	Gibco	41965-062
	4.5 g/ml			
	10 % FBS/FCS	(50 ml)	Gibco invitrogen	10270106
	100 U/I Pen/strep	(5 ml)	gibco life technologies	15140-122
	10 mM HEPES	(5 ml)	gibco life technologies	15630-056
	1 x MEM NEAA	(5 ml)	gibco life technologies	11140-035
	2 mM L-glutamine	(5 ml)	Gibco life technologies	25030-024
Medium without FCS	DMEM high glucose	(500 ml)		
	4.5 g/ml			
	100 U/I Pen/strep	(5 ml)		
	10 mM HEPES	(5 ml)		
	1 x MEM NEAA	(5 ml)		
	2 mM L-glutamine	(5 ml)		
Medium with ITS	Medium without FCS	(50 ml)		
	1 x ITS	(1 ml)		

3.1.5 Antibodies

Antibody	Manufacturer	Cat. number
anti-SphK1 (rabbit polyclonal anti human)	Cell Signalling Technologies	3297

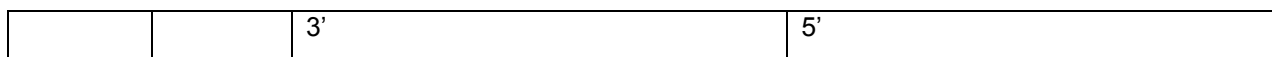
anti-SphK2 (rabbit polyclonal anti human)	Sigma Aldrich	SAB1411112
anti-GAPDH (rabbit polyclonal anti human)	Proteintech	10494-1-AP
secondary antibody (goat polyclonal anti rabbit HRP)	Thermo Scientific – life technologies	32260

3.1.6 qRT-PCR Primers & TaqMan Assays

qRT-PCR primers were purchased from Sigma Aldrich.

Primer Sequences:

Gene	Species	Forward Primer	Reverse Primer
S1PR1	human	5'-GCCCATGGCCAACTCACTTCTGA-3'	3'-GCTGACAGGGCCACAAACATAC-5'
S1PR2	human	5'-GCTGCCACTTGACGACTTCTCC-3'	3'-GCTTCTCTCTGCCTTGCTCAG-5'
S1PR3	human	5'-CAATAGCAGCCACTCTCCGAAGGT-3'	3'-GGCAGGCTGTTGGTCAAAGTAAGG-5'
S1PR4	human	5'-TCCTCAACTCGGCGGTCAAC-3'	3'-CGTTCCTGCTCCCCATACA-5'
S1PR5	human	5'-GCCATGGCCAACTCACTTCTGA-3'	3'-CACCTTTGGCTGCATTTCTACA-5'
claudin-1	human	5'-CAGTCAATGCCAGGTACGAATTT-3'	3'-AAGTAGGGCACCTCCCAGAAG-5'
claudin-4	human	5'-TGTACCAACTGCCTGGAGGAT-3'	3'-GACACCGGCACTATCACCATAA-5'
occludin	human	5'-GATGAGCAGCCCCCAAT-3'	3'-GGTGAAGGCACGTCCTGTGT-5'
ZO-1	human	5'-ACAGTGCCTAAAGCTATTCCTGTGA-3'	3'-TCGGGAATGGCTCCTTGAG-5'
ZO-2	human	5'-CGGTAAATACCGTGAGGCAAA-	3'-GGGAACCACTGGGTGTAATTCA-



FAM labelled TaqMan Assays were purchased from Applied Biosystems.

Gene	Species	Assay number
b-Actin	human	Hs99999903_m1
CCL20	human	Hs01011368_m1
IFN γ	human	Hs00989291_m1
IL-10	human	Hs00961622_m1
IL-13	human	Hs00174379_m1
IL-33	human	Hs00369211_m1
IL-4	human	Hs00174122_m1
IL-5	human	Hs01548712_g1
IL-8	human	Hs00174103_m1
RANTES	human	Hs00982282_m1
SphK1	human	Hs01116530_g1
SphK2	human	Hs01016543_g1
TSLP	human	Hs00263639_m1
SGPL1	human	Hs00187407_m1

3.1.7 SDS Page

12 %SDS Gel	Composition
separation gel (final volume 10,6 ml)	3 ml Acrylamide 50 µl 10 % APS 4.4 ml DDW 2.5 ml running buffer 100 µl 10 %SDS 10 µl TEMED
stacking gel (final volume 2,5175ml)	500 µl Acrylamide 12.5 µl 10 % APS 1.35 ml DDW 25 µl 10 % SDS 625 µl stacking buffer 5 µl TEMED

3.2 Methods

3.2.1 Cell Culture

Cultivation of Cells

1. Human colon adenoma carcinoma cells (CaCo2 clone TC7), kindly provided by Dr. Monique Rousset (INSERM, Paris, France) and stored in liquid nitrogen, were thawed when needed.
2. Cells were defrozen at 37 °C, immediately transferred into a 15 ml Falcon tube (TPP; 91015) containing complete medium, and centrifuged at 800 x g for 5 min (Allegra x12R Centrifuge, BACKMANN Coulter). Pellet was resuspended in complete medium. Cells were transferred to T75 cultivation flask (nunc; 156499/157400) and incubated in a 37 °C humidified 5 % CO₂ incubator (CO₂ incubator TYP 112010; Thermo-Scientific/ ILMVAG GmbH; BBD622Q).
3. Cells were passaged every 3-4 days at approximately 80 % confluence. Cells were detached from plastic using 0.05 % Trypsin-EDTA and cell numbers were estimated using a cell counter (TC10 automated cell counter, BIO Rad).
4. For cultivation, cells were seeded at a density of 5 x 10³ cells/cm². Therefore, 3.75 x 10⁵ cells were placed in a T75 cultivation flask.

Freezing Protocol

1. Prior to freezing, cells were cultured in complete medium supplemented with 20 % FBS instead of 10 % (DMEM + 20 % FCS) until they reached 80 % confluency.
2. 1 x 10⁶ cells were resuspended in 900 µl Complete Medium + 20 % FCS, 100 µl DMSO was added and cell suspension was transferred into a CryoTube™ Vial (Thermo Scientific; 363401).
3. Tubes containing cells were placed in an isopropanol chamber and stored at -80 °C for 2 days before being transferred to liquid nitrogen tanks.

Mycoplasma Test

Cells were checked for mycoplasma contamination according to MycoAlert mycoplasma detection kit protocol.

1. 1 ml of cell supernatant was centrifuged for 5 min at 200 x g.
2. 50 µl of cell supernatant, 50 µl positive and 50 µl negative control (applied in test kit) were transferred to one well of a 96 well plate, respectively.

3. 50 μ l MycoAlert Reagent (applied in test kit) was added to the samples and incubated at room temperature for 5 min.
4. Luminescence was measured with Infinite M200 Pro (TECAN) to define the basement luminescence (measure a).
5. 50 μ l MycoAlert substrate (applied in kit) was added to the test solution as well as to the control samples and incubated for 10 min at room temperature.
6. Luminescence was measured again (measure b) and mycoplasma contamination was determined using the b/a measure ratio. If ratio was smaller than 0.9, no mycoplasma contamination was present and cells were used for experiments.

3.2.2 Cell Stimulation

1. For experiments, cells were seeded in complete medium at a density of 6×10^4 cells/cm² in:
 - a. 12 well plates (TTP; 92012) with a total of 2.28×10^5 cells per well
 - b. 12 well transwell plates (12 Well Cell Culture Receiver Plate; MerckMillipore; PIMWS 1250; and 12 well Millicell Hanging cell culture Inserts; MerckMillipore; PIHT15R48) at a total of 6.6×10^4 cells per insert
 - c. 24 well transwell plates (Falcon 24 Well TC-Treated Cell Polystyrene Permeable Support Companion Plate; Corning; 353504 with Falcon Permeable Support 24 well plate inserts; Corning; 353492) with a total of 1.80×10^4 cells per insert
 - d. 96 well plates (Nunc™ MicroWell™ 96-Well Optical-Bottom Plates with Polymer Base; Thermo Scientific nunc; 165305) containing 1.92×10^4 cells per well.
2. Cells were cultivated for 21 days to fully differentiate. Medium was changed every second day.
3. For cultivation in transwell plates, FCS-free medium was applied apically from day 7 of cultivation.
4. In case of S1P stimulation, ITS was used to replace FCS in basolateral well on day 20.
5. On day 21 experiments were performed. Fresh complete medium, FCS-free medium or ITS containing-medium was applied and cells were stimulated with:

Poly (D,L-lactide-co-glycolide) Microparticles and coating substances

Cells cultured in 12 well plates were stimulated apically with: 10 µg/ml AAL, 10 µg/ml NA, 10 µg/ml WGA, 10 µg/ml OVA, 10 µg/ml uncoated Particle (Plain-MP), 10 µg/ml Particle coated with AAL (AAL-MP), 10 µg/ml Particle coated with NA (NA-MP), 10 µg/ml Particle coated with WGA (WGA-MP) for 1, 2, 3 and 6 hours or remained unstimulated for controls.

S1P

Cells in 12 well transwell plates were stimulated basolaterally with 100 nM S1P (S1P in methanol + 1 % BSA) or vehicle control (methanol + 1 % BSA) for 30 min, 2, and 4 hours. To test the effect of S1P2 antagonist JTE-013, cells were stimulated basolaterally with 1 µM JTE-013 10 min prior to stimulation (30 min and 4 hours) with 500 nM S1P and vehicle control, respectively.

TNFα

Cells in 12 well transwell plates were stimulated on the basolateral side with 100 ng/ml or 250 ng/ml TNFα (in 1 x PBS + 0.1% BSA) and vehicle control (1 x PBS + 0.1 % BSA) for 30 min, 1, 2, 4, 6 and 8 hours, respectively.

3.2.3 Analysis of Gene Expression by Real-time PCR

RNA Extraction and Isolation

All steps were performed at room temperature, if not indicated otherwise. For RNA isolation, RNeasy Mini Kit (QIAGEN) was used.

1. Cells were harvested using 700 µl TRIZOL reagent, transferred to 1.5 ml Eppendorf tubes, and placed on benchtop for 5 minutes.
2. 140 µl chloroform per tube were added and mixed by vigorous shaking for 15 seconds.
3. Samples were placed on benchtop for 2 minutes prior to centrifugation at 12000 x g for 15 minutes. After centrifugation, sample consisted of three phases: an upper colourless aqueous phase (containing RNA), a white intermediate and a lower red phase.
4. The upper aqueous phase was carefully transferred into a new 1.5 ml Eppendorf tube. 1.5 volumes 100 % ethanol were added and mixed by pipetting up and down several times.
5. Up to 700 µl of the samples were transferred into RNeasy Minispinn columns in 2 ml collection tubes (supplied in Kit) and centrifuged at ≥ 10000 x g for 30 sec. The flow through was discarded.

6. Step 5 was repeated with remaining sample.
7. 500 µl Buffer RPE (supplied in Kit) were added to the columns and centrifuged at $\geq 10000 \times g$ for 30 seconds. Flow through was discarded.
8. Again, 500 µl Buffer RPE were added to the columns and centrifuged at $\geq 10000 \times g$ for 2 min. RNeasy Mini Spin columns were carefully transferred to new 1.5 ml Eppendorf tubes
9. 30 µl RNase free water (supplied in Kit) was added directly onto RNeasy Mini spin column membranes and RNA was eluted with centrifugation at $\geq 10000 \times g$ for 1 minute.
If DNase treatment was performed, RNA was eluted in 50 µl RNase free water prior to DNase treatment.

DNase Treatment:

10. 6 µl Turbo DNase, 10 µl DNase Buffer and 34 µl RNase free water were added to 50 µl eluted RNA.
11. The samples were incubated at 37 °C for 30 min and placed on ice afterwards.
12. 100 µl Phenol-Chloroform per sample were added and mixed by vigorous shaking for 1 min.
13. RNA isolation protocol was repeated starting from step 3. Final elution of RNA in step 10. was performed in 30 µl RNase free water.

RNA concentrations and purity were measured with nanodrop ND-1000 Spectrophotometer (peqLab Biotechnologie GmbH). Samples were stored at -80 °C.

Reverse Transcription PCR

For RT-PCR, High Capacity cDNA Reverse Transcription Kit without RNase Inhibitor was used.

1. Kit components (10 x Buffer, 25 x dNTP Mix, 10 x RT Random Primers) were thawed on ice.
2. 1 µg RNA per sample was diluted with nuclease free water to a final volume of 10 µl and placed on ice.

- 2 x RT master mix was prepared according to High Capacity cDNA Reverse Transcription Kit protocol (Applied Biosystems):

Table 1: Protocol for RT-PCR Master Mix for one reaction

2 x Master Mix	Volume/Reaction [μl]
10 x RT Buffer	2,00
25 x dNTP Mix (100mM)	0,80
10 x RT Random Primers	2,00
MultiScribe Reverse Transcriptase	1,00
Nuclease-free H ₂ O	4,20
Total per Reaction	10,00

- 10 μ l RT master mix was added to RNA sample (step 2) and RT-PCR was performed using MyCycler (BioRad). PCR settings according to High Capacity cDNA Reverse Transcription Kit protocol (Applied Biosystems) were used: 25 °C for 10 min, 37 °C for 120 min, 85 °C for 5 min and samples were left at 4 °C until further process/storage.
- The final cDNA was diluted 1:5 in nuclease free water and stored at -20 °C.

Quantitative Real-time PCR

SYBR-GREEN

qRT-PCR was performed according to SYBR Green Mix Protocol.

- Lyophilized primers were diluted in RNase free water (RNeasy Mini Kit; QIAGEN) according to technical datasheet to obtain a stock solution of 100 μ M and stored at -20 °C.
- Mixes of 10 μ M forward and 10 μ M reverse primer in RNase free water (QIAGEN) were prepared for further experiments and stored at -20 °C.
- Efficiency of primers was tested before usage
 - A standard dilution of cDNA samples was prepared 1 (undiluted cDNA), 1:10, 1:50, 1:100, 1:1000.
 - To test if primers specifically bind cDNA, 1 μ g RNA per sample was diluted in 10 μ l nuclease free water to match the starting concentration of RT-PCR and further diluted 1:5 in nuclease free water to simulate the concentration of cDNA.
 - To test for primer dimers, nuclease free water was used as non-template control.

- Master Mix was prepared for technical triplicates according to SYBR-Green protocol:

Table 2: Protocol for qPCR Master Mix for one technical triplicate

Master Mix	Volume/triplicate [μ l]
SYBR Green MM	15
Primer Mix (10 μ M fw + 10 μ M rev)	2.4
Nuclease-free H ₂ O	8.7
Total per Reaction	26.10

- Per triplicate 1.5 μ l cDNA, 1.5 μ l RNA, and 1.5 μ l nuclease free water, were added to the master mix, respectively.
- 10 μ l sample was placed per well in a 384 well plate (384 well plate micro AMP Optical 384 well reaction plate with barcode; Applied Biosystems; 4309849) and plates were run on a 7900HT Fast Real Time PCR machine (Applied Biosystems). For efficiency testing, a dissociation curve was added at the end of the run.

Table 3: Quantitative real time PCR Program for Primer testing with SYBR-Green

	UNG incubation	Polymerase activation	PCR Denaturation	Annealing	Dissociation curve		
Temperature[$^{\circ}$ C]	50	95	95	60	95	60	95
Time [sec]	120	600	15	60	15	60	15
			40 cycles				

For gene expression analysis, β -actin was used as endogenous control.

Results were analysed using SDS 2.4 and RQ Manager 1.2.1 from Applied Biosystems.

TaqMan

qRT-PCR was performed according to TaqMan Universal Master Mix Protocol (Applied Biosystems). β -actin was used as endogenous control.

- Master mix was prepared according to protocol, each sample was run in technical triplicates:

Table 4 Protocol for quantitative real time PCR Master Mix for triplicate

Master Mix	Volume/triplicae [μ l]
TaqMan Universal Master Mix	15
FAM labelled TaqMan assay	1.5
Nuclease-free H ₂ O	8.7
Total per Reaction	25.2

2. 1.6 µl cDNA or 1.6 µl nuclease free water as non template control was added to the master mix
3. 10 µl sample per well was placed per well in a 384 well plate. qRT-PCR was run on a 7900HT Fast Real Time PCR machine according to protocol.

Table 5: Quantitative real time PCR Program for gene expression analysis with TaqMan.

	UNG incubation	Polymerase activation	PCR Denaturation	Annealing
Temperature[°C]	50	95	95	60
Time [sec]	120	600	15	60
			40 cycles	

3.2.4 Analysis of Protein Expression by Western Blot:

Protein Extraction

Protein extraction was performed on ice, if not otherwise indicated

1. Cells were washed with 1 ml ice cold 1 x PBS
2. 500 µl lysis buffer per sample were added, cells were scraped (CytoOne USA scientific; CC7600-0220) off and placed into 1.5 ml Eppendorf tubes.
3. 10 µl protease inhibitor was added and sample was vigorously vortexed.
4. Afterwards, tubes were placed on a rotator for 30 min at 4 °C
5. To remove the cell debris, the suspension was centrifuged at 12000 rpm for 20 min at 4 °C.
6. The supernatant containing the protein lysates (approximately 500 µl) was transferred to a new tube and the pellet was discarded.
7. Samples were stored at -80 °C.

Determination of Protein Concentration

Protein concentration was determined using Pierce BCA Protein Assay Kit according to protocol (Thermo Scientific).

1. Standard dilutions and sample dilutions were prepared in nuclease free H₂O.
 - a) BSA Standard dilutions (Albumin Standard; Thermo Scientific; 23209):
2000 µg/ml, 1500 µg/ml, 1000 µg/ml, 750 µg/ml, 500 µg/ml, 250 µg/ml, 125 µg/ml, 25 µg/ml, and 0 µg/ml were prepared.
 - b) Samples were diluted 1:10, 1:20, and 1:40 in nuclease free H₂O with a final volume of 100µl.

- c) For the working reagent 50 parts of Pierce BCA Protein Assay Reagent A were mixed with 1 part Pierce BCA Protein Assay Reagent B.
2. 25µl standard and sample were transferred into a 96 well plate in technical duplicates, respectively. 200 µl working reagent was added per well.
3. The plate was covered with parafilm and incubated at 37 °C for 30 min.
4. Absorbance was measured at 562 nm with an Infinite PRO Reader (TECAN).

To determine the protein concentration, standard curve and standard curve equation were determined using Microsoft Excel 2013 and concentrations for measured samples were calculated

SDS Page

For electrophoresis, the Mini Protean 3 System of Bio Rad was used.

1. 12 % SDS Gel with 10 wells was prepared:
 - a. First, the separation gel (approx. 3 ml) was filled in the gap between the glass plates and covered with 1 ml isopropanol to remove potential air bubbles.

After complete polymerisation (approx. 10 min), isopropanol was removed.
 - b. Next, the stacking gel (approx. 2 ml) was filled on top of the separation gel and a comb forming 10 wells was inserted carefully.
 - c. After polymerisation (approx. 5 min), the comb was removed and wells were rinsed with DDW several times to ensure gel-free wells.
 - d. Glass plates were set into an electrophoresis chamber and electrophoresis buffer was added.
2. 25 µg protein in 15 µl lysis buffer were mixed with 5 µl sample buffer and heated at 95 °C for 3 min.
3. 5 µl Page Ruler Plus Prestained Protein Ladder (Thermo Scientific; 26619) and 20 µl of the samples were loaded into wells.
4. Electrophoresis was run at 30 mA for 40 min using a Power Pac 3000 (Bio Rad).

Western Blot

For western blots, Mini Trans-Blot® Electrophoretic Transfer Cell (Bio Rad; 170-3930) was used. GAPDH staining was used as endogenous control.

1. Filter paper (extra thick blot paper; Bio Rad; 1703968), nitrocellulose membrane (Protean BA 83; GE Healthcare Life Sciences; 10401396), and sponge were soaked in cold transfer buffer for 5-10 min.
2. The Mini Gel Holder Cassette was loaded according to figure 3:

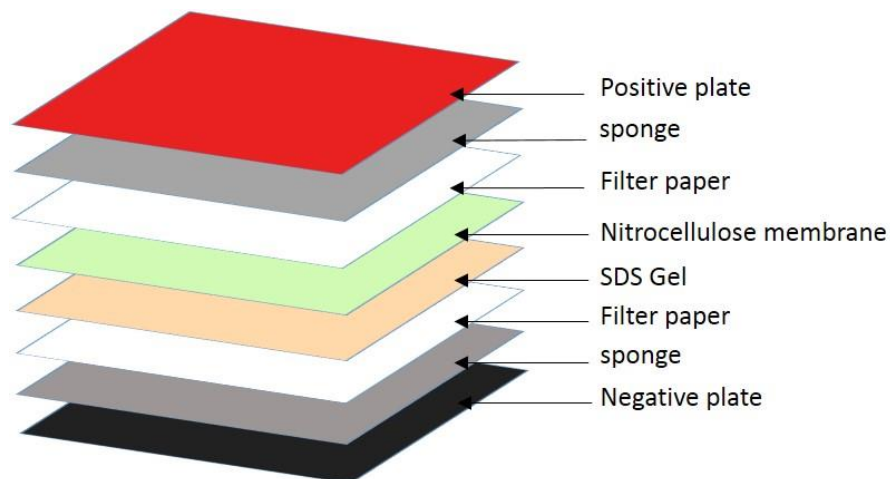


Figure 3: Loading of western blot cassette

3. The cassette was transferred to the Mini Transfer-Blot Core, which was added to the blotting chamber. A magnetic stirrer and a cooling unit were added and the blotting chamber was filled with cold transfer buffer and placed on ice.
4. Transfer was run at 250 mA for 90 min using Bio Rad Power Pac 300 (Bio Rad; 1703968).
5. After blotting, the nitrocellulose membrane was washed in washing buffer
6. To block unspecific binding, the membrane was incubated in blocking buffer on a shaker for 2 hours at room temperature.
7. Primary antibody was diluted 1:1000 in 10 ml blocking solution, added to the membrane, and incubated overnight at 4°C.
8. The next day, the blot was washed with washing buffer 3 times à 10 minutes at room temperature.
9. Secondary antibody diluted 1:10.000 in 10 ml blocking buffer was added to the membrane and incubated for 1 hour on a shaker at room temperature.

10. Afterwards, the membrane was washed 3 times à 10 minutes with washing buffer.

11. The blot was developed with Super Signal West Pico Chemiluminescent Substrate (Thermo Scientific; 34080) and pictures were taken with Versa Doc Imager 4000MP (Bio Rad):

a. For the protein ladder the configuration were:

Exposure time	2 sec
Gain	0.5
Application	Weisslicht 4x4
Light mode	LED
Color	White
Dark Type	Referenced dark subtraction
Ref. Bkgd Time	60 sec
Emission Filter	None

b. For the stained proteins the following setups were used:

Exposure time	300 sec
Gain	0.5
Application	Chemi Ultra Sensitivity
Light mode	Emissive
Dark Type	Referenced dark subtraction
Ref. Bkgd Time	60 sec
Emission Filter	4

12. The membrane was washed with washing buffer and stripped with stripping buffer for 15 minutes.

13. After washing with washing buffer, 3 times à 10 minutes, primary antibody for endogenous control analysis was added and the protocol repeated starting at step 7.

3.2.5 Trans-Epithelial Electrical Resistance

For TEER measurement, CaCo2 cells were grown on 24 well transwell plates for 21 days.

1. Before usage, measure chamber (6 mm Culture Cup, World Precious Instruments; ENDOHM-6) was disinfected using microzid. Complete medium was

filled in chamber until meniscus in measure chamber levelled meniscus of medium in inserted transwell.

2. Baseline TEER of each transwell insert was measured three times with epithelial volt-ohm-meter EVOM2 (World Precious Instruments) and mean values were calculated.
3. Cells were stimulated on basolateral side with 100 nM S1P, 500 nM S1P, vehicle control, or remained unstimulated. Stimulation was performed in duplicates.
4. TEER was measured after 1, 2, 4, 6, 8, 10, 24, 26, 28, and 30 hours. Per insert 3 measurements were done at each time point and mean values were used for further analysis.

3.2.6 Calcium Mobilization Assay

Experiments were performed according to Fluo-4 Direct protocol at room temperature. Cells plated on 96 well plates were used for experiments. Each stimulation was done in triplicates.

1. 10 ml Fluo-4 Direct calcium assay buffer was added to 1 bottle Fluo-4 calcium assay reagent, mixed and 3.25 ml aliquots were stored at -20 °C (Component A).
2. 1 ml Fluo-4 Direct calcium assay buffer was added to a vial containing 77 mg probenecid, mixed and stored at -20 °C (Component B).
3. 10 ml HBSS was mixed with 200 µl HEPES and stored at 4 °C (Component C)
4. 3.25 ml component A was mixed with 3.25 ml component C and 130 µl component B. The assay reagent was prewarmed at 37 °C for approx. 5 min.
5. In 96 well plates containing cells, cultivation medium was removed and 100 µl assay reagent per well was added.
6. Cells were incubated in dark for 30 min at 37 °C followed by 30 min at room temperature.
7. Plate was centrifuged at 400 x g for 5 min.
8. Plate was transferred to a TECAN Infinite Pro 300 machine and the fluorescence was measured with the following protocol:

Kinetic cycle

Duration	2 min
Kinetic interval	3 sec

Kinetic condition executive commands at cycle 5

Channel A	Injector
Volume	50 μ l
Speed	100 μ l/sec
Refill speed	100 μ l/sec
Refill mode	500 μ l

Fluorescence Intensity (well wise)

Excitation	490 nm
Emission	525 nm
Gain	160 manual
Number of flashes	25
Integration time	25 μ sec
Lag, settle time	0

9. After 12 seconds ligands were added using the injector:

- a. 1 x PBS
- b. Vehicle control (methanol+ 1 % BSA in 1 x PBS)
- c. 1 nM S1P final concentration in well
- d. 10 nM S1P final concentration in well
- e. 100 nM S1P final concentration in well
- f. 1000 nM S1P final concentration in well
- g. 1 μ M calcium ionophor final concentration in well

10. The changes in fluorescence were analysed with graph pad prism 5.

3.3 Statistics

Experiments were performed in three to four separate experiments. Significant outliers were determined with Grub's test.

To compare independent variables, one- or two-way analysis of variance with Bonferroni correction was performed in GraphPad Prism5. $P < 0.05$ was considered statistically significant.

For TEER measurements, the mean of the stimulation condition was calculated with Microsoft Excel 2013 for every experiment. To estimate the electrical resistance per cm^2 (Ωcm^2) the calculated average was inserted in the Formula:

$$\text{unit area resistance } (\Omega\text{cm}^2) = (\Omega * \pi * d^2) / 4$$

Ωmean measurement

πratio of a circle's circumference to its diameter

deffective diameter of cell culture insert

To calculate the difference in resistance ($\Delta\Omega\text{cm}^2$) over time, Ωcm^2 of time point 0 was subtracted from the other time points. Further analysis was performed with GraphPad Prism5.

In Calcium mobilization assays, the mean fluorescence for each condition at time point 0 was calculated with Excel 2013. The fluorescence of each stimulation condition was normalized in GraphPad Prism 5 to its mean. To calculate the changes over time, the mean of the normalized data was analysed in GraphPad.

Western blot pictures were analysed with Image Lab 5.2.1 of Bio Rad. The relative expression was calculated, compared to control and further analysed with GraphPad Prism5.

4. Results

4.1 Influence of Sphingosine-1-Phosphate on Intestinal Epithelial Cells

4.1.1 Expression of S1P Metabolizing Enzymes in Intestinal Epithelial Cells

To investigate whether or not IECs express S1P metabolizing enzymes, gene expression analysis of SphKs and SGPL was performed in CaCo2 cells. Relative mRNA expression levels show that CaCo2 cells express SGPL (average Ct 24.656) (Fig 4 A) as well as SphK2 (average Ct 26.824) and lower levels of SphK1 (average Ct 30.114) mRNA (Fig 4 B).

To determine if the presence of basolateral S1P alters gene expression of its metabolizing enzymes, CaCo2 monolayers were stimulated with S1P for 30 min, 2 and 4 hours. Neither SGPL (Fig 4 C) nor SphK1 (Fig 4 D) and SphK2 (Fig 4 E) expression were significantly changed over time compared to vehicle control stimulated cells.

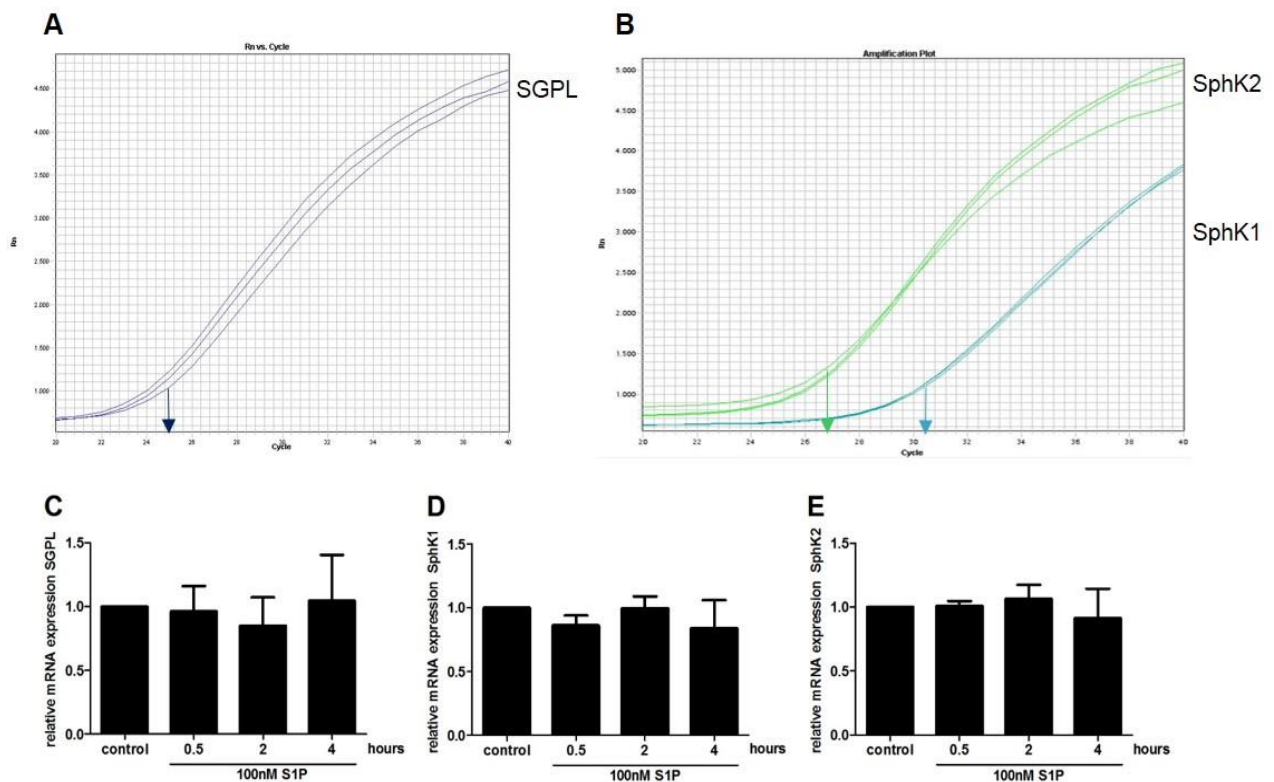


Figure 4: Relative mRNA expression of S1P lyase (SGPL) and sphingosine kinases (SphKs) in CaCo2 cells. Fully differentiated and FCS-deprived CaCo2 cells were stimulated basolaterally with vehicle control or 100 nM S1P for 30 min, 2 or 4 hours. Analysis of quantitative real-time PCR data shows expression of (A) SGPL and (B) SphKs mRNAs. (A-B): Data represents one of four separate experiments. (C-E): Data from four experiments (mean \pm SEM) are presented as fold change in comparison with vehicle control.

To determine if other cell signal proteins could influence gene expression of SphKs and consequently S1P production, CaCo2 monolayers were stimulated basolaterally with TNF α . Consistently with previous experiments, vehicle control stimulated cells showed high expression of SphK2 (average Ct 29.268) and low expression of SphK1 (average Ct 32.261) (Fig 5 A, B). SphK1 levels did not change after stimulation with TNF α (data not shown), and in western blot analysis SphK1 could not be detected (Fig 5 E, F). However, SphK2 gene expression was down-regulated over time when cells were stimulated with 100 ng/ml TNF α (Fig 5 C) or 250 ng/ml TNF α (Fig 5 D), respectively. This effect could be confirmed on protein-level when cells were stimulated with 250 ng/ml TNF α (Fig 5 H, J), but not with 100 ng/ml (Fig 5 G, I).

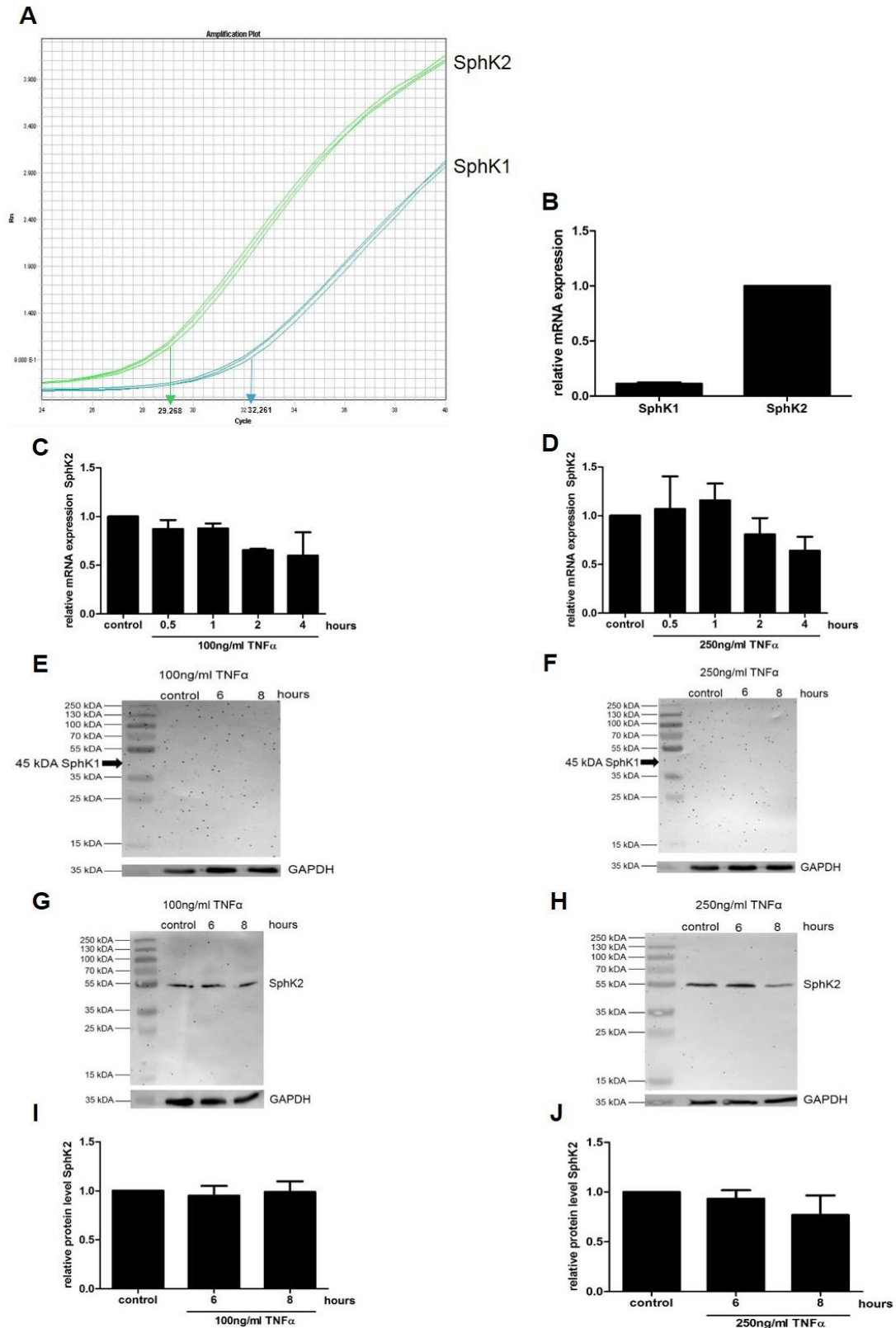


Figure 5: Effect of TNF α stimulation on SphK mRNA expression. Fully differentiated and FCS-deprived CaCo2 cells were stimulated basolaterally with vehicle control, 100 ng/ml or 250 ng/ml TNF α . Cells were stimulated for 30 min, 1, 2 or 4 hours and quantitative real-time PCR was performed to evaluate the relative mRNA expression levels of SphK1 and SphK2 (A, B) as well as the changes in expression over time (C, D). Cells were stimulated basolaterally with vehicle control, 100 ng/ml or 250 ng/ml TNF α for 6 and 8 hours to determine protein expression of SphK1 (E, F) and SphK2 (G, H) in Western Blot experiments. Protein levels were quantified against GAPDH to determine changes over time (I, J). Data from three experiments (mean \pm SEM) are presented as fold change in comparison with vehicle control.

4.1.2 Influence of S1P Signalling on Cytokine and Tight Junction Expression

To explore if CaCo2 cells express S1P receptors, qRT-PCR was performed. CaCo2 cells showed expression of S1P2 (average Ct 29.405) and low expression of S1P3 (average Ct value 34.070) whereas S1P1, S1P4, and S1P5 were not expressed (Fig 6 A, B).

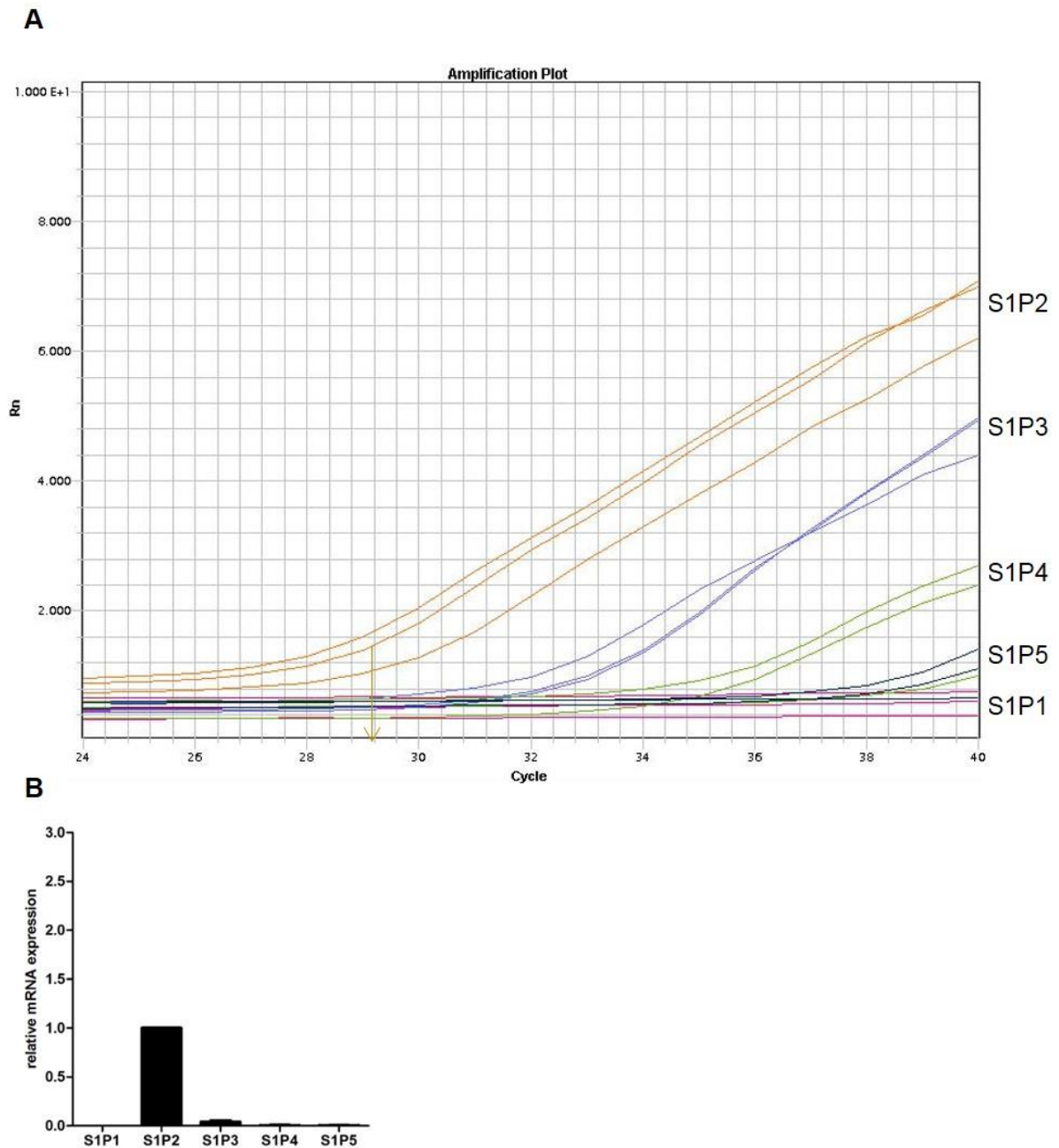


Figure 6: Expression of S1P receptors in CaCo2 cells: (A) mRNA levels of S1P receptors of fully differentiated and FCS-deprived CaCo2 cells were quantified with qRT-PCR and (B) analysed relative to S1P2. Data of four experiments (mean±SEM) represent fold changes of relative mRNA expression.

Calcium release assays were performed to analyse the possibility that apical S1P induces signalling in IECs via S1P receptors. PBS stimulation was used as mock treatment of unstimulated cells and vehicle control stimulation as baseline. Furthermore, calcium ionophor was used as positive control since it leads to the complete release of internally stored calcium. Measurement of fluorescence signals over time showed no difference between cells stimulated with PBS, vehicle control or different concentrations of S1P (Fig 7) However, stimulation with calcium ionophor induced elevated fluorescence levels (Fig 7).

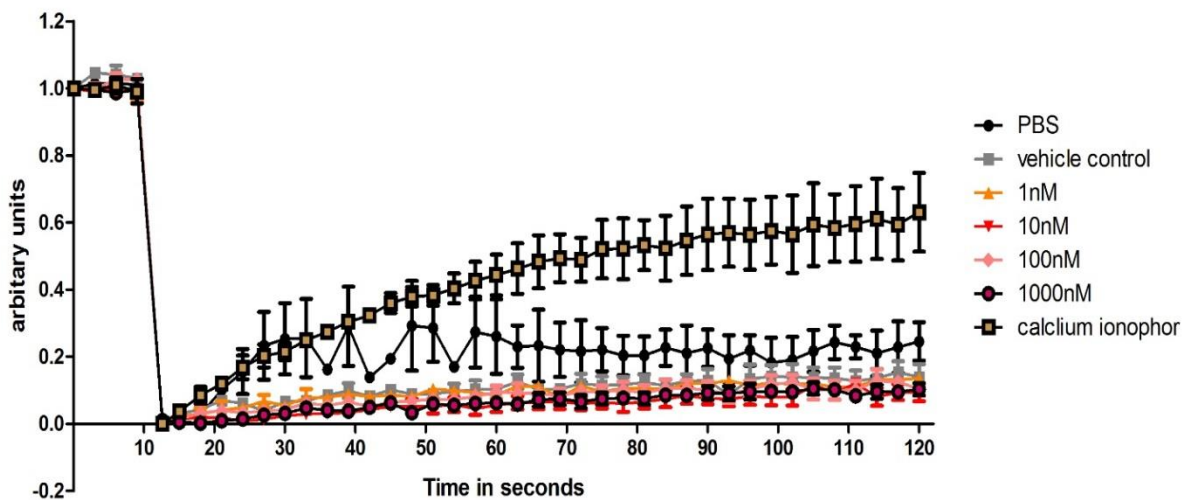


Figure 7: Effect of apical S1P stimulation on calcium release over time. 21 day old FCS-deprived CaCo2 monolayers were stimulated apically with either PBS (●), vehicle control (■), S1P (1nM ▲, 10nM ▼, 100nM ◆, 1000nM ●) or positive control (calcium ionophor ■). Changes in fluorescence were measured for 12 seconds before and 108 seconds after stimulation. Data from three experiments (mean±SEM) represent changes fluorescence.

To investigate if IECs respond to basolateral S1P, CaCo2 cell monolayers were stimulated with 100 nM and 500 nM S1P, respectively. In addition, JTE-013, a specific S1P2 antagonist, was used to determine whether or not S1P2 is involved in signalling. Cells stimulated with vehicle control were used to determine baseline expression. Stimulation with 100 nM S1P (Fig 8 A), and 500 nM S1P did not alter S1P2 levels (Fig 8 B black bars) compared to control. Incubation with JTE-013 prior to S1P stimulation did not significantly alter S1P2 mRNA expression (Fig 8 B white bars).

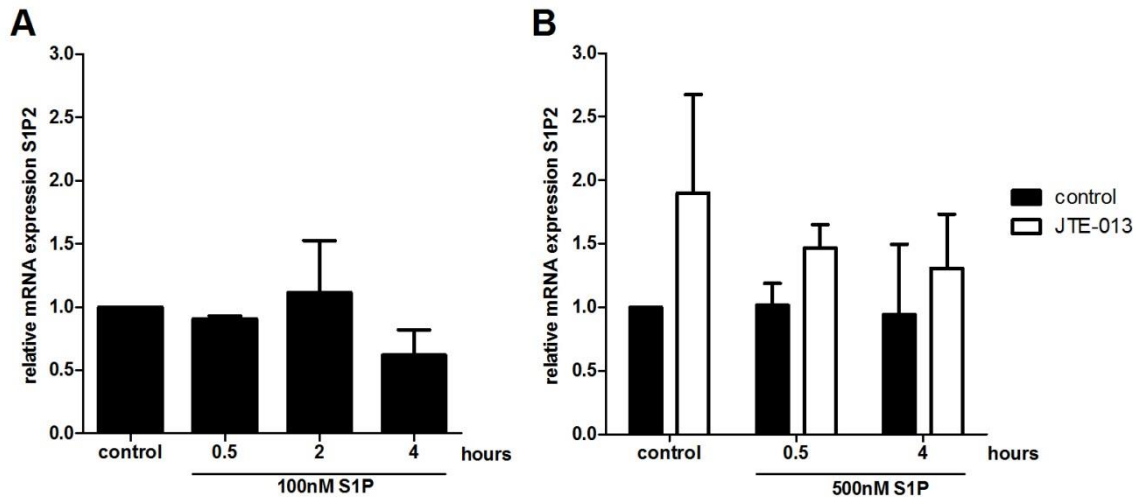
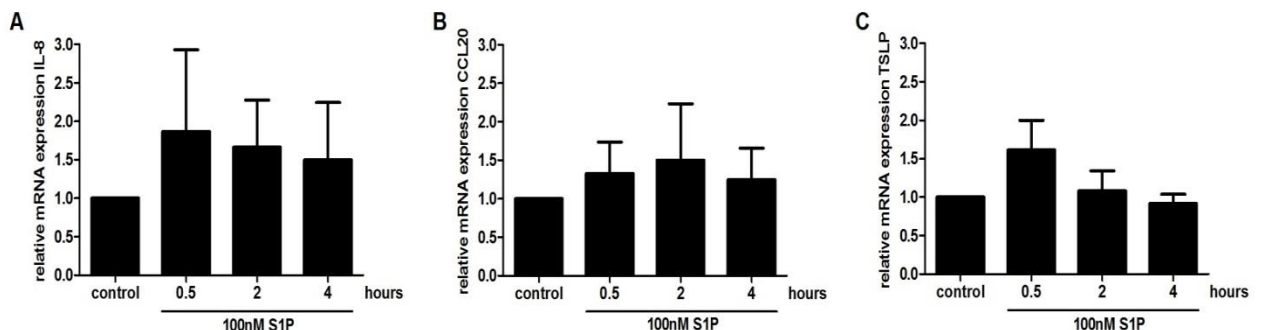


Figure 8: Changes in S1P2 expression after S1P stimulation. Fully differentiated and FCS-deprived CaCo2 cells were stimulated basolaterally with vehicle control and (A) 100 nM S1P or (B) 500 nM S1P for 30 min, 2 and 4 hours with and without 1 μ M JTE-013 pre-treatment. Changes in S1P2 receptor mRNA expression after stimulation were quantified with qRT-PCR. Data from four experiments (mean \pm SEM) are represented as fold change relative to vehicle control.

To determine if expression of pro- or anti-inflammatory cytokines is regulated by S1P, CaCo2 monolayers were stimulated with 100 nM S1P on the basolateral side. The pro-inflammatory cytokines IL-4 and IL-5, mainly found in Th2 mediated allergic reactions, INF γ and RANTES as well as the anti-inflammatory cytokine IL-10 were not expressed, neither in unstimulated CaCo2 cells nor in cells stimulated with S1P (data not shown). However, expression of IL-8 showed a slight, but not significant increase after stimulation with 100 nM S1P (Fig 9 A). Furthermore, CCL20 levels, which are important for the formation and function of mucosal lymphoid tissue, were increased in cells stimulated with 100 nM S1P stimulated cells compared to control (Fig 9 B). This increase, however, was not statistically significant; the same was true for the pro-inflammatory cytokine TSLP (Fig



9 C).

Figure 9: Changes in relative cytokine mRNA expression after basolateral stimulation with 100 nM S1P. FCS-deprived CaCo2 monolayers cultured for 21 days on transwells were stimulated basolaterally with vehicle control or 100 nM S1P for 30 min, 2 and 4 hours. Quantitative real-time PCR was performed to evaluate the changes in relative mRNA expression levels of (A) IL-8, (B) CCL20 and (C) TSLP over time. Relative cytokine

mRNA expression levels of four experiments (mean±SEM) are represented as fold change in comparison to vehicle control.

To explore if S1P is not only able to alter the cytokine expression but also regulates the barrier integrity of IECs, TEER measurements were conducted. Overtime an increase of TEER (Fig 9 A) in untreated (Fig 10 A \blackrightarrow), vehicle control (Fig 10 A \blackrightarrow), 100 nM S1P (Fig 10 A \blackrightarrow) and 500 nM S1P (Fig 10 A \blackrightarrow) stimulated cells could be observed. Relative quantification of the data showed that basolateral treatment with 500 nM S1P resulted in significantly elevated TEER levels after 10, 26, 28 and 30 hours (Fig 10 B black bars), whereas stimulation with 100 nM S1P caused an increase in TEER levels that was not statistically significant (Fig 10 B white bars).

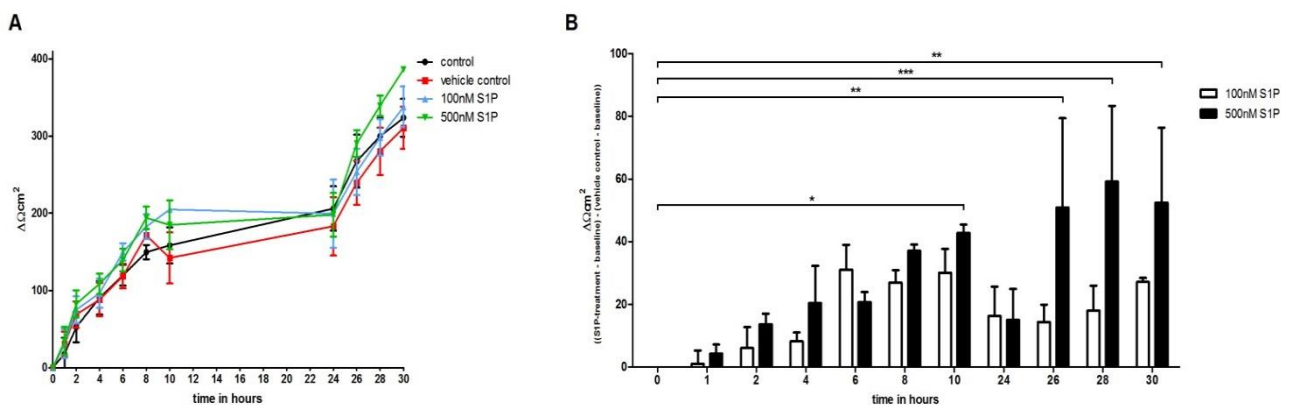


Figure 10: S1P enhances trans-epithelial electrical resistance over time. Fully differentiated FCS-deprived CaCo2 monolayers remained either untreated (control \blackrightarrow) or were stimulated basolaterally with vehicle control (\blackrightarrow), 100 nM (\blackrightarrow) or 500 nM (\blackrightarrow) S1P. Data from three experiments (mean±SEM) are expressed as (A) delta TEER over time for 30 hours in 2 hour intervals and (B) as relative changes after S1P (100 nM or 500 nM) treatment. Significance was calculated with 2-way ANOVA with Bonferroni correction for multiple comparison. *P<0.05, **P<0.01, ***P<0.001

Correspondingly, stimulation of CaCo2 cells with 100 nM S1P caused regulation of claudin-1 (Fig 11 A), claudin-4 (Fig 11 C), ZO-1 (Fig 11 G) and ZO-2 (Fig 11 I) mRNA. Occludin mRNA expression was not regulated by 100 nM S1P stimulation (Fig 11 E). Contradicting the enhanced TEER levels, stimulation of cell monolayers with 500 nM S1P did not alter gene expression of TJ proteins (Fig 11 B, D, F, H, J black bars). However, in cells pre-treated with JTE-013, elevated claudin-1 (Fig 11 B white bar), occludin (Fig 11 F white bar) and ZO-2 (Fig 11 J white bar) levels could be detected after 30 min S1P stimulation (500 nM). Additionally, 4 hours stimulation with 500 nM S1P after JTE-013 pre-treatment resulted in higher ZO-1 levels compared to control cells (Fig 11 H white bar). Only claudin-4 expression levels were not influenced by pre-treatment of cells with JTE-013 (Fig 11 D white bars).

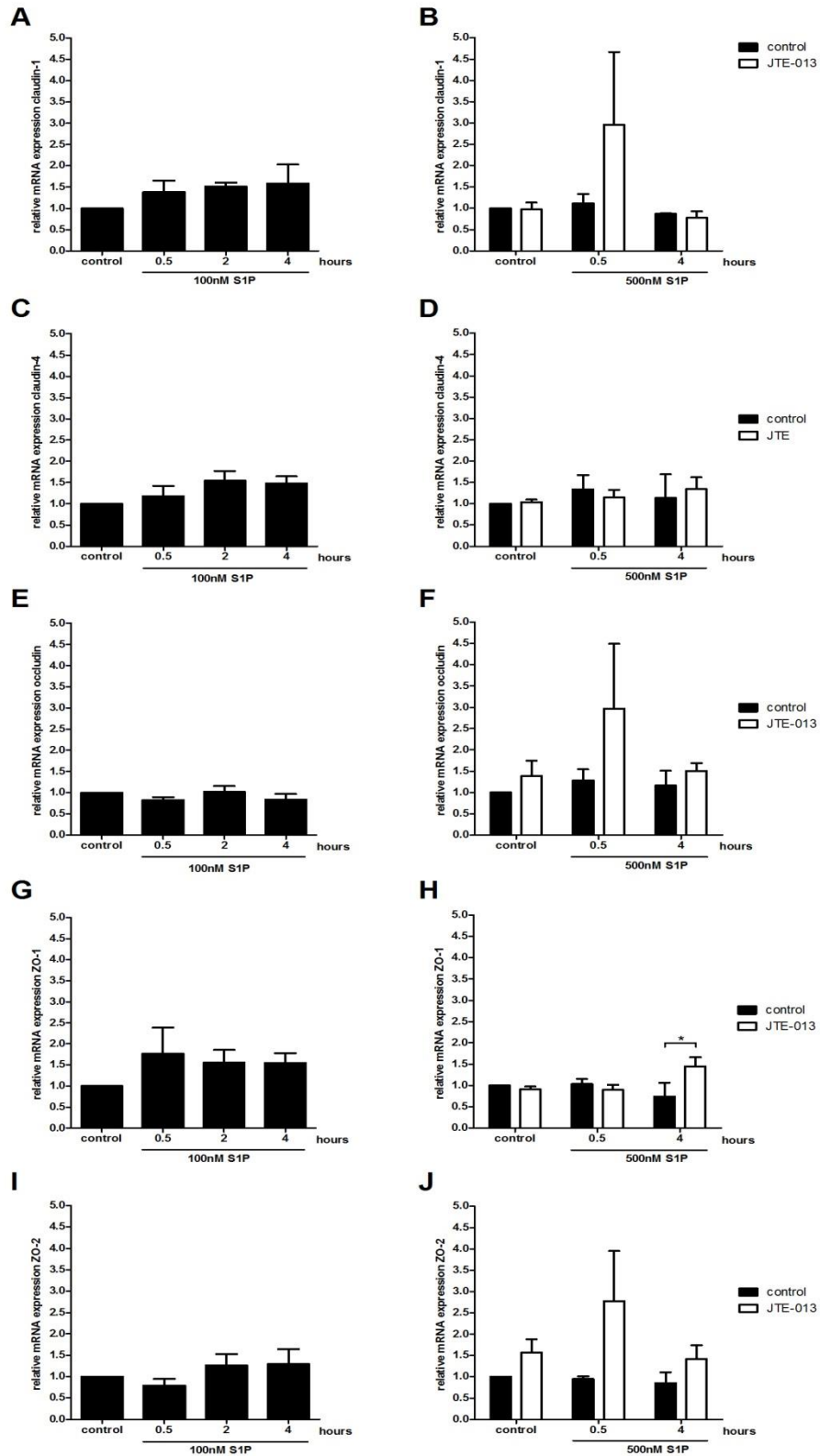


Figure 11: S1P regulates tight junction protein mRNA expression in CaCo2 cells. Fully differentiated FCS-depleted CaCo2 cells were stimulated basolaterally (A, C, E, G, I) with vehicle control and 100 nM for 30 min, 2 or 4 hours and (B, D, F, H, J) with 500 nM (back bar) or 1 μ M JTE prior to 500 nM S1P (white bar) for 30 min or 4h. Data represents changes in relative mRNA expression of, claudin-1 (A, B), claudin-4 (C, D), occludin (E, F) zonula occludens-1 (G, H) and zonula occludens-2 (I, J) of four experiments (mean \pm SEM). Significance was calculated with one-way ANOVA as well as two-way ANOVA with Bonferroni correction for multiple comparison. *P<0.05

4.2 Effect of Poly-(D, L-lactide-co-glycolide) Microparticles on Intestinal Epithelial Cells

4.2.1 Influence of Targeted and Coated Microparticle Treatment on Cytokine Expression

To investigate whether oral application of poly (D,L-lactide-co-glycolide) (PLGA) microparticles (MPs) loaded with OVA and coated with neuraminidase of *vibrio cholera* (NA), aleuria aurantia lectin (AAL) or wheat germ agglutinin (WGA) influences IECs to induce cytokine production (Fig 12-15), mRNA expression analysis after apical stimulation was performed. Untreated CaCo2 cells were used as control to determine baseline expression. Cells were stimulated with coating substances (AAL, NA and WGA) alone to investigate their influence on cytokine expression as well as to determine if the changes after MPs stimulation are related to them. Furthermore, OVA alone was used to investigate the effect of the allergen alone on CaCo2 cells. Cytokines associated with allergy IL-4, IL-5, IL-13, the pro-inflammatory cytokine INF γ as well as the regulatory cytokine IL-10 was neither expressed in unstimulated nor in stimulated cells (data not shown).

Analysis of IL-8 levels revealed that incubation with NA is able to induce IL-8 expression. A significant induction of IL-8 overtime with an increase until 3 hours after stimulation could be observed (Fig 12 A, E). Furthermore, IL-8 levels were significantly higher after 3 hours compared to stimulation with other coating substances or OVA alone (Fig 12 A). This upregulating effect of IL-8 mRNA expression after NA stimulation could also be seen in comparison to cells stimulated with OVA (Fig 12 E). Additionally, cells stimulated with NA-MPs revealed increasing IL-8 levels over time again with the highest peak after 3 hours (Fig 12 B, D). AAL stimulation resulted in increased IL-8 mRNA levels after 2 hours of stimulation, but no further regulation thereafter (Fig 12 C). Moreover, AAL-MP also resulted in elevated IL-8 levels after 2 hours of stimulation compared to Plain-MPs (Fig 12 D). Treatment with WGA resulted in significant upregulation of IL-8 expression after 3 hours of stimulation (Fig 12 G). In contrast IL-8 mRNA expression levels were significantly stronger regulated if CaCo2 cells were stimulated for 3 hours with Plain-MP compared to WGA-MPs (Fig 12 H).

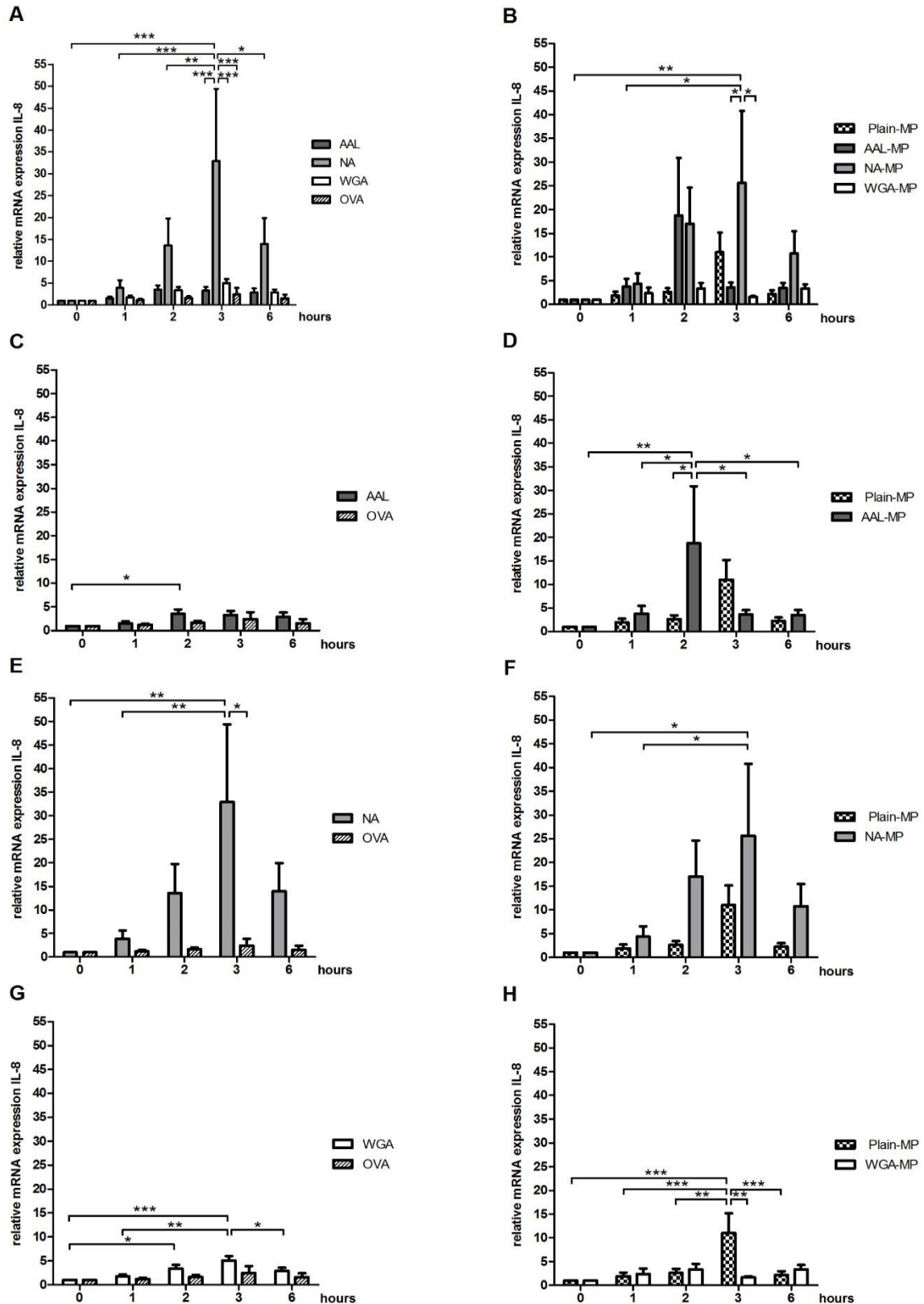


Figure 12: Effect of allergen loaded targeted microparticle stimulation on IL-8 mRNA expression. Fully differentiated CaCo2 cells were stimulated with (A, C, E, G) AAL (■), NA (▒), WGA (□) or OVA (▨) for 0,1,2,3 or 6 hours or (B, D, F, H) allergen loaded MPs, Plain-MP (▩), coated with AAL-MP (■), NA-MP (▒) or WGA-MP (□) for 0,1,2,3 or 6 hours. Data represent fold change of relative IL-8 mRNA expression of four experiments (mean±SEM) compared to unstimulated control cells. Significance was calculated with two-way ANOVA with Bonferroni correction for multiple comparison. *P<0.05, **P<0.01, ***P<0.001.

Stimulation of CaCo2 cells with NA for 3 hours resulted in significant induction of CCL20 expression (Fig 13 A, E). Furthermore, NA-MPs incubation increased CCL-20 levels over time with the highest peak after 6 hours of stimulation compared to CaCo2 cells stimulated with Plain-MPs, AAL-MPs or WGA-MPs (Fig 13 B). AAL (Fig 13 C) and WGA (Fig 13 G) treatment was not able to change CCL-20 mRNA levels. Compared to this, treatment with OVA alone resulted in enhanced CCL20 expression after 3 hours of treatment (Fig 13 C, G). Furthermore, treatment of CaCo2 cells with Plain-MPs resulted in higher levels of CCL20 after 3 hours compared to treatment with AAL-MPs (Fig13 D). In contrast to WGA, WGA-MPs raised CCL20 levels significantly after 6 hours of treatment compared to Plain-MP (Fig 13 H).

The pro-inflammatory cytokine RANTES was significantly upregulated after 2 hours of AAL treatment in comparison with NA or OVA stimulation (Fig 14 A). However, the observed changes in RANTES mRNA expression after AAL treatment were not significant compared to OVA stimulation (Fig 14 C). Moreover, incubation with NA (Fig 14 E) or WGA (Fig 14 G) did not induce changed RANTES expression levels. Treatment of cells with Plain-MPs resulted in elevated RANTES levels after 3 hours of stimulation compared to treatment with coated MPs (Fig 14 B). Neither AAL-MPs (Fig 14 D) nor WGA-MPs (Fig 14 H) induced significantly changed RANTES expression when compared to stimulation with Plain-MP. However, 6 hours of treatment with NA-MPs resulted in significant upregulation of RANTES levels (Fig 14 F).

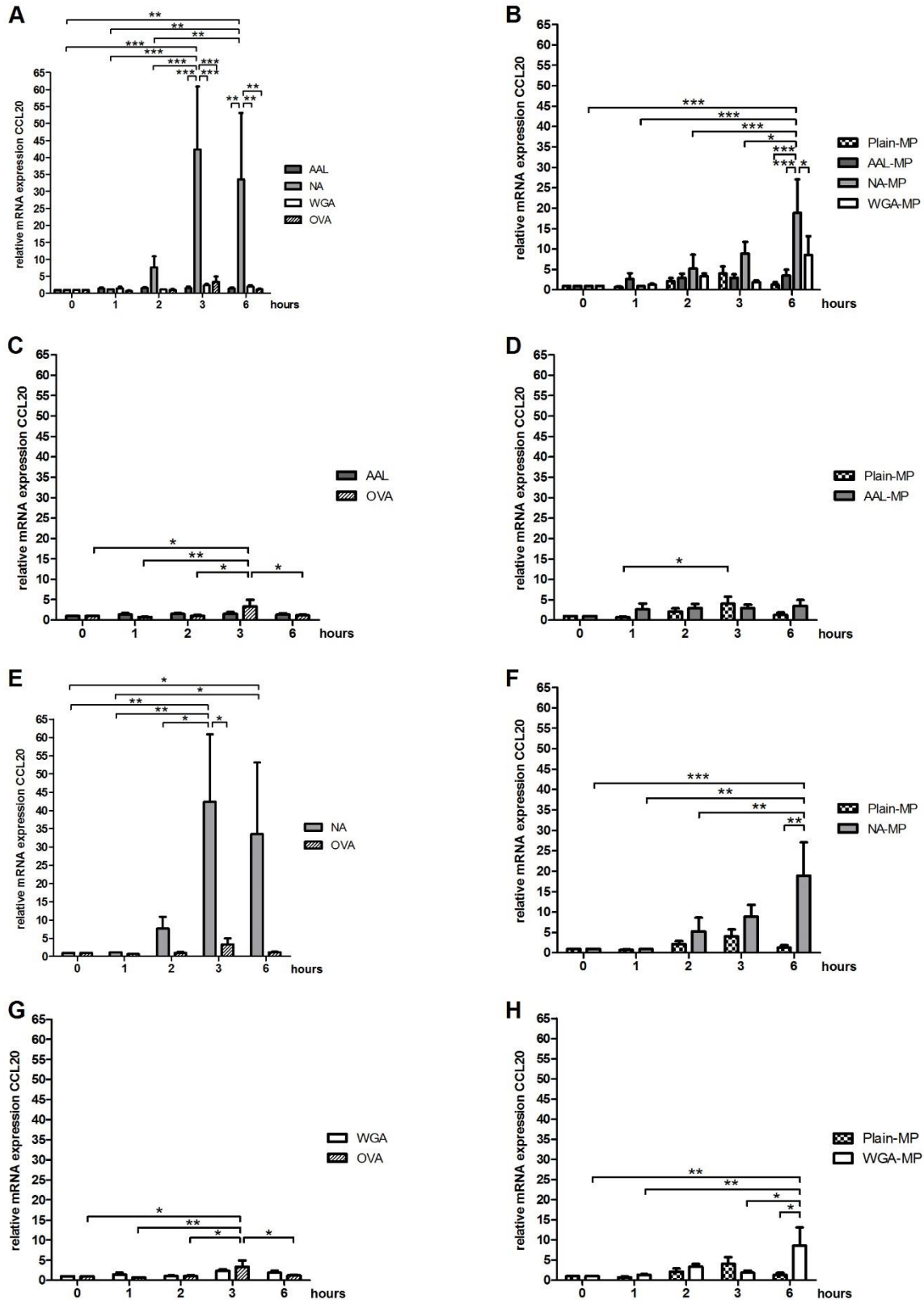


Figure 13: Influence of microparticle stimulation on CCL20 mRNA expression. CaCo2 monolayers cultivated for 21 days were either stimulated with (A, C, E, G) AAL (■), NA (■), WGA (□) or OVA (▨) for 0,1,2,3 or 6 hours or (B, D, F, H) allergen loaded MPs, Plain-MP (▩), targeted with AAL-MP (■), NA-MP (■) or WGA-MP (□) for 0,1,2,3 or 6 hours. Data represent fold change of relative CCL20 mRNA expression of four experiments (mean±SEM) compared to unstimulated control cells. Significance was calculated with two-way ANOVA with Bonferroni correction for multiple comparison. *P<0.05, **P<0.01, ***P<0.001.

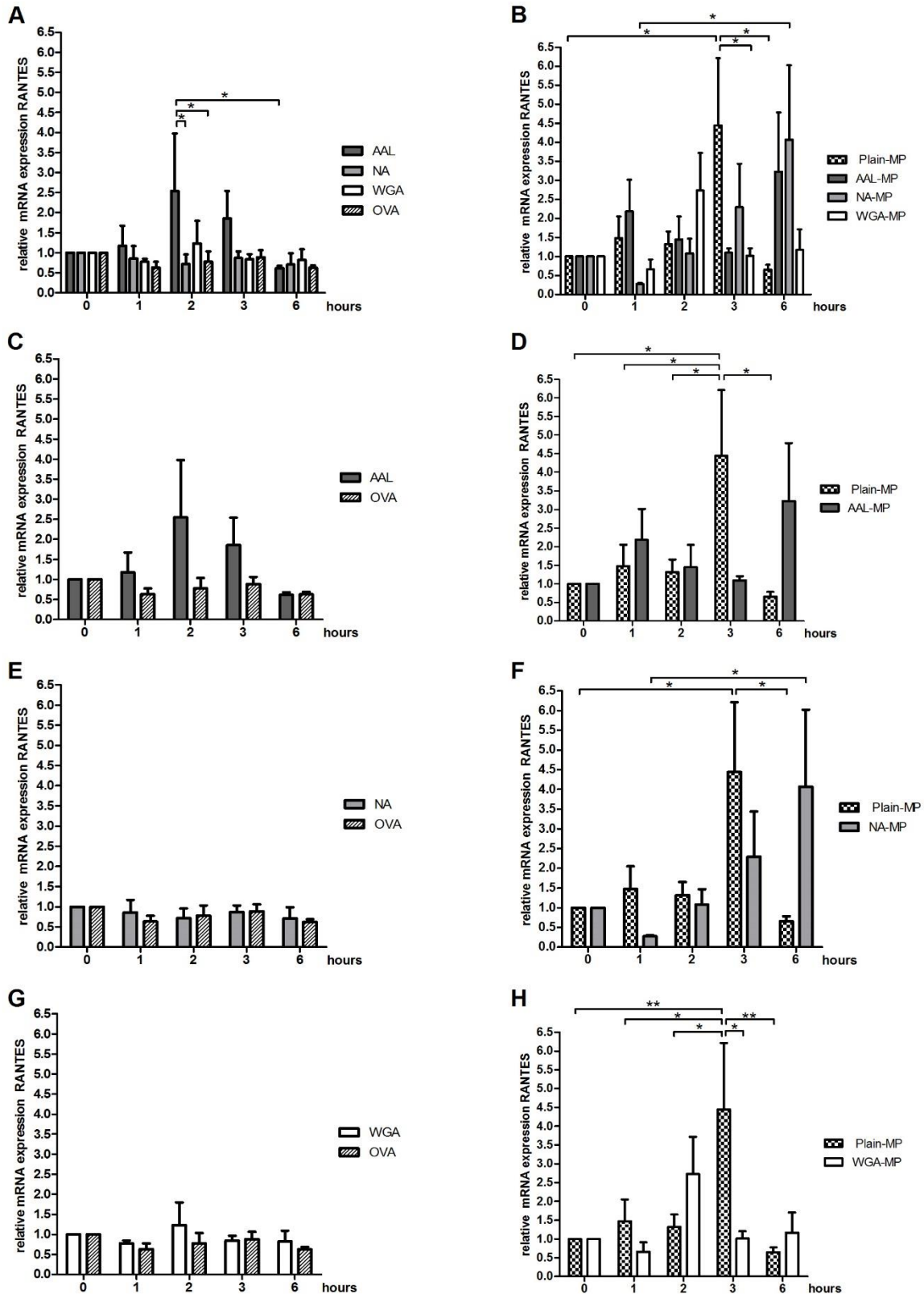


Figure 14: Changes in RANTES mRNA expression after microparticle treatment. Fully differentiated CaCo2 cells were either stimulated with (A, C, E, G) AAL (■), NA (■) WGA (□) or OVA (▨) for 0,1,2,3 or 6 hours or (B, D, F, H) allergen loaded MPs, Plain-MP (▩), targeted with AAL-MP (■), NA-MP (■) or WGA-MP (□) for 0,1,2,3 or 6 hours. Data represent fold change of relative RANTES mRNA expression of four experiments (mean±SEM) compared to unstimulated control cells. Significance was calculated with two-way ANOVA with Bonferroni correction for multiple comparison. *P<0.05, **P<0.01, ***P<0.001.

TSLP expression levels were neither significantly changed by treatment with AAL, NA, WGA nor OVA (Fig 15 A). Moreover, AAL (Fig 15 C) and WGA (Fig 15 G) treatment did not result in any significant TSLP level changes compared to stimulation with OVA alone. However, stimulation with NA resulted in significant induction of TSLP after 3 hours of incubation compared to OVA treatment (Fig 15 E). Incubation with AAL-MPs resulted in increased TSLP levels after 2 hours compared to other MPs treatments (Fig 15 B). Compared to Plain-MPs treatment, incubation with AAL-MPs did not induce significant changes in TSLP expression (Fig15 D). Furthermore, NA-MPs treatment was not able to change TSLP levels significantly compared to Plain-MPs (Fig 15 F). Treatment with WGA-MPs for 2 hours resulted in significantly higher TSLP levels compared to Plain-MPs (Fig 15 H), whereas Plain-MPs induced stronger TSLP expression in intestinal epithelial cells compared to WGA-MPs stimulation (Fig 15 H).

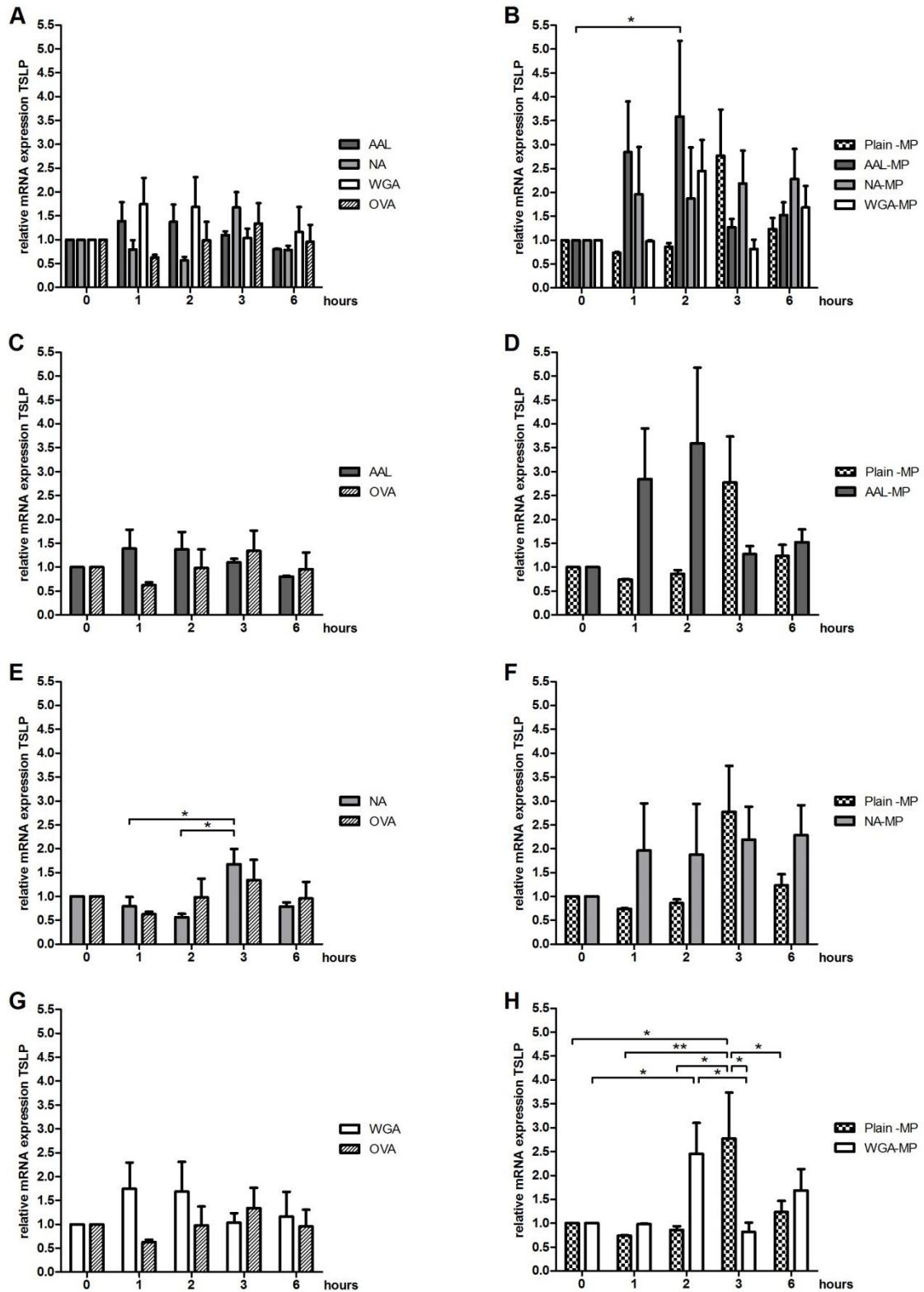


Figure 15: Influence of microparticle treatment on mRNA expression levels of TSLP. CaCo2 monolayers were stimulated with (A, C, E, G) AAL (■), NA (■), WGA (□) or OVA (▨) for 0,1,2,3 or (B, D, F, H) 6 hours or allergen loaded MPs, Plain-MP (▤), targeted with AAL-MP (■), NA-MP (■) or WGA-MP (□) for 0,1,2,3 or 6 hours. Data represent fold change of relative TSLP mRNA expression of four experiments (mean±SEM) compared to unstimulated control cells. Significance was calculated with two-way ANOVA with Bonferroni correction for multiple comparison. *P<0.05, **P<0.01.

4.2.2 Effect of Particle Stimulation on Tight Junction Formation of Intestinal Epithelial Cells

Since we observed induction of cytokine mRNA upon stimulation with coating substances as well as coated or uncoated allergen loaded MPs, we further aimed to evaluate TJ formation of IECs on mRNA levels. Again untreated cells (0) were used to evaluate baseline expression levels.

Neither AAL, NA, WGA nor OVA were able to induce significant changes in claudin-1 mRNA expression levels over time in stimulate CaCo2 cells (Fig 16 A, C, E, G). Although Plain-MP stimulation drastically induced claudin-1 levels after 6 hours compared to other stimulants (Fig 16 B), this effect could not be observed when compared to AAL-MP (Fig 16 D) or NA-MP (Fig 16 F), respectively. Furthermore, stimulation with WGA-MP did not alter claudin-1 expression levels significantly compared to Plain-MP stimulation (Fig 16 H).

Stimulation of cells with WGA resulted in higher levels of claudin-4 expression over time compared to CaCo2 cells stimulated with OVA (Fig 17 G) or NA (Fig 17 A). However, WGA-MPs were not able to induce elevated expression levels of claudin-4 (Fig 17 H). Despite the fact that AAL stimulation induced higher claudin-4 levels (Fig 17 C), stimulation with AAL-MPs did not alter the expression significantly (Fig 17 D). Furthermore, OVA compared to AAL (Fig 17 C) or NA (Fig17 E) was able to induce elevated levels after 2 hours of stimulation. However, Plain-MP stimulation did not change expression levels (Fig 17 B, D, F, H). After 3 hours of stimulation, NA-MPs significantly enhanced expression levels of claudin-4 compared to Plain-MPs (Fig 17 F), AAL-MPs or WGA MPs (Fig 17 B).

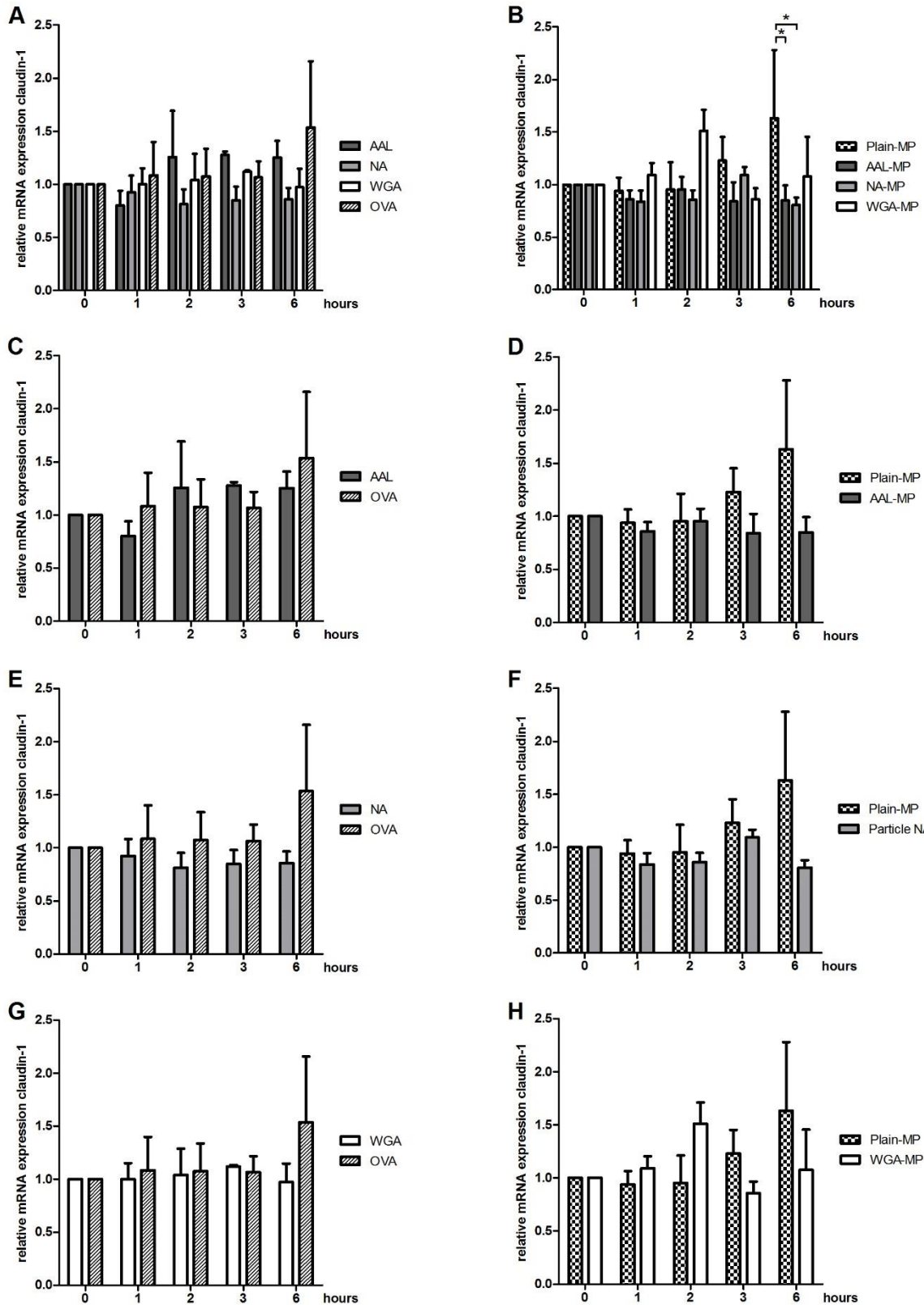


Figure 16: Changes in claudin-1 mRNA expression after particle stimulation. CaCo2 cells, cultured for 21 days were stimulated on the apical side with either (A, C, E, G) targeting substances, AAL (■), NA (■), WGA (□), OVA (▨) or (B, D, F, H) with allergen loaded MPs: Plain-MP (▨), AAL-MP (■), NA-MP (■) or WGA-MP (□) for 0,1,2,3, and 6 hours. Data represent fold change of relative claudin-1 mRNA expression of four experiments (mean±SEM) compared to unstimulated control cells. Significance was calculated with two-way ANOVA with Bonferroni correction for multiple comparison. *P<0.05, **P<0.01, ***P<0.001.

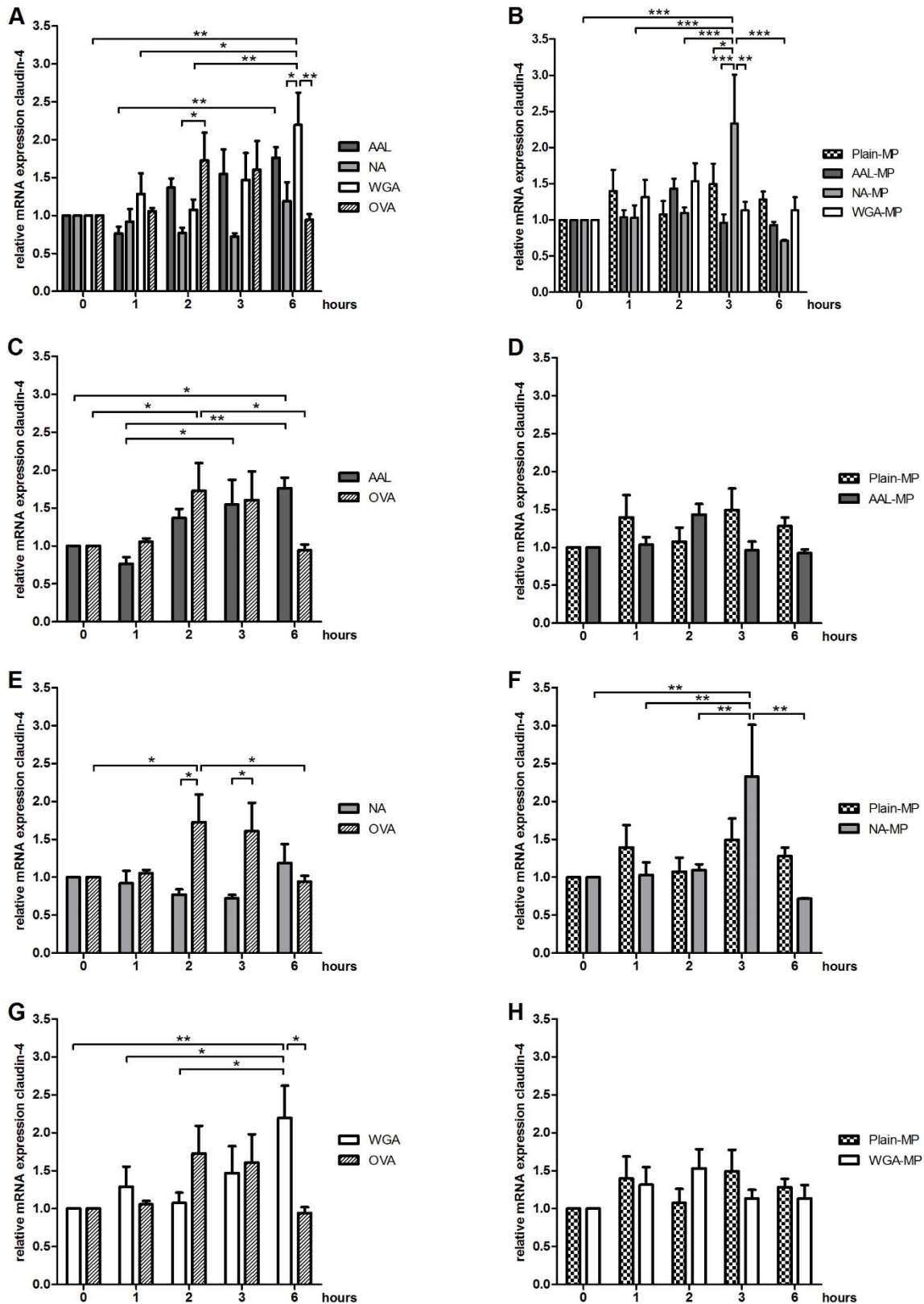


Figure 17: Effect of particle stimulation on mRNA expression of claudin-4. Fully differentiated CaCo2 monolayers were stimulated on the apical side with either (A, C, E, G) AAL (■), NA (■), WGA (□) or OVA (▨) or (B, D, F, H) with allergen loaded MPs: Plain-MP (▨), AAL-MP (■), NA-MP (■) or WGA-MP (□) for 0,1,2,3 and 6 hours. Data represent fold change of relative claudin-4 mRNA expression of four experiments (mean±SEM) compared to unstimulated control cells. Significance was calculated with two-way ANOVA with Bonferroni correction for multiple comparison. *P<0.05, **P<0.01, ***P<0.001.

Treatment of CaCo2 cells for 2 hours with AAL resulted in elevated occludin levels compared to NA, WGA or OVA stimulation (Fig 18 A, C). Neither NA (Fig 18 E) nor WGA (Fig 18 G) resulted in changes of occludin levels over time. Furthermore, 3 hours of stimulation with Plain-MP induced occludin expression levels (Fig 18 B), whereas AAL-MP (Fig 18 D), NA-MP (Fig 18 F) or WGA-MP (Fig 18 H) were not able to influence

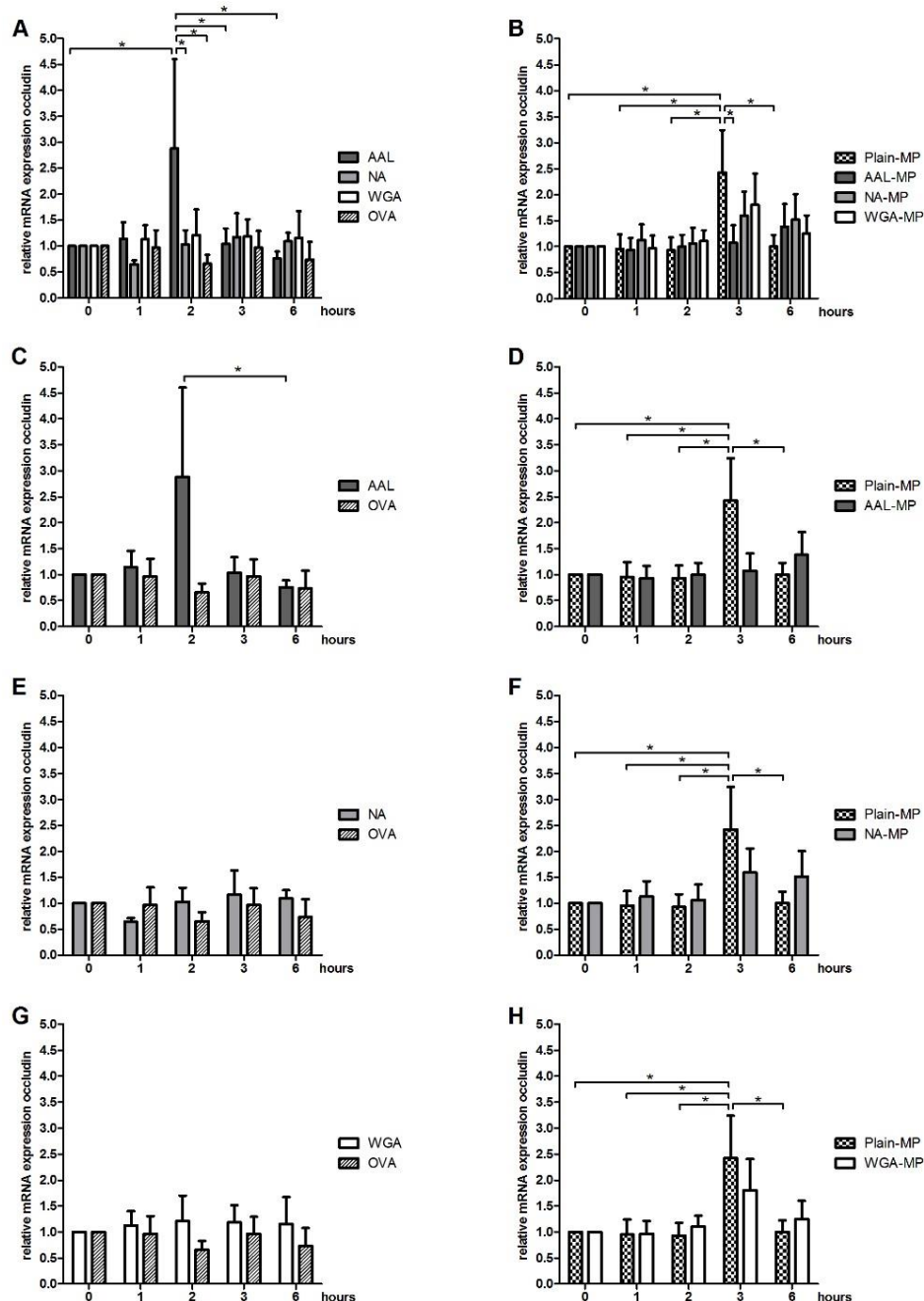


Figure 18: Influence of microparticle stimulation on occludin expression. CaCo2 monolayers cultivated for 21 days were either stimulated with (A, C, E, G) AAL (■), NA (■) WGA (■) or OVA (▨) for 0,1,2,3 or 6 hours or (B, D, F, H) allergen loaded MPs: Plain-MP (▨), AAL-MP (■), NA-MP (■) or WGA-MP (■) for 0,1,2,3 or 6 hours. Data represent fold change of relative occludin mRNA expression of four experiments (mean±SEM) compared to unstimulated control cells. Significance was calculated with two-way ANOVA with Bonferroni correction for multiple comparison. *P<0.05. **P<0.01. ***P<0.001

expression.

Stimulation with neither AAL (Fig 19 A, C), NA (Fig 19 A, E), WGA (Fig 19 A, G) nor OVA (Fig 19 A) was able to significantly alter ZO-1 expression levels in CaCo2 cells. Furthermore, stimulation with AAL-MP (Fig 19 B, D), NA-MP (Fig 19 B, F), WGA-MP (Fig 19 B, H) or Plain- MP (Fig 19 B) did not change ZO-1 levels over time either.

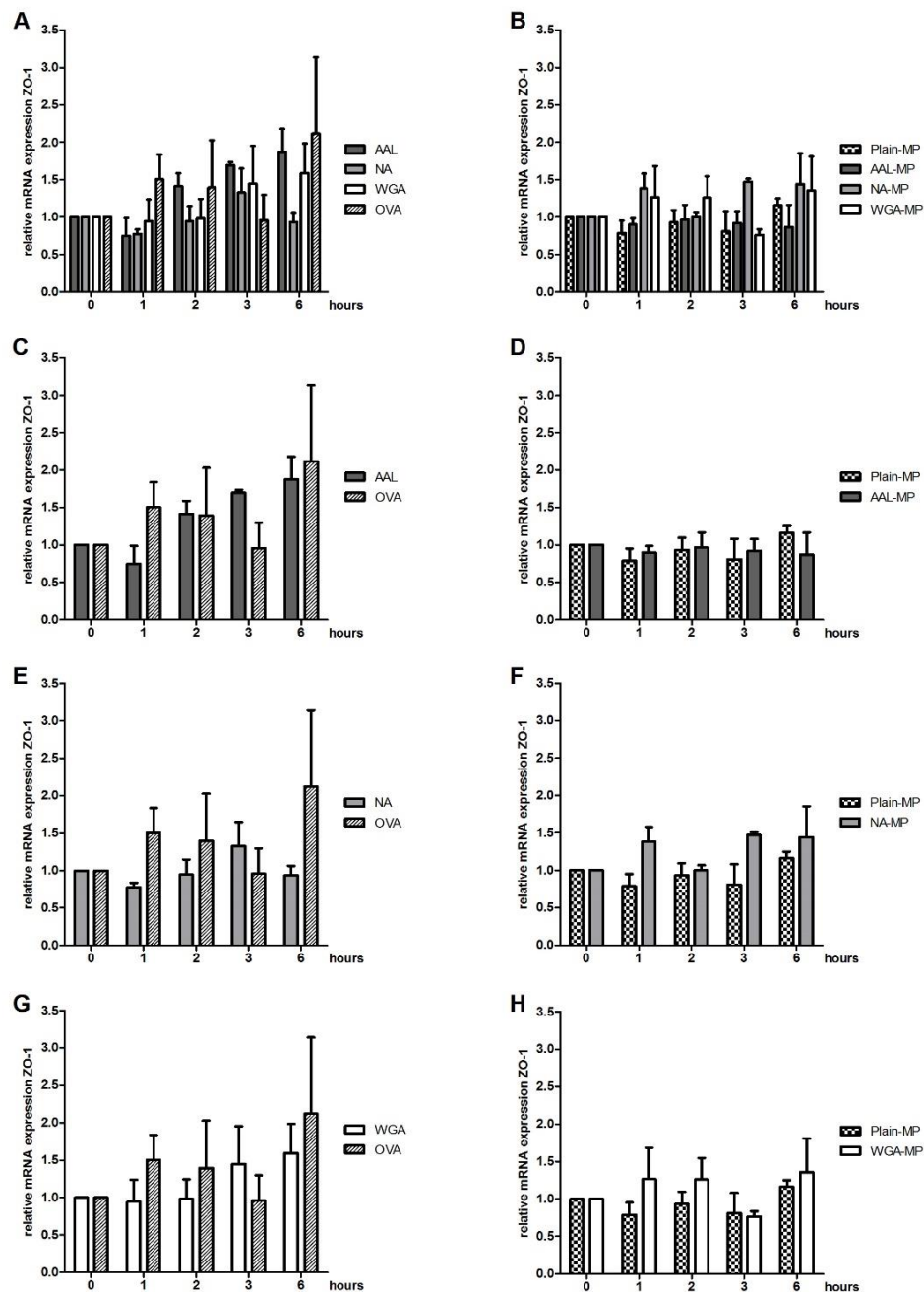


Figure 19: Changes in zonula occludens-1 mRNA expression after microparticle stimulation. Fully differentiated CaCo2 monolayers were stimulated for 0,1,2,3 or 6 hours with (A, C, E, G): AAL (■), NA (▒), WGA (□), OVA (▨) or (B, D, F, H) with allergen loaded MPs: Plain-MP (▩), AAL-MP (■), NA-MP (▒) or WGA-MP (□). Data represent fold change of relative ZO-1 mRNA expression of four experiments (mean±SEM) compared to unstimulated control cells. Significance was calculated with two-way ANOVA with Bonferroni correction for multiple comparison.

Analysis of ZO-2 expression showed no regulation through stimulation with AAL (Fig 20 A, C), NA (Fig 20 A, E), WGA (Fig 20 A, G) or OVA (Fig 20 A). Furthermore, AAL-MP (Fig 20 B, D), NA-MP (Fig 20 B, F) or Plain-MP (Fig 20 B) stimulation did not alter expression levels. However, 6 hours of stimulation with WGA-MPs resulted in significant elevated ZO-2 mRNA expression levels over time (Fig 20 H).

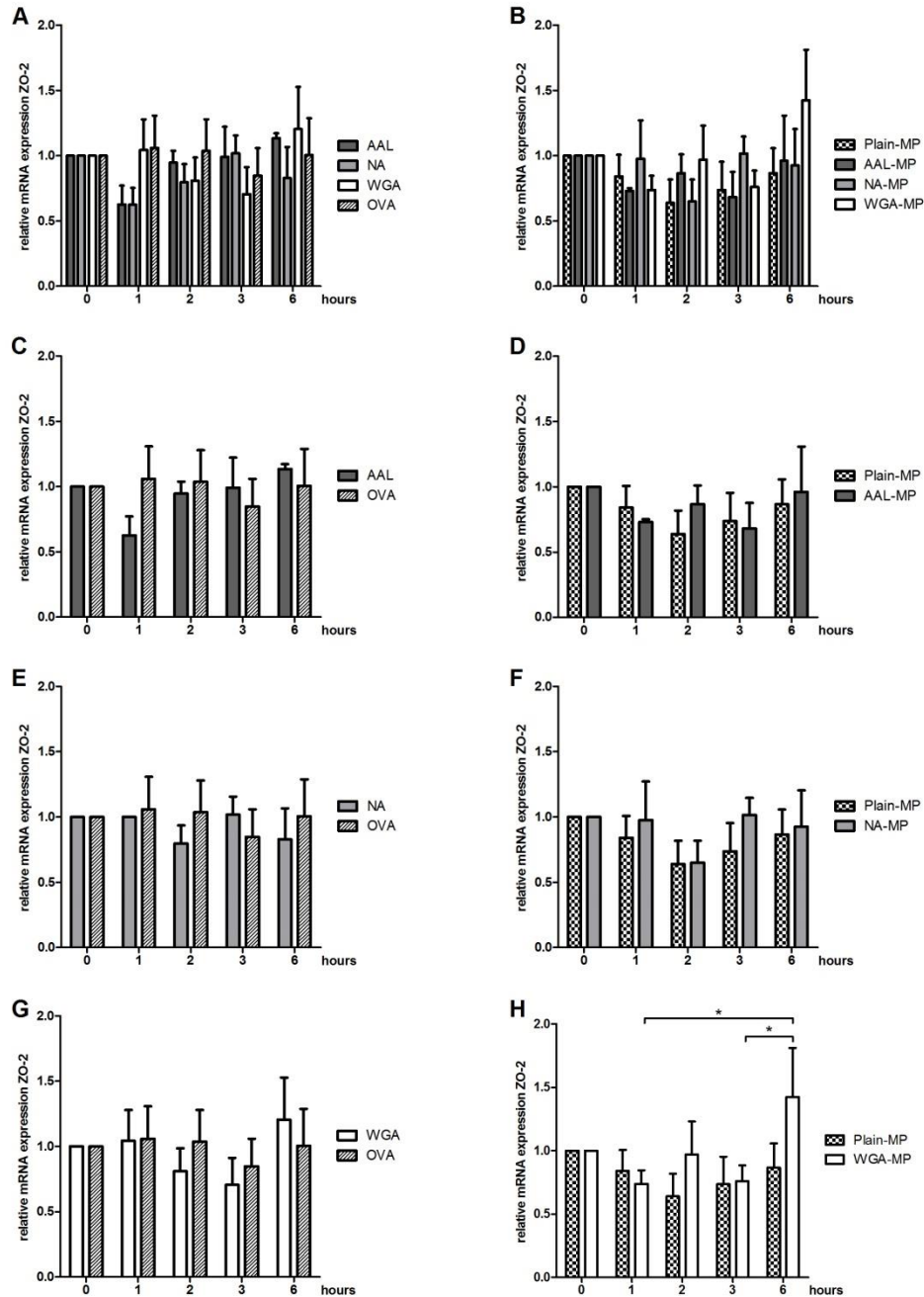


Figure 20: Changes in zonula occludens-2 protein expression after microparticle stimulation. Fully differentiated CaCo2 monolayers were stimulated for 0,1,2,3 or 6 hours with (A, C, E, G): AAL (■), NA (■), WGA (□), OVA (▨) or (B, D, F, H) with allergen loaded MPs: Plain-MP (▩), AAL-MP (■), NA-MP (■) or WGA-MP (□). Data represent fold change of relative ZO-2 mRNA expression of four experiments (mean±SEM) compared to unstimulated control cells. Significance was calculated with two-way ANOVA with Bonferroni correction for multiple comparison. *P<0.05

5. Discussion

The intestinal epithelium is the largest barrier of the human body which provides protection against environmental factors while maintaining tolerance towards commensal microbes and food derived antigens⁸⁵. In food allergies, impaired barrier function of the intestinal epithelium is found^{7,9,222}. A potent contributor to the establishment of allergic reactions is the bioactive lipid S1P, which is produced upon mast cell activation and released by degranulation²²³. Not much is known about the effect of S1P on the intestinal epithelium. The aim of this study was to investigate the influence of S1P on IECs as well as their possible contribution to the establishment of the S1P gradient between blood and tissue. Furthermore, we explored the effect of allergen loaded MPs on the barrier integrity of IECs as well as cytokine production to explore their options as novel treatment possibility for oral immunotherapy of food allergy.

The human colon carcinoma cell line CaCo2 is the most abundant cell line used for the *in vitro* study of the intestinal epithelium, since so far human IECs are not cultivable in their polarized form. CaCo2 cells acquire a small intestinal epithelial phenotype upon 21 days of cultivation, resulting in formation of a tight monolayer with an apical brush border as well as polarized cells^{224,225}. The formation of this functional monolayer is influenced by various culture conditions like the passage of the cell culture, seeding density and medium composition^{226–228}. To compare studies between laboratories, a highly standardized cultivation protocol is used, which we also applied for this thesis^{227,229,230}. Since CaCo2 cells differentiate into polarized enterocytes, they are widely used to predict drug absorption and intestinal permeability^{231–233}. Like in other *in vitro* models, CaCo2 culture studies have limitations. Even though the cells differentiate into a tight monolayer of small intestinal enterocytes, forming villi and crypt structures, no other contributor of the intestinal barrier is present. Therefore, a careful interpretation of the obtained results is necessary. Further studies such as co-culture experiments with mucus producing cells, immune cells or *in vivo* models are needed to allow for a reliable interpretation and elucidation of underlying mechanisms.

In a recent study using CaCo2 cells, peanut allergens were able to disrupt the monolayer by alterations of the TJ localisation¹³². Another study using CaCo2 cells and a food allergy mouse model revealed S1P as an important factor influencing the integrity of the intestinal epithelial barrier¹⁸⁸. This bioactive lipid is an important signalling molecule in allergic and other inflammatory reactions¹⁷⁹⁻¹⁸⁶. Through the expression of different S1P receptor subtypes on allergy effector cells, it is able to recruit Th2 lymphocytes as well as mast cells towards the side of inflammation^{195,196}. Since SphK1 of mast cells gets activated via FcεRI crosslinking, which results in the production of high S1P amounts as

well as the degranulation of mast cells, S1P is an important mediator in allergic reactions such as fibrosis, contraction of smooth muscle cells and vascular permeability^{172,173,179,181,183–185,234,235}. However, not much is known about the influence of S1P, its metabolizing enzymes or receptor expression on IECs.

Our study reveals that CaCo2 cells express SphK1 at low and SphK2 at higher levels, which allows the assumption that the cells are able to produce S1P from the degradation of food or membrane sphingolipids^{138,236,237}. Dietary sphingolipids, like sphingomyelin, are processed in the gut to sphingosine monomers and both delivered to and absorbed by the apical side of the small IECs^{238,239}. The presence of SphKs in small IECs provides them with the possibility to generate S1P and secrete it to regulate intestinal immune responses. This is consistent with studies showing the regulatory role of dietary sphingolipids and their metabolising enzymes on intestinal inflammation^{240–246}. In addition to the production of S1P by SphKs in CaCo2 cells, our data imply the possible degradation of S1P through the expressed SGPL. This provides evidence that IECs might contribute to the establishment of a S1P gradient and therefore are able to regulate the migration of lymphocytes and other effector cells in case of inflammation, as seen in other tissue cells which express SGPL²⁴⁷. Contrary to assumptions, the simulation of an inflammatory state with high mucosal S1P levels, basolateral S1P stimulation of CaCo2 cells did not influence the mRNA expression of the metabolizing enzymes. However, we neither investigated the protein expression nor the activity of SphKs and SGPL in this context. It might be possible that the presence of S1P downregulates its kinase and upregulates SGPL activity.

Another factor to simulate inflammation of the intestine is the pro-inflammatory cytokine TNF α , which is found in high doses in inflammatory bowel disease and food allergy^{113,248–250}. High TNF α levels alter structure and function of TJs and thereby impair the intestinal barrier function^{248,251,252}. This effect could be enhanced by the release of S1P of IECs through the TNF α mediated activation of SphKs^{170,171,154}. In our experiments, however, TNF α did not enhance the expression levels of SphKs neither on mRNA levels nor on protein levels. In contrast, TNF α stimulation induced a downregulation of the pro-apoptotic SphK2²⁵³ over time, which seemed to be concentration dependent on protein level but independent on mRNA level. These results could provide evidence that through downregulation of SphK2, TNF α induces pro-survival effects in IECs. Since this is the first study which shows the influence of TNF α on SphK2, further studies are needed to verify these findings as well as to identify the intracellular signalling pathway and to explore if TJ formation is impaired or not.

During inflammation and allergic reactions, the elevated tissue S1P levels efficiently recruit effector lymphocytes like Th2 cells and mast cells ^{147,171,174,187}. This recruitment is mediated through the expression of the S1P1 receptor on the surface of the immune cells ²⁵⁴. Other S1P surface receptors are responsible for their activation and the release of their mediators ²⁵⁴. In human airway smooth muscle cells, activation of expressed S1P2 and S1P3 results in re-modelling of the muscle cells as well as in hyper reactivity ^{183,255}. Additionally, through basolateral S1P2 expression, human lung epithelial cells produce and release IL-8 upon S1P stimulation ²⁵⁶. Since IECs are important contributors to the intestinal immunity through the release of regulatory and inflammatory cytokines ³⁸, we were interested if IECs are also able to react towards S1P levels via the expression of one or more S1P receptors. The evaluation of real time-qPCR results revealed the mRNA presence of S1P2 and S1P3 in lower amounts. Basolateral stimulation with different S1P concentrations showed no regulation of S1P2 mRNA expression. Even co-incubation with JTE-013, a specific S1P2 antagonist, did not significantly alter expression of S1P2 mRNA; only a slightly higher baseline receptor mRNA expression was found in the cells when incubated with JTE-013. These results show that CaCo2 cells express S1P receptors on mRNA levels, which is not regulated by basolateral S1P stimulation. However, our data do not indicate if the cells also express the receptors on protein levels and whether they are expressed on the apical and/or basolateral membrane. Good antibodies for S1P receptors, as for most G protein-coupled receptors, are not available. However, using a calcium release assay, we were at least able to show that CaCo2 cells do not respond towards apical S1P stimulation via a typical Gq/Gi coupled calcium signalling. Since it is known that S1P2 and S1P3 couple to Gq and Gi, these receptors are most probably not expressed on the apical side and might influence the immune function of IECs upon basolateral S1P exposure like lung epithelial cells ^{158,257}. In endothelial as well as in lung epithelial cells, S1P was found to induce the release of cytokines and therefore mediate inflammation ^{257,258}. However, our results indicate only slight increases in inflammatory and the complete absence of allergy mediating cytokine expression. In a food allergy model, S1P signalling impaired the intestinal barrier function, which would be in accordance with the impaired barrier function found in food allergic patients ^{188,259}. Nonetheless, our results indicate that S1P has a protective function on the intestinal barrier, since it enhances the TEER formation over time in a dose dependent manner. Correspondingly, TJ mRNA expression was found to be slightly upregulated in IECs after S1P stimulation. However, this effect does not seem to be S1P2 dependent since co-stimulation with JTE-013, a S1P2 specific antagonist, did not have a significant impact on TJ mRNA expression. The upregulation of occludin and ZO-2 mRNA after 30min of S1P stimulation in JTE-013 pre-treated cells shows that block of S1P2 signalling leads to

enhanced TJ formation. However, the strong induction is lost after longer S1P stimulation suggesting the induction of other signalling pathways in the regulation of TJ formation. During inflammation, several mediators are released besides S1P and probably adding up to the relatively small effect we are measuring by just picking one mediator. In addition, several different cell types play crucial roles during inflammation. Future experiments using co-cultures of CaCo2 cells with PBMCs might help to understand the complex situation in the intestinal epithelium.

Apart from S1P, other factors are able to influence the barrier formation of the intestinal epithelium and may contribute to the leaky gut syndrome found in food allergic patients^{116,117}. The permeability of IECs is thereby influenced by various cytokines and chemokines which are produced during allergic reactions^{122–128}. This allows for enhanced allergen passage which contributes to the severity of the adverse reaction towards food^{113–115,131,132}. Severe systemic reactions and rising numbers of food allergy patients involve the high need for a curative treatment^{105,113,114}. The only approach to cure food allergy is the application of OIT, which aims to re-establish oral tolerance towards the food allergen^{190–192}. Through the regulation of Th2 cytokines and mast cell mediators, OIT would allow IECs to rebuild an effective barrier¹⁹⁰. During OIT, rising dosages of allergen are administered to the patients resulting in a desensitization followed by an induced tolerance^{191,194}. To enhance the delivery efficiency of bioavailable allergen to the intestine during OIT, allergens are encapsulated into lectin functionalised MPs^{193,211–215,260}. The functionalisation of MPs allows the specific targeting of diverse IECs and thereby facilitates antigen uptake, internalisation and varying immune responses^{193,213–215,217,260}. Another coating approach is the functionalisation of MPs with the NA from *vibrio cholera*, which allows the specific targeting of M-cells²¹⁹. Compared to lectin coated MPs, NA-MPs facilitate enhanced binding, allergen uptake and modulation of immune responses [unpublished data]. However, not much is known about the influence of MP binding on the intestinal permeability as well as the stimulation of IECs.

Here we could show that allergen loaded, coated MPs are able to induce an immune response in IECs. Stimulation with AAL-MPs, NA-MPs as well as WGA-MPs resulted in upregulation of IL-8 mRNA expression levels, with NA-MPs showing the strongest induction. This effect seems to be due to NA, because NA stimulation alone induced a significant upregulation of IL-8 mRNA expression. Release of IL-8 by IECs is associated with the attraction of neutrophils which promote an early inflammatory response²⁶¹. The enhanced IL-8 mRNA expression after NA and NA-MPs stimulation might indicate that NA possesses an important adjuvant function to enhance the immune response. In addition, stimulation with WGA-MPs and NA-MPs resulted in enhanced levels of CCL20

expression, which is associated with the chemotactic recruitment of lymphocytes and the formation of mucosal lymphoid tissues^{262,263}. Thereby NA-MPs induced higher expression levels than WGA-MPs allowing the assumption that NA-MPs induce a stronger response in IECs. The high expression of CCL20 after NA stimulation alone further facilitates the assumption that NA has an important adjuvant function. An increased expression of RANTES after NA-MPs stimulation provides evidence that the stimulated IECs are able to recruit lymphocytes towards the side of inflammation¹. However, the effect seems to be NA mediated since NA stimulation alone did not induce a higher RANTES expression. The upregulation of TSPL expression after MP stimulation suggests that IECs recruit DCs towards the side of inflammation and limit their ability to produce pro-inflammatory cytokines^{38,83}. This leads to the conclusion that coated MPs, especially NA-MPs, induce a prominent immune response in IECs which might contribute to the establishment of immunomodulation and successful OIT.

Since food allergic patients suffer from a leaky gut syndrome⁹, it was of special importance to evaluate the intestinal barrier integrity after MP incubation. Our results indicate that MPs do not interfere with the barrier integrity of the intestinal epithelium. In contrast, an enhanced claudin-4 and ZO-2 expression was observed after MP stimulation, indicating a possible protective effect on the intestinal barrier integrity.

In conclusion we suggest that IECs might contribute to the establishment of a S1P gradient through the production of S1P via SphK2 and the degradation via SGPL. Furthermore, the cells possess the ability to respond upon S1P levels because they express S1P2 and S1P3 most likely on the basolateral side. Furthermore, S1P appears to have a protective function on IECs by enhanced TJ formation and induction of inflammatory cytokines.

Furthermore, our results indicate that MPs, in particular, NA-MPs, induce IECs to produce IL-8, CCL20, RANTES and TSLP which are associated with lymphocyte recruitment and the induction of an inflammatory immune response. Additionally, functionalised MPs induce claudin-4 and ZO-2 expression in IECs.

In any case, further studies are needed to evaluate if the observed effects of S1P and MPs are also seen on protein level and in *in vivo* model organisms.

6. References

1. Abbas, A. K., Lichtman, A. H. & Pillai, S. *Cellular and Molecular Immunology*. (Elsevier, 2011).
2. Groschwitz, K. R. & Hogan, S. P. Intestinal barrier function: molecular regulation and disease pathogenesis. *J. Allergy Clin. Immunol.* **124**, 3–20; quiz 21–2 (2009).
3. Alberts, B. *et al. Molecular Biology of The Cell*. (Garland Science, 2008).
4. Kunzelmann, K. & Mall, M. Electrolyte transport in the mammalian colon: mechanisms and implications for disease. *Physiol. Rev.* **82**, 245–289 (2002).
5. Bröer, S. Amino acid transport across mammalian intestinal and renal epithelia. *Physiol. Rev.* **88**, 249–286 (2008).
6. Ferraris, R. P. Dietary and developmental regulation of intestinal sugar transport. *Biochem. J.* **360**, 265–276 (2001).
7. Yu, L. C.-H. Intestinal Epithelial Barrier Dysfunction in Food Hypersensitivity. *J. Allergy* **2012**, 1–11 (2012).
8. Van Itallie, C. M. & Anderson, J. M. Claudins and Epithelial Paracellular Transport. *Annu. Rev. Physiol.* **68**, 403–429 (2006).
9. Liu, Z., Li, N. & Neu, J. Tight junctions, leaky intestines, and pediatric diseases. *Acta Paediatr.* **94**, 386–393 (2005).
10. Michielan, A. & Incà, R. D. Intestinal Permeability in Inflammatory Bowel Disease: Pathogenesis, Clinical Evaluation, and Therapy of Leaky Gut. *Mediators Inflamm.* **2015**, (2015).
11. Furuse, M. *et al.* Occludin: A novel integral membrane protein localizing at tight junctions. *J. Cell Biol.* **23**, 1777–1788 (1993).
12. Wong, V. & Gumbiner, B. M. A synthetic peptide corresponding to the extracellular domain of occludin perturbs the tight junction permeability barrier. *J. Cell Biol.* **136**, 399–409 (1997).
13. Nusrat, A. *et al.* Multiple Protein Interactions Involving Proposed Extracellular Loop Domains of the Tight Junction Protein Occludin. *Mol. Biol. Cell* **16**, 1725–1734 (2005).
14. Furuse, M. *et al.* Direct association of occludin with ZO-1 and its possible involvement in the localization of occludin at tight junctions. *J. Cell Biol.* **27**, 1617–1626 (1994).
15. Itoh, M., Morita, K. & Tsukita, S. Characterization of ZO-2 as a MAGUK family member associated with tight as well as adherens junctions with a binding affinity to occludin and α catenin. *J. Biol. Chem.* **274**, 5981–5986 (1999).
16. Furuse, M., Fujita, K., Hiiragi, T., Fujimoto, K. & Tsukita, S. Claudin-1 and -2: novel integral membrane proteins localizing at tight junctions with no sequence similarity to occludin. *J. Cell Biol.* **141**, 1539–50 (1998).
17. Morita, K., Furuse, M., Fujimoto, K. & Tsukita, S. Claudin multigene family encoding four-transmembrane domain protein components of tight junction strands. *Proc. Natl. Acad. Sci. U. S. A.* **96**, 511–516 (1999).
18. Krause, G. *et al.* Structure and function of claudins. *Biochim. Biophys. Acta - Biomembr.* **1778**, 631–645 (2008).
19. Itoh, M. *et al.* Direct binding of three tight junction-associated MAGUKs, ZO-1, ZO-

- 2, and ZO-3, with the COOH termini of claudins. *J. Cell Biol.* **147**, 1351–1363 (1999).
20. Tang, V. W. & Goodenough, D. A. Paracellular Ion Channel at the Tight Junction. *Biophys. J.* **84**, 1660–1673 (2003).
 21. Hartsock, A. & Nelson, W. J. Adherens and tight junctions: Structure, function and connections to the actin cytoskeleton. *Biochim. Biophys. Acta - Biomembr.* **1778**, 660–669 (2008).
 22. Perez-Moreno, M. & Fuchs, E. Catenins: Keeping Cells from Getting Their Signals Crossed. *Dev. Cell* **11**, 601–612 (2006).
 23. Ebnet, K. Organization of multiprotein complexes at cell-cell junctions. *Histochem. Cell Biol.* **130**, 1–20 (2008).
 24. Turnbaugh, P. J. *et al.* A core gut microbiome in obese and lean twins. *Nature* **457**, 480–484 (2009).
 25. Turnbaugh, P. J. *et al.* The effect of diet on the human gut microbiome: a metagenomic analysis in humanized gnotobiotic mice. *Sci. Transl. Med.* **1**, 6ra14 (2009).
 26. De Filippo, C. *et al.* Impact of diet in shaping gut microbiota revealed by a comparative study in children from Europe and rural Africa. *Proc. Natl. Acad. Sci. U. S. A.* **107**, 14691–14696 (2010).
 27. Mariat, D. *et al.* The Firmicutes/Bacteroidetes ratio of the human microbiota changes with age. *BMC Microbiol.* **9**, (2009).
 28. Sekirov, I., Russell, S. L., Antunes, L. C. M. & Finlay, B. B. Gut Microbiota in Health and Disease. *Physiol. Rev.* **90**, 859–904 (2010).
 29. Purchiaroni, F. *et al.* The role of intestinal microbiota and the immune system. *Eur. Rev. Med. Pharmacol. Sci.* **17**, 323–33 (2013).
 30. Clarke, T. B. *et al.* Recognition of peptidoglycan from the microbiota by Nod1 enhances systemic innate immunity. *Nat. Med.* **16**, 228–231 (2010).
 31. Round, J. L., O’Connell, R. M. & Mazmanian, S. K. Coordination of tolerogenic immune responses by the commensal microbiota. *J. Autoimmun.* **34**, 220–225 (2010).
 32. Gutzeit, C., Magri, G. & Cerutti, A. Intestinal IgA production and its role in host-microbe interaction. *Immunol Rev.* **141**, 520–529 (2014).
 33. Brandtzaeg, P. Presence of J chain in human immunocytes containing various immunoglobulin classes. *Nature* **252**, 418–419 (1974).
 34. Brandtzaeg, P. & Prydz, H. Direct evidence for an integrated function of J chain and secretory component in epithelial transport of immunoglobulins. *Nature* **309**, 23–29 (1984).
 35. Phalipon, A. *et al.* Secretory component: A new role in secretory IgA-mediated immune exclusion in vivo. *Immunity* **17**, 107–115 (2002).
 36. Strugnell, R. A. & Wijburg, O. L. The role of secretory antibodies in infection immunity. *Nat. Rev. Microbiol.* **8**, 68–71 (2010).
 37. Ivanov, I. I. & Honda, K. Intestinal commensal microbes as immune modulators. *Cell Host Microbe* **12**, 496–508 (2012).
 38. Zeuthen, L. H., Fink, L. N. & Frokiaer, H. Epithelial cells prime the immune response to an array of gut-derived commensals towards a tolerogenic phenotype

- through distinct actions of thymic stromal lymphopoietin and transforming growth factor- β . *Immunology* **123**, 197–208 (2007).
39. Macpherson, A. J., Köller, Y. & McCoy, K. D. The bilateral responsiveness between intestinal microbes and IgA. *Trends Immunol.* **36**, 1–11 (2015).
 40. Mathias, A., Pais, B., Favre, L., Benyacoub, J. & Corthésy, B. Role of secretory IgA in the mucosal sensing of commensal bacteria. *Gut Microbes* **5**, 688–695 (2014).
 41. Atuma, C., Strugala, V., Allen, a & Holm, L. The adherent gastrointestinal mucus gel layer: thickness and physical state in vivo. *Am. J. Physiol. Gastrointest. Liver Physiol.* **280**, G922–G929 (2001).
 42. Johansson, M. E. V, Larsson, J. M. H. & Hansson, G. C. The two mucus layers of colon are organized by the MUC2 mucin, whereas the outer layer is a legislator of host-microbial interactions. *PNAS* **108**, 4659–4665 (2011).
 43. Turner, J. R. Intestinal mucosal barrier function in health and disease. *Nat. Rev. Immunol.* **9**, 799–809 (2009).
 44. Johansson, M. E. V *et al.* The inner of the two Muc2 mucin-dependent mucus layers in colon is devoid of bacteria. *Proc. Natl. Acad. Sci. U. S. A.* **105**, 15064–9 (2008).
 45. Sansonetti, P. J. War and Peace at Mucosal Surfaces. *Nat. Rev. Immunol.* **4**, 953–964 (2004).
 46. Zasloff, M. Antimicrobial Peptides in health and Disease. *N. Engl. J. Med.* **347**, 1199–1200 (2002).
 47. Zasloff, M. Antimicrobial peptides of multicellular organisms. *Nature* **415**, 389–395 (2002).
 48. Matsuzaki, K. Why and how are peptide-lipid interactions utilized for self-defense? Magainins and tachyplesins as archetypes. *Biochim. Biophys. Acta - Biomembr.* **1462**, 1–10 (1999).
 49. Shai, Y. Mechanism of the binding, insertion and destabilization of phospholipid bilayer membranes by ??-helical antimicrobial and cell non-selective membrane-lytic peptides. *Biochim. Biophys. Acta - Biomembr.* **1462**, 55–70 (1999).
 50. Mukherjee, S. *et al.* Antibacterial membrane attack by a pore-forming intestinal C-type lectin. **505**, 103–107 (2014).
 51. Zanetti, M. Cathelicidins, multifunctional peptides of the innate immunity. *J. Leukoc. Biol.* **75**, 39–48 (2004).
 52. De Yang *et al.* LL-37, the neutrophil granule- and epithelial cell-derived cathelicidin, utilizes formyl peptide receptor-like 1 (FPRL1) as a receptor to chemoattract human peripheral blood neutrophils, monocytes, and T cells. *J. Exp. Med.* **192**, 1069–74 (2000).
 53. Koczuła, R. *et al.* An angiogenic role for the human peptide antibiotic LL-37 / hCAP-18. *J. Clin. Invest.* **111**, 1665–1672 (2003).
 54. Heilborn, J. D. *et al.* The cathelicidin anti-microbial peptide LL-37 is involved in re-epithelialization of human skin wounds and is lacking in chronic ulcer epithelium. *J. Invest. Dermatol.* **120**, 379–389 (2003).
 55. Peterson, L. W. & Artis, D. Intestinal epithelial cells: regulators of barrier function and immune homeostasis. *Nat. Rev. Immunol.* **14**, 141–53 (2014).
 56. Hall, P. a, Coates, P. J., Ansari, B. & Hopwood, D. Regulation of cell number in the

- mammalian gastrointestinal tract: the importance of apoptosis. *J. Cell Sci.* **107** , 3569–3577 (1994).
57. van der Flier, L. G. & Clevers, H. Stem cells, self-renewal, and differentiation in the intestinal epithelium. *Annu. Rev. Physiol.* **71**, 241–260 (2009).
 58. Marshman, E., Booth, C. & Potten, C. S. The intestinal epithelial stem cell. *BioEssays* **24**, 91–98 (2002).
 59. Schmidt, G. H., Winton, D. J. & Ponder, B. a. Development of the pattern of cell renewal in the crypt-villus unit of chimaeric mouse small intestine. *Development* **103**, 785–790 (1988).
 60. Mallow, E. *et al.* Human Enteric Defensins. *J. Biol. Chem.* **271**, 4038–4045 (1996).
 61. Karam, S. M. Lineage Commitment and Maturation of Epithelial Cells in the Gut. *Bioscience* **4**, 286–298 (1999).
 62. Porter, E. M., Bevins, C. L., Gosh, D. & Ganz, T. The multifaceted Paneth cell. *Cell. Mol. Life Sci.* **59**, 1081–1095 (2002).
 63. Battle, E. *et al.* β -catenin and TCF mediate cell positioning in the intestinal epithelium by controlling the expression of EphB/EphrinB. *Cell* **111**, 251–263 (2002).
 64. Porter, E. M. *et al.* Localization of human intestinal defensin 5 in Paneth cell granules . Localization of Human Intestinal Defensin 5 in Paneth Cell Granules. *Microbiology* **65**, 2389–2395 (1997).
 65. Neutra, M. & Leblond, C. Synthesis in the of the Carbohydrate As Shown of Mucus By Electron Golgi Complex Microscope With of Goblet Glucose-H. *J. Cell Biol.* **30**, 119–136 (1966).
 66. Specian, R. D. & Neutra, M. R. Mechanism of rapid mucus secretion in goblet cells stimulated by acetylcholine. *J. Cell Biol.* **85**, 626–640 (1980).
 67. Johansson, M. E. V *et al.* Bacteria penetrate the inner mucus layer before inflammation in the dextran sulfate colitis model. *PLoS One* **5**, e12238 (2010).
 68. Schonhoff, S. E., Giel-Moloney, M. & Leiter, A. B. Minireview: Development and differentiation of gut endocrine cells. *Endocrinology* **145**, 2639–2644 (2004).
 69. Posovszky, C. & Wabitsch, M. Regulation of appetite, satiation, and body weight by enteroendocrine cells. Part 1: Characteristics of enteroendocrine cells and their capability of weight regulation. *Horm. Res. Paediatr.* **83**, 1–10 (2015).
 70. Vaishnava, S. *et al.* The antibacterial lectin RegIII γ promotes the spatial segregation of microbiota and host in the intestine. *Science* **334**, 255–8 (2011).
 71. Tolhurst, G., Reimann, F. & Gribble, F. M. Intestinal sensing of nutrients. *Handb. Exp. Pharmacol.* **209**, 309–35 (2012).
 72. Crawley, S. W., Mooseker, M. S. & Tyska, M. J. Shaping the intestinal brush border. *J. Cell Biol.* **207**, 441–51 (2014).
 73. Shifrin, D. A. *et al.* Enterocyte microvillus-derived vesicles detoxify bacterial products and regulate epithelial-microbial interactions. *Curr. Biol.* **22**, 627–631 (2012).
 74. Campbell, E. L. *et al.* Resolvin E1-induced intestinal alkaline phosphatase promotes resolution of in fl ammation through LPS detoxi fi cation. *Pnas* **107**, 14298–14303 (2010).
 75. Untersmayr, E. *et al.* The high affinity IgE receptor Fc epsilonRI is expressed by

- human intestinal epithelial cells. *PLoS One* **5**, e9023 (2010).
76. Kaiserlian, D., Lachaux, A., Grosjean, I., Grabert, P. & Bonnefoy, J. Intestinal epithelial cells express the CD23 / Fc γ RII molecule: enhanced expression in enteropathies. *Immunology* **80**, 90–95 (1993).
 77. Hershberg, R. M. *et al.* Highly polarized HLA class II antigen processing and presentation by human intestinal epithelial cells. *J. Clin. Invest.* **102**, 792–803 (1998).
 78. Miron, N. & Cristea, V. Enterocytes: active cells in tolerance to food and microbial antigens in the gut. *Clin. Exp. Immunol.* **167**, 405–12 (2012).
 79. Sanderson, I. & Walker, W. Uptake and transport of macromolecules by the intestine: possible role in clinical disorders (an update). - PubMed - NCBI. *Gastroenterology* **104**, 622–39 (1993).
 80. Mantis, N. J. *et al.* Selective adherence of IgA to murine Peyer's patch M cells: evidence for a novel IgA receptor. *J. Immunol.* **169**, 1844–1851 (2002).
 81. Winstead, C. J. Follicular helper T cell-mediated mucosal barrier maintenance. *Immunol. Lett.* **162**, 39–47 (2014).
 82. Jung, C., Hugot, J.-P. & Barreau, F. Peyer's Patches: The Immune Sensors of the Intestine. *Int. J. Inflamm.* **2010**, 1–12 (2010).
 83. Sheridan, B. S. & Lefrançois, L. Intraepithelial Lymphocytes: To Serve and Protect. *Curr. Gastroenterol. Rep.* **12**, 513–521 (2010).
 84. A.M.C., F. & H.L., W. Oral tolerance. *Immunol. Rev.* **206**, 232–259 (2005).
 85. Meyer, T., Ullrich, R. & Zeitz, M. Oral tolerance induction in humans. *Exp. Mol. Pathol.* **93**, 449–454 (2012).
 86. Rescigno, M. *et al.* Dendritic cells express tight junction proteins and penetrate gut epithelial monolayers to sample bacteria. *Nat. Immunol.* **2**, 361–367 (2001).
 87. Liu, L. M. & Macpherson, G. G. Lymph-borne (veiled) dendritic cells can acquire and present intestinally administered antigens. *Immunology* **73**, 281–286 (1991).
 88. Schulz, O. *et al.* Intestinal CD103+, but not CX3CR1+, antigen sampling cells migrate in lymph and serve classical dendritic cell functions. *J. Exp. Med.* **206**, 3101–3114 (2009).
 89. Scheinecker, C., McHugh, R., Shevach, E. M. & Germain, R. N. Constitutive Presentation of a Natural Tissue Autoantigen Exclusively by Dendritic Cells in the Draining Lymph Node. *J. Exp. Med.* **196**, 1079–1090 (2002).
 90. Spahn, T. W. *et al.* Mesenteric lymph nodes are critical for the induction of high-dose oral tolerance in the absence of Peyer's patches. *Eur. J. Immunol.* **32**, 1109–1113 (2002).
 91. Sonoda, E., Matsumoto, R. & Hitoshi, Y. Transforming Growth Factor β induces IgA production and acts additively with Interleukin 5 for IgA production. *J. Exp. Med.* **170**, 1415–1420 (1989).
 92. Borsutzky, S., Cazac, B. B., Roes, J. & Guzman, C. A. TGF- β Receptor Signaling Is Critical for Mucosal IgA Responses. *J. Immunol.* **173**, 3305–3309 (2004).
 93. Hammerschmidt, S. I. *et al.* Stromal mesenteric lymph node cells are essential for the generation of gut-homing T cells in vivo. *J. Exp. Med.* **205**, 2483–2490 (2008).
 94. Iwata, M. *et al.* Retinoic acid imprints gut-homing specificity on T cells. *Immunity* **21**, 527–38 (2004).

95. Sun, C.-M. *et al.* Small intestine lamina propria dendritic cells promote de novo generation of Foxp3 T reg cells via retinoic acid. *J. Exp. Med.* **204**, 1775–1785 (2007).
96. Castro-Sánchez, P. & Martín-Villa, J. M. Gut immune system and oral tolerance. *Br. J. Nutr.* **109**, S3–S11 (2013).
97. Chen, Y., Kuchroo, V. K., Inobe, J., Hafler, D. a & Weiner, H. L. Regulatory T cell clones induced by oral tolerance: suppression of autoimmune encephalomyelitis. *Science* **265**, 1237–1240 (1994).
98. Groux, H. *et al.* A CD4+ T-cell subset inhibits antigen-specific T-cell responses and prevents colitis. *Nature* **389**, 737–742 (1997).
99. Zhang, X., Izikson, L., Liu, L. & Weiner, H. L. Activation of CD25+CD4+ Regulatory T Cells by Oral Antigen Administration. *J. Immunol.* **167**, 4245–4253 (2001).
100. Nakamura, K., Kitani, A. & Strober, W. Cell contact-dependent immunosuppression by CD4(+)CD25(+) regulatory T cells is mediated by cell surface-bound transforming growth factor beta. *J. Exp. Med.* **194**, 629–44 (2001).
101. Fontenot, J. D., Gavin, M. A. & Rudensky, A. Y. Foxp3 programs the development and function of CD4+CD25+ regulatory T cells. *Nat. Immunol.* **4**, 330–336 (2003).
102. Ostroukhova, M. *et al.* Tolerance induced by inhaled antigen involves CD4(+) T cells expressing membrane-bound TGF-beta and FOXP3. *J. Clin. Invest.* **114**, 28–38 (2004).
103. Appleman, L. J. & Boussiotis, V. a. T cell anergy and costimulation. *Immunol. Rev.* **192**, 161–180 (2003).
104. Wasserman, S. & Watson, W. Food allergy. *Allergy, Asthma Clin. Immunol.* **7**, S7 (2011).
105. Untersmayr, E. & Jensen-Jarolim, E. Mechanisms of type I food allergy. *Pharmacol. Ther.* **112**, 787–98 (2006).
106. Untersmayr, E. *et al.* Antacid medication inhibits digestion of dietary proteins and causes food allergy: A fish allergy model in Balb/c mice. *J. Allergy Clin. Immunol.* **112**, 616–623 (2003).
107. Diesner, S. C., Knittelfelder, R., Krishnamurthy, D. & Gajdzik, L. Dose-dependent food allergy induction against ovalbumin under acid-suppression: A murine food allergy model. *Immunol Lett* **121**, 45–51 (2008).
108. Untersmayr, E. & Jensen-Jarolim, E. Europe PMC Funders Group The role of protein digestibility and antacids on food allergy outcomes. *J. Allergy Clin. Immunol.* **121**, 1301–1310 (2010).
109. Vickery, B., Chin, S. & Burks, A. W. Pathophysiology of Food Allergy. *Pediatr. Clin North Am* **58**, 363–376 (2011).
110. Sokol, C. L. & Medzhitov, R. Emerging functions of basophils in protective and allergic immune responses. *Mucosal Immunol.* **3**, 129–137 (2010).
111. Geha, R. S., Jabara, H. H. & Brodeur, S. R. The regulation of immunoglobulin E class-switch recombination. *Nat. Rev. Immunol.* **3**, 721–732 (2003).
112. Cianferoni, A. Food allergy. *Allergol. Int.* **20**, 931–945 (2009).
113. Galli, S. J. & Tsai, M. Mast cells in allergy and infection: Versatile effector and regulatory cells in innate and adaptive immunity. *Eur. J. Immunol.* **40**, 1843–1851 (2010).

114. Galli, S. J., Grimaldeston, M. & Tsai, M. Immunomodulatory mast cells: negative, as well as positive, regulators of immunity. *Nat. Rev. Immunol.* **8**, 478–486 (2008).
115. Galli, S. J., Tsai, M. & Piliponsky, A. M. The development of allergic inflammation. *Nature* **454**, 445–454 (2008).
116. Ventura, M. T. *et al.* Intestinal permeability in patients with adverse reactions to food. *Dig. Liver Dis.* **38**, 732–736 (2006).
117. Andre, C., Andre, F., Colin, L. & Cavagna, S. Measurement of intestinal permeability to mannitol and lactulose as a means of diagnosing food allergy and evaluating therapeutic effectiveness of disodium cromoglycate. *Ann. Allergy* **59**, 127–30 (1987).
118. Berin MC, Kiliaan AJ, Yang PC, Groot JA, Taminiou JA, P. M. Rapid transepithelial antigen transport in rat jejunum: impact of sensitization and the hypersensitivity reaction. *Gastroenterology* **113**, 856–864 (1997).
119. Yang, P. C., Berin, M. C., Yu, L. C. H., Conrad, D. H. & Perdue, M. H. Enhanced intestinal transepithelial antigen transport in allergic rats is mediated by IgE and CD23 (FcεRII). *J. Clin. Invest.* **106**, 879–886 (2000).
120. Yu, L. C. H. *et al.* Enhanced Transepithelial Antigen Transport in Intestine of Allergic Mice Is Mediated by IgE/CD23 and Regulated by Interleukin-4. doi:10.1053/gast.2001.26470
121. Tu, Y. & Perdue, M. H. CD23-mediated transport of IgE / immune complexes across human intestinal epithelium: role of p38 MAPK. *Pathology* **5**, 532–538 (2006).
122. Musch, M. W. *et al.* T cell activation causes diarrhea by increasing intestinal permeability and inhibiting epithelial Na⁺/K⁺-ATPase. *J. Clin. Invest.* **110**, 1739–1747 (2002).
123. Berin, M. C., Yang, P. C., Ciok, L., Wasserman, S. & Perdue, M. H. Role for IL-4 in macromolecular transport across human intestinal epithelium. *Am. J. Physiol.* **276**, C1046–52 (1999).
124. Wisner, D. M., Harris, L. R., Green, C. L. & Poritz, L. S. Opposing Regulation of the Tight Junction Protein Claudin-2 by Interferon-γ and Interleukin-4. *J. Surg. Res.* **144**, 1–7 (2008).
125. Ceponis, P. J. M., Botelho, F., Richards, C. D. & McKay, D. M. Interleukins 4 and 13 Increase Intestinal Epithelial Permeability by a Phosphatidylinositol 3-Kinase Pathway. Lack of Evidence for STAT 6 Involvement. *J. Biol. Chem.* **275**, 29132–29137 (2000).
126. Heller, F., Fromm, A., Gitter, A. H., Mankertz, J. & Schulzke, J.-D. Epithelial apoptosis is a prominent feature of the epithelial barrier disturbance in intestinal inflammation: effect of pro-inflammatory interleukin-13 on epithelial cell function. *Mucosal Immunol.* **1**, S58–S61 (2008).
127. Brandt, E. B. *et al.* Mast cells are required for experimental oral allergen-induced diarrhea. *J. Clin. Invest.* **112**, 1666–1677 (2003).
128. Jacob, C. *et al.* Mast Cell Tryptase Controls Paracellular Permeability of the Intestine: Role of Protease-Activated Receptor 2 and β-Arrestins. *J. Biol. Chem.* **280**, 31936–31948 (2005).
129. Lee, J. J. *et al.* Eosinophils alter colonic epithelial barrier function: role for major basic protein. *Am J Physiol Gastrointest Liver Physiol* **289**, 890–897 (2005).
130. Wan, H., Winton, H. L., Soeller, C., E. A. Der p 1 facilitates transepithelial allergen

- delivery by disruption of tight junctions. *J Clin Invest.* **104**, 123–133 (1999).
131. Starkl, P. *et al.* Heating Affects Structure, Enterocyte Adsorption and Signalling, As Well as Immunogenicity of the Peanut Allergen Ara h 2 Europe PMC Funders Group. *Open Allergy J.* **4**, 24–34 (2011).
 132. Price, D. B., Ackland, M. L., Burks, W., Knight, M. I. & Suphioglu, C. Peanut Allergens Alter Intestinal Barrier Permeability and Tight Junction Localisation in Caco-2 Cell Cultures ¹. *Cell. Physiol. Biochem.* **33**, 1758–1777 (2014).
 133. Greenspon, J. *et al.* Sphingosine-1-Phosphate Protects Intestinal Epithelial Cells from Apoptosis Through the Akt Signaling Pathway. **54**, 499–510 (2009).
 134. Jiang, P. *et al.* Sphingosine kinase 1 overexpression stimulates intestinal epithelial cell proliferation through increased c-Myc translation. *Am. J. Physiol. Cell Physiol.* **304**, C1187–97 (2013).
 135. Thamilselvan, V., Li, W., Sumpio, B. E. & Basson, M. D. Sphingosine-1-phosphate stimulates human Caco-2 intestinal epithelial proliferation via p38 activation and activates ERK by an independent mechanism. *In Vitro Cell. Dev. Biol. Anim.* **38**, 246–253 (2002).
 136. Greenspon, J. *et al.* Sphingosine-1-phosphate regulates the expression of adherens junction protein E-cadherin and enhances intestinal epithelial cell barrier function. *Dig. Dis. Sci.* **56**, 1342–53 (2011).
 137. Yatomi, Y., Welch, R. J. & Igarashi, Y. Distribution of sphingosine 1-phosphate, a bioactive sphingolipid, in rat tissues. *FEBS Lett.* **404**, 173–174 (1997).
 138. Kurek, K. *et al.* Metabolism, physiological role, and clinical implications of sphingolipids in gastrointestinal tract. *Biomed Res. Int.* **2013**, 908907 (2013).
 139. Futerman, A. H. & Riezman, H. The ins and outs of sphingolipid synthesis. *Trends Cell Biol.* **15**, 312–318 (2005).
 140. Duan, R.-D. *et al.* Purification, localization, and expression of human intestinal alkaline sphingomyelinase. *J. Lipid Res.* **44**, 1241–1250 (2003).
 141. Nilsson, Å. & Duan, R. D. Alkaline sphingomyelinases and ceramidases of the gastrointestinal tract. *Chem. Phys. Lipids* **102**, 97–105 (1999).
 142. Duan, R. D., Cheng, Y., Yang, L., Ohlsson, L. & Nilsson, A. Evidence for specific ceramidase present in the intestinal contents of rats and humans. *Lipids* **36**, 807–812 (2001).
 143. Kohno, M. *et al.* Intracellular role for sphingosine kinase 1 in intestinal adenoma cell proliferation. *Mol. Cell. Biol.* **26**, 7211–23 (2006).
 144. Murate, T. *et al.* Cell Type-specific Localization of Sphingosine Kinase 1a in Human Tissues. *J. Histochem. Cytochem.* **49**, 845–855 (2001).
 145. Chen, H., Born, E., Mathur, S. N. & Field, F. J. Cholesterol and sphingomyelin syntheses are regulated independently in cultured human intestinal cells, CaCo-2: role of membrane cholesterol and sphingomyelin content. *J. Lipid Res.* **34**, 2159–2167 (1993).
 146. Merrill, A. H., Nixon, D. W. & Williams, R. D. Activities of serine palmitoyltransferase (3-ketosphinganine synthase) in microsomes from different rat tissues. *J. Lipid Res.* **26**, 617–22 (1985).
 147. Pappu, R. *et al.* Promotion of lymphocyte egress into blood and lymph by distinct sources of sphingosine-1-phosphate. *Science* **316**, 295–298 (2007).

148. Venkataraman, K. *et al.* Vascular Endothelium As a Contributor of Plasma Sphingosine 1-Phosphate. *Circ. Res.* **102**, 669–676 (2008).
149. Yamanaka, M. *et al.* Sphingosine kinase 1 (SPHK1) is induced by transforming growth factor- β and mediates TIMP-1 up-regulation. *J. Biol. Chem.* **279**, 53994–54001 (2004).
150. Spiegel, S. & Milstien, S. Sphingosine-1-phosphate: an enigmatic signalling lipid. *Nat. Rev. Mol. Cell Biol.* **4**, 397–407 (2003).
151. Spiegel, S. & Milstien, S. Functions of the multifaceted family of sphingosine kinases and some close relatives. *J. Biol. Chem.* **282**, 2125–2129 (2007).
152. Shu, X., Wu, W., Mosteller, R. D. & Broek, D. Sphingosine kinase mediates vascular endothelial growth factor-induced activation of ras and mitogen-activated protein kinases. *Mol. Cell. Biol.* **22**, 7758–68 (2002).
153. Pettus, B. *et al.* The sphingosine kinase 1/sphingosine-1-phosphate pathway mediates COX-2 induction and PGE2 production in response to TNF- α . *FASEB J.* **17**, 1411–1421 (2003).
154. Billich, A. *et al.* Basal and induced sphingosine kinase 1 activity in A549 carcinoma cells: function in cell survival and IL-1 β and TNF- α induced production of inflammatory mediators. *Cell. Signal.* **17**, 1203–1217 (2005).
155. Igarashi, N. *et al.* Sphingosine kinase 2 is a nuclear protein and inhibits DNA synthesis. *J. Biol. Chem.* **278**, 46832–46839 (2003).
156. Olivera, A. & Spiegel, S. Sphingosine-1-phosphate as second messenger in cell proliferation induced by PDGF and FCS mitogens. *Nature* **363**, 210–211 (1993).
157. Mitra, P. *et al.* Role of ABCC1 in export of sphingosine-1-phosphate from mast cells. *Proc. Natl. Acad. Sci. U. S. A.* **103**, 16394–9 (2006).
158. Rosen, H., Gonzalez-Cabrera, P. J., Sanna, M. G. & Brown, S. Sphingosine 1-phosphate receptor signaling. *Annu. Rev. Biochem.* **78**, 743–68 (2009).
159. Stunff, H. Le, Galve-Roperh, I., Peterson, C., Milstien, S. & Spiegel, S. Sphingosine-1-phosphate phosphohydrolase in regulation of sphingolipid metabolism and apoptosis. *J. Cell Biol.* **158**, 1039–1049 (2002).
160. Mandala, S. M. *et al.* Sphingoid base 1-phosphate phosphatase: a key regulator of sphingolipid metabolism and stress response. *Proc. Natl. Acad. Sci. U. S. A.* **95**, 150–155 (1998).
161. Bandhuvula, P., Fyrst, H. & Saba, J. D. A rapid fluorescence assay for sphingosine-1-phosphate lyase enzyme activity. *J. Lipid Res.* **48**, 2769–2778 (2007).
162. Oskouian, B. *et al.* Sphingosine-1-phosphate lyase potentiates apoptosis via p53- and p38-dependent pathways and is down-regulated in colon cancer. *PNAS* **103**, 17384–17389 (2006).
163. Sanchez, T. & Hla, T. Structural and functional characteristics of S1P receptors. *J. Cell. Biochem.* **92**, 913–22 (2004).
164. Ancellin, N. & Hla, T. Differential pharmacological properties and signal transduction of the sphingosine 1-phosphate receptors EDG-1, EDG-3, and EDG-5. *J. Biol. Chem.* **274**, 18997–19002 (1999).
165. Lee, M.-J., Evans, M. & Hla, T. The Inducible G Protein-coupled Receptor edg-1 Signals via the G β 1/Mitogen-activated Protein Kinase Pathway*. *J. Biol. Chem.* **271**, 11272–11279 (1996).

166. Ishii, I. *et al.* Selective Loss of Sphingosine 1-Phosphate Signaling with No Obvious Phenotypic Abnormality in Mice Lacking Its G Protein-coupled Receptor, LP B3/EDG-3. *J. Biol. Chem.* **276**, 33697–33704 (2001).
167. Sugimoto, N., Takuwa, N., Okamoto, H., Sakurada, S. & Takuwa, Y. Inhibitory and Stimulatory Regulation of Rac and Cell Motility by the G_{12/13}-Rho and G_i Pathways Integrated Downstream of a Single G Protein-Coupled Sphingosine-1-Phosphate Receptor Isoform. *Mol. Cell. Biol.* **23**, 1534–1545 (2003).
168. Jolly, P. S. *et al.* Transactivation of sphingosine-1-phosphate receptors by FcεRI triggering is required for normal mast cell degranulation and chemotaxis. *J. Exp. Med.* **199**, 959–70 (2004).
169. Rosen, H. & Goetzl, E. J. Sphingosine 1-phosphate and its receptors: an autocrine and paracrine network. *Nat. Rev. Immunol.* **5**, 560–70 (2005).
170. Matloubian, M. *et al.* Lymphocyte egress from thymus and peripheral lymphoid organs is dependent on S1P receptor 1. *Nature* **427**, 355–60 (2004).
171. Kunisawa, J. *et al.* Sphingosine 1-phosphate dependence in the regulation of lymphocyte trafficking to the gut epithelium. *J. Exp. Med.* **204**, 2335–2348 (2007).
172. Hughes, J. E. *et al.* Sphingosine-1-phosphate induces an antiinflammatory phenotype in macrophages. *Circ. Res.* (2008). doi:10.1038/nm.2071.Generation
173. Scherer, E. Q., Yang, J., Canis, M., Reimann, K. & Ivanov, K. Tumor necrosis factor- α enhances microvascular tone and reduces blood flow in the cochlea via enhanced sphingosine-1-phosphate signaling. *Stroke* **41**, 2618–2624 (2010).
174. Maeda, Y. *et al.* Migration of CD4 T Cells and Dendritic Cells toward Sphingosine 1-Phosphate (S1P) Is Mediated by Different Receptor Subtypes: S1P Regulates the Functions of Murine Mature Dendritic Cells via S1P Receptor Type 3. *J. Immunol.* **178**, 3437–3446 (2007).
175. Jenne, C. N. *et al.* T-bet-dependent S1P5 expression in NK cells promotes egress from lymph nodes and bone marrow. *J. Exp. Med.* **206**, 2469–2481 (2009).
176. Allende, M. L. *et al.* Sphingosine-1-phosphate Lyase Deficiency Produces a Pro-inflammatory Response While Impairing Neutrophil Trafficking. *J. Biol. Chem.* **286**, 7348–7358 (2010).
177. Kunisawa, J. *et al.* Sphingosine 1-phosphate regulates peritoneal B-cell trafficking for subsequent intestinal IgA production. *Blood* **109**, 3749–3756 (2007).
178. Gohda, M. *et al.* Sphingosine 1-phosphate regulates the egress of IgA plasmablasts from Peyer's patches for intestinal IgA responses. *J. Immunol.* **180**, 5335–5343 (2008).
179. Ammit, A. J. *et al.* Sphingosine 1-phosphate modulates human airway smooth muscle cell functions that promote inflammation and airway remodeling in asthma. *FASEB J.* **15**, 1212–1214 (2001).
180. Prieschl, E. E., Csonga, R., Novotny, V., Kikuchi, G. E. & Baumruker, T. The Balance between Sphingosine and Sphingosine-1-phosphate Is Decisive for Mast Cell Activation after Fcε Receptor I Triggering. *J. Exp. Med.* **190**, 1–8 (1999).
181. Pushparaj, P. N. *et al.* Sphingosine Kinase1 Is Pivotal for FcεRI-Mediated Mast Cell Signaling and Functional Responses In Vitro and In Vivo. *J. Immunol.* **183**, 221–227 (2009).
182. Olivera, A. *et al.* Sphingosine-1-phosphate can promote mast cell hyper-reactivity through regulation of contactin-4 expression. *J. Leukoc. Biol.* **94**, 1013–24 (2013).

183. Kume, H. *et al.* Sphingosine 1-phosphate causes airway hyper-reactivity by rho-mediated myosin phosphatase inactivation. *J. Pharmacol. Exp. Ther.* **320**, 766–773 (2007).
184. Roviezzo, F. *et al.* Sphingosine-1-phosphate/sphingosine kinase pathway is involved in mouse airway hyperresponsiveness. *Am. J. Respir. Cell Mol. Biol.* **36**, 757–62 (2007).
185. Rosenfeldt, H. M. *et al.* Sphingosine-1-phosphate stimulates contraction of human airway smooth muscle cells. *FASEB J.* **17**, 1789–99 (2003).
186. Szczepaniak, W., Pitt, B. R. & MvVerry, B. J. S1P2 receptor-dependent Rho-kinase activation mediates vasoconstriction in the murine pulmonary circulation induced by sphingosine 1-phosphate. *Am J Physiol Lung Cell Mol Physiol* **299**, L137–L145 (2010).
187. Kurashima, Y. *et al.* Sphingosine 1-phosphate-mediated trafficking of pathogenic Th2 and mast cells for the control of food allergy. *J. Immunol.* **179**, 1577–85 (2007).
188. Diesner, S. C. *et al.* Sphingosone-kinase 1 and 2 contribute to oral sensitization and effector phase in a mouse model of food allergy. *Immunol Lett.* **141**, 210–219 (2012).
189. Yang, Y.-H. & Chiang, B.-L. Novel approaches to food allergy. *Clin. Rev. Allergy Immunol.* **46**, 250–7 (2014).
190. Kulis, M., Vickery, B. P. & Burks, A. W. Pioneering immunotherapy for food allergy: Clinical outcomes and modulation of the immune response. *Immunol. Res.* **49**, 216–226 (2010).
191. Le, U. H. & Burks, A. W. Oral and sublingual immunotherapy for food allergy. *World Allergy Organ. J.* **7**, 35–41 (2014).
192. Varshney, P. *et al.* A randomized controlled study of peanut oral immunotherapy (OIT): clinical desensitization and modulation of the allergic response. *J. Allergy Clin. Immunol.* **127**, 654–660 (2011).
193. Diesner, S. C., Wang, X.-Y., Jensen-Jarolim, E., Untersmayr, E. & Gabor, F. Use of lectin-functionalized particles for oral immunotherapy. *Ther. Deliv.* **3**, 277–290 (2012).
194. Patriarca, G. *et al.* Oral desensitizing treatment in food allergy: clinical and immunological results. *Aliment. Pharmacol. Ther.* **17**, 459–465 (2003).
195. Witt, C. & Kissel, T. Morphological characterization of microspheres, films and implants prepared from poly(lactide-co-glycolide) and ABA triblock copolymers: Is the erosion controlled by degradation, swelling or diffusion? *Eur. J. Pharm. Biopharm.* **51**, 171–181 (2001).
196. Lima, K. M. & Rodrigues, J. M. Poly-DL-lactide-co-glycolide microspheres as a controlled release antigen delivery system. *Brazilian J. Med. Biol. Res.* **32**, 171–180 (1999).
197. Schöll, I., Boltz-Nitulescu, G. & Jensen-Jarolim, E. Review of novel particulate antigen delivery systems with special focus on treatment of type I allergy. *J. Control. Release* **104**, 1–27 (2005).
198. O'Hagan, D. T. & Singh, M. Microparticles as vaccine adjuvants and delivery systems. *Expert Rev. Vaccines* **2**, 269–83 (2003).
199. Jones, D. H., Corris, S., McDonald, S., Clegg, J. C. S. & Farrar, G. H. Poly(DL-lactide-co-glycolide)-encapsulated plasmid DNA elicits systemic and mucosal antibody responses to encoded protein after oral administration. *Vaccine* **15**, 814–

- 817 (1997).
200. Igartua, M. *et al.* Enhanced immune response after subcutaneous and oral immunization with biodegradable PLGA microspheres. *J. Control. Release* **56**, 63–73 (1998).
 201. Thomas, C., Gupta, V. & Ahsan, F. Influence of surface charge of PLGA particles of recombinant hepatitis B surface antigen in enhancing systemic and mucosal immune responses. *Int. J. Pharm.* **279**, 41–50 (2009).
 202. Hillery, A. M. & Florence, A. T. The effect of adsorbed poloxamer 188 and 407 surfactants on the intestinal uptake of 60-nm polystyrene particles after oral administration in the rat. *Int. J. Pharm.* **132**, 123–130 (1996).
 203. Gaumet, M., Gurny, R. & Delie, F. Interaction of biodegradable nanoparticles with intestinal cells: The effect of surface hydrophilicity. *Int. J. Pharm.* **390**, 45–52 (2010).
 204. Gaumet, M., Gurny, R. & Delie, F. Localization and quantification of biodegradable particles in an intestinal cell model: The influence of particle size. *Eur. J. Pharm. Sci.* **36**, 465–473 (2009).
 205. Desai, M., Labhassetwar, V., Walter, E., Levy, R. & Amidon, G. The mechanism of uptake of biodegradable microparticles in Caco-2 cells is size dependent. *Pharmaceutical Res.* **14**, 1568–1573 (1997).
 206. Brayden, D. J. & Baird, A. W. Microparticle vaccine approaches to stimulate mucosal immunisation. *Microbes Infect.* **3**, 867–876 (2001).
 207. Eldridge, J. H., Meulbroek, J. A., Staas, J. K., Tice, T. R. & Gilley, R. M. Vaccine-containing biodegradable microspheres specifically enter the gut-associated lymphoid tissue following oral administration and induce a disseminated mucosal immune response. *Adv. Exp. Med. Biol.* **251**, 191–202 (1989).
 208. Garinot, M. *et al.* PEGylated PLGA-based nanoparticles targeting M cells for oral vaccination. *J. Control. Release* **120**, 195–204 (2007).
 209. Schöll, I. *et al.* Allergen-loaded biodegradable poly (D , L -lactic-co-glycolic) acid nanoparticles down-regulate an ongoing Th2 response in the BALB / c mouse model. *Clin Exp Allergy* **34**, 315–321 (2004).
 210. Batanero, E., Barral, P., Villalba, M. & Rodríguez, R. Encapsulation of Ole e 1 in biodegradable microparticles induces Th1 response in mice: A potential vaccine for allergy. *J. Control. Release* **92**, 395–398 (2003).
 211. Gabor, F., Stangl, M. & Wirth, M. Lectin-mediated bioadhesion: Binding characteristics of plant lectins on the enterocyte-like cell lines Caco-2, HT-29 and HCT-8. *J. Control. Release* **55**, 131–142 (1998).
 212. Gabor, F., Bogner, E., Weissenboeck, A. & Wirth, M. The lectin-cell interaction and its implications to intestinal lectin-mediated drug delivery. *Adv. Drug Deliv. Rev.* **56**, 459–480 (2004).
 213. Wirth, M., Hamilton, G. & Gabor, F. Lectin-mediated drug targeting: quantification of binding and internalization of Wheat germ agglutinin and Solanum tuberosum lectin using Caco-2 and HT-29 cells. *J. Drug Target.* **6**, 95–104 (1998).
 214. Walter, F. *et al.* Functionalisation of allergen-loaded microspheres with wheat germ agglutinin for targeting enterocytes. *Biochem. Biophys. Res. Commun.* **315**, 281–287 (2004).
 215. Roth-Walter, F. *et al.* M cell targeting with Aleuria aurantia lectin as a novel approach for oral allergen immunotherapy. *J. Allergy Clin. Immunol.* **114**, 1362–

- 1368 (2004).
216. Crennell, S., Garman, E., Laver, G., Vimr, E. & Taylor, G. Crystal structure of *Vibrio cholerae* neuraminidase reveals dual lectin-like domains in addition to the catalytic domain. *Structure* **2**, 535–544 (1994).
 217. Roth-Walter, F. *et al.* Targeting antigens to murine and human M-cells with *Aleuria aurantia* lectin-functionalized microparticles. *Immunol. Lett.* **100**, 182–188 (2005).
 218. Hinou, H., Kurogochi, M., Shimizu, H. & Nishimura, S. I. Characterization of *Vibrio cholerae* neuraminidase by a novel mechanism-based fluorescent labeling reagent. *Biochemistry* **44**, 11669–11675 (2005).
 219. Mantis, N. J., Frey, A. & Neutra, M. R. Accessibility of glycolipid and oligosaccharide epitopes on rabbit villus and follicle-associated epithelium. *Am J Physiol Gastrointest Liver Physiol* **278**, G915–G923 (2000).
 220. Galen, J. E. *et al.* Role of *Vibrio cholerae* Neuraminidase in the Function of Cholera Toxin. *Infect. Immun.* **60**, 406–415 (1992).
 221. Moustafa, I. *et al.* Sialic acid recognition by *Vibrio cholerae* neuraminidase. *J. Biol. Chem.* **279**, 40819–40826 (2004).
 222. Gitter, A. H., Bendfeldt, K., Schulzke, J. D. & Fromm, M. Leaks in the epithelial barrier caused by spontaneous and TNF-alpha-induced single-cell apoptosis. *FASEB J.* **14**, 1749–1753 (2000).
 223. Price, M. M., Oskeritzian, C. A., Milstien, S. & Spiegel, S. Sphingosine-1-phosphate synthesis and functions in mast cells. *Futur. Lipidol* **3**, 665–674 (2008).
 224. Pinto, M. *et al.* Enterocyte-like Differentiation and Polarization of the Human Colon Carcinoma Cell Line Caco-2 in Culture. *Biol Cell* **47**, 323–330 (1983).
 225. Chantret, I., Barbat, A., Dussaulx, E., Brattain, M. G. & Zweibaum, A. Epithelial Polarity , Villin Expression , and Enterocytic Differentiation of Cultured Human Colon Carcinoma Cells : A Survey of Twenty Cell Lines Epithelial Polarity , Villin Expression , and Enterocytic Differentiation of Cultured Human Colon Carcinoma C. *Cancer Res* **48**, 1936–1942 (1988).
 226. Zucco, F. *et al.* An inter-laboratory study to evaluate the effects of medium composition on the differentiation and barrier function of Caco-2 cell lines. *Altern. Lab. Anim.* **33**, 603–18 (2005).
 227. Sambuy, Y. *et al.* The Caco-2 cell line as a model of the intestinal barrier: influence of cell and culture-related factors on Caco-2 cell functional characteristics. *Cell Biol. Toxicol.* **21**, 1–26 (2005).
 228. Natoli, M. *et al.* Cell growing density affects the structural and functional properties of Caco-2 differentiated monolayer. *J. Cell. Physiol.* **226**, 1531–43 (2011).
 229. Ferruzza, S., Rossi, C., Scarino, M. L. & Sambuy, Y. A protocol for differentiation of human intestinal Caco-2 cells in asymmetric serum-containing medium. *Toxicol. In Vitro* **26**, 1252–5 (2012).
 230. Ferruzza, S., Rossi, C., Sambuy, Y. & Scarino, M. L. Serum-reduced and serum-free media for differentiation of Caco-2 cells. *ALTEX* **30**, 159–68 (2013).
 231. Hidalgo, I., Raub, T. & Borchardt, R. Characterization of the Human Colon Carcinoma Cell Line (Caco-2) as a Model Permeability. *Gastroenterology* **96**, 736–749 (1989).
 232. Shah, P., Jogani, V., Bagchi, T. & Misra, A. Role of Caco-2 cell monolayers in prediction of intestinal drug absorption. *Biotechnol. Prog.* **22**, 186–98

233. Smetanová, L., Stětinová, V., Svoboda, Z. & Kvetina, J. Caco-2 cells, biopharmaceutics classification system (BCS) and biowaiver. *Acta medica* **54**, 3–8 (2011).
234. Watterson, K. R., Ratz, P. H. & Spiegel, S. The role of sphingosine-1-phosphate in smooth muscle contraction. *Cell. Signal.* **17**, 289–98 (2005).
235. Idzko, M. *et al.* Local application of FTY720 to the lung abrogates experimental asthma by altering dendritic cell function. *J. Clin. Invest.* **116**, 2935–2944 (2006).
236. Schmelz, E. M., Crall, K. J., Larocque, R., Dillehay, D. L. & Merrill, A. H. Uptake and metabolism of sphingolipids in isolated intestinal loops of mice. *J. Nutr.* **124**, 702–712 (1994).
237. Vesper, H. *et al.* Sphingolipids in food and the emerging importance of sphingolipids to nutrition. *J. Nutr.* **129**, 1239–1250 (1999).
238. Nilsson, A. & Duan, R.-D. Absorption and lipoprotein transport of sphingomyelin. *J. Lipid Res.* **47**, 154–171 (2006).
239. Garmy, N., Taïeb, N., Yahi, N. & Fantini, J. Apical uptake and transepithelial transport of sphingosine monomers through intact human intestinal epithelial cells: Physicochemical and molecular modeling studies. *Arch. Biochem. Biophys.* **440**, 91–100 (2005).
240. Mazzei, J. C. *et al.* Suppression of intestinal inflammation and inflammation-driven colon cancer in mice by dietary sphingomyelin: importance of peroxisome proliferator-activated receptor γ expression. *J. Nutr. Biochem.* **22**, 1160–71 (2011).
241. Fischbeck, A. *et al.* Sphingomyelin induces cathepsin D-mediated apoptosis in intestinal epithelial cells and increases inflammation in DSS colitis. *Gut* **60**, 55–65 (2011).
242. Sjöqvist, U. *et al.* Chronic colitis is associated with a reduction of mucosal alkaline sphingomyelinase activity. *Inflamm. Bowel Dis.* **8**, 258–63 (2002).
243. Maines, L. W. *et al.* Suppression of ulcerative colitis in mice by orally available inhibitors of sphingosine kinase. *Dig. Dis. Sci.* **53**, 997–1012 (2008).
244. Nyberg, L., Duan, R. D. & Nilsson, Å. A mutual inhibitory effect on absorption of sphingomyelin and cholesterol. *J. Nutr. Biochem.* **11**, 244–249 (2000).
245. Duan, R. D. *et al.* Identification of human intestinal alkaline sphingomyelinase as a novel ecto-enzyme related to the nucleotide phosphodiesterase family. *J. Biol. Chem.* **278**, 38528–38536 (2003).
246. Furuya, H., Ohkawara, S., Nagashima, K., Asanuma, N. & Hino, T. Dietary sphingomyelin alleviates experimental inflammatory bowel disease in mice. *Int. J. Vitam. Nutr. Res.* **78**, 41–48 (2008).
247. Fyrst, H. & Saba, J. D. Sphingosine-1-phosphate lyase in development and disease: Sphingolipid metabolism takes flight. *Biochim. Biophys. Acta* **1781**, 448–458 (2008).
248. Schmitz, H. *et al.* Tumor necrosis factor- α (TNF α) regulates the epithelial barrier in the human intestinal cell line HT-29/B6. *J. Cell Sci.* **112**, 137–146 (1999).
249. MacDonald, T. T., Hutchings, P., Choy, M. Y., Murch, S. & Cooke, A. Tumour necrosis factor- α and interferon- γ production measured at the single cell level in normal and inflamed human intestine. *Clin. Exp. Immunol.* **81**, 301–305 (1990).
250. Sicherer, S. H. & Sampson, H. A. Food allergy. *J. Allergy Clin. Immunol.* **125**,

- S116–S125 (2010).
251. Janes, K. a. *et al.* The Response of Human Epithelial Cells to TNF Involves an Inducible Autocrine Cascade. *Cell* **124**, 1225–1239 (2006).
 252. Arrieta, M. C., Madsen, K., Doyle, J. & Meddings, J. Reducing small intestinal permeability attenuates colitis in the IL10 gene-deficient mouse. *Gut* **58**, 41–48 (2009).
 253. Maceyka, M. SphK1 and SphK2, Sphingosine Kinase Isoenzymes with Opposing Functions in Sphingolipid Metabolism. *J. Biol. Chem.* **280**, 37118–37129 (2005).
 254. Rivera, J., Proia, R. L. & Olivera, A. The alliance of sphingosine-1-phosphate and its receptors in immunity. *Nat Rev Immunol.* **8**, 753–763 (2009).
 255. Fuerst, E. *et al.* Sphingosine-1-phosphate induces pro-remodelling response in airway smooth muscle cells. *Allergy* **69**, 1531–9 (2014).
 256. O’Sullivan, M. J., Hirota, N. & Martin, J. G. Sphingosine 1-phosphate (S1P) induced interleukin-8 (IL-8) release is mediated by S1P receptor 2 and nuclear factor kB in BEAS-2B cells. *PLoS One* **9**, e95566 (2014).
 257. O’Sullivan, M. J., Hirota, N. & Martin, J. G. Sphingosine 1-phosphate (S1P) induced interleukin-8 (IL-8) release is mediated by S1P receptor 2 and nuclear factor kB in BEAS-2B cells. *PLoS One* **9**, e95566 (2014).
 258. Fernández-Pisonero, I. *et al.* Lipopolysaccharide and sphingosine-1-phosphate cooperate to induce inflammatory molecules and leukocyte adhesion in endothelial cells. *J. Immunol.* **189**, 5402–10 (2012).
 259. Pizzuti, D. *et al.* In vitro model for IgE mediated food allergy. *Scand. J. Gastroenterol.* **46**, 177–87 (2011).
 260. Roth-Walter, F. *et al.* Mucosal targeting of allergen-loaded microspheres by Aleuria aurantia lectin. *Vaccine* **23**, 2703–2710 (2005).
 261. Kucharzik, T. *et al.* Acute induction of human IL-8 production by intestinal epithelium triggers neutrophil infiltration without mucosal injury. *Gut* **54**, 1565–72 (2005).
 262. Sierro, F. *et al.* Flagellin stimulation of intestinal epithelial cells triggers CCL20-mediated migration of dendritic cells. *Proc. Natl. Acad. Sci. U. S. A.* **98**, 13722–7 (2001).
 263. Mabbott, N. A., Donaldson, D. S., Ohno, H., Williams, I. R. & Mahajan, A. Microfold (M) cells: important immunosurveillance posts in the intestinal epithelium. *Mucosal Immunol.* **6**, 666–77 (2013).

7. Appendix

7.1 List of Tables

Table 1: Protocol for RT-PCR Master Mix for one reaction	47
Table 2: Protocol for qPCR Master Mix for one technical triplicate	48
Table 3: Quantitative real time PCR Program for Primer testing with SYBR-Green.....	48
Table 4 Protocol for quantitative real time PCR Master Mix for triplicate	48
Table 5: Quantitative real time PCR Program for gene expression analysis with TaqMan.	49

7.2 List of Figures

Figure 1: Schematic picture of the intestinal epithelium and involved intestinal epithelial cells. The intestinal epithelium is structured into villi and crypts to enhance its surface area and covers those with mucus to protect itself against harmful agents. To further enhance its surface area, the intestinal epithelial cells (IECs) form microvilli towards the apical located lumen, also called brush border, where they absorb the nutrient components and release them into the basolateral located lamina propria (left side). The IECs consist of various cell types which are located at different positions along the crypt-villus axis. The cells are constantly renewed by pluripotent stem cells, influenced by stromal cell released factors, and move along the crypt-villus axis towards the villi tops where they are shed into the lumen and undergo apoptosis (middle). Various factors protect the intestinal epithelium from harmful agents and pathogens. The overlying microbiota releases microbe associated molecular patterns (MAMP's) - if stimulated by certain factors - into the underlying mucus layers. These MAMP's and other foreign antigens, are recognised by secreted Immunoglobulin A (sIgA) and antimicrobial peptides (AMP's). Furthermore, antigens within the lamina propria or sampled by dendritic cells (DCs) through the IECs, are processed by macrophages as well as DCs and presented to lymphocytes (B and T cells) which further shape the immunologic response by releasing antibodies, cytokines and chemokines which recruit further cells, like mast cells (right side).....20

Figure 2: Schematic drawing of M-cell with beneath lying Peyer patch. Antigens are able to pass the intestinal epithelium through microfold (M) cells, which are embedded in the surrounding follicle associated epithelium and barely covered with mucus. Entering the beneath lying dome region of the Peyer's Patch, the antigen is processed by dendritic cells (DCs) and macrophages which present them to naïve B cells in the follicle areas or naïve T helper (Th) cells in the inter-follicular areas of the PP's. Through the presentation, the lymphocytes get activated and differentiate into specific effector cells, like IgA plasma cells, before they either move to the connected mesenteric lymph nodes or are released into the lamina propria.22

Figure 3: Loading of western blot cassette.....51

Figure 4: Relative mRNA expression of S1P lyase (SGPL) and sphingosine kinases (SphKs) in CaCo2 cells. Fully differentiated and FCS-deprived CaCo2 cells were stimulated basolaterally with vehicle control or 100 nM S1P for 30 min, 2 or 4 hours. Analysis of quantitative real-time PCR data shows expression of (A) SGPL and (B) SphKs mRNAs. (A-B): Data represents one of four separate experiments. (C-E): Data from four

experiments (mean±SEM) are presented as fold change in comparison with vehicle control.....56

Figure 5: Effect of TNF α stimulation on SphK mRNA expression. Fully differentiated and FCS-deprived CaCo2 cells were stimulated basolaterally with vehicle control, 100 ng/ml or 250 ng/ml TNF α . Cells were stimulated for 30 min, 1, 2 or 4 hours and quantitative real-time PCR was performed to evaluate the relative mRNA expression levels of SphK1 and SphK2 (A, B) as well as the changes in expression over time (C, D). Cells were stimulated basolaterally with vehicle control, 100 ng/ml or 250 ng/ml TNF α for 6 and 8 hours to determine protein expression of SphK1 (E, F) and SphK2 (G, H) in Western Blot experiments. Protein levels were quantified against GAPDH to determine changes over time (I, J). Data from three experiments (mean±SEM) are presented as fold change in comparison with vehicle control.58

Figure 6: Expression of S1P receptors in CaCo2 cells: (A) mRNA levels of S1P receptors of fully differentiated and FCS-deprived CaCo2 cells were quantified with qRT-PCR and (B) analysed relative to S1P2. Data of four experiments (mean±SEM) represent fold changes of relative mRNA expression.....59

Figure 7: Effect of apical S1P stimulation on calcium release over time. 21 day old FCS-deprived CaCo2 monolayers were stimulated apically with either PBS (●), vehicle control (■), S1P (1nM ▲, 10nM ▼, 100nM ◆, 1000nM ◇) or positive control (calcium ionophor ■). Changes in fluorescence were measured for 12 seconds before and 108 seconds after stimulation. Data from three experiments (mean±SEM) represent changes fluorescence.60

Figure 8: Changes in S1P2 expression after S1P stimulation. Fully differentiated and FCS-deprived CaCo2 cells were stimulated basolaterally with vehicle control and (A) 100 nM S1P or (B) 500 nM S1P for 30 min, 2 and 4 hours with and without 1 μ M JTE-013 pre-treatment. Changes in S1P2 receptor mRNA expression after stimulation were quantified with qRT-PCR. Data from four experiments (mean±SEM) are represented as fold change relative to vehicle control.61

Figure 9: Changes in relative cytokine mRNA expression after basolateral stimulation with 100 nM S1P. FCS-deprived CaCo2 monolayers cultured for 21 days on transwells were stimulated basolaterally with vehicle control or 100 nM S1P for 30 min, 2 and 4 hours. Quantitative real-time PCR was performed to evaluate the changes in relative mRNA expression levels of (A) IL-8, (B) CCL20 and (C) TSLP over time. Relative cytokine mRNA expression levels of four experiments (mean±SEM) are represented as fold change in comparison to vehicle control.....61

Figure 10: S1P enhances trans-epithelial electrical resistance over time. Fully differentiated FCS-depleted CaCo2 monolayers remained either untreated (control \blackleftarrow) or were stimulated basolaterally with vehicle control (\blackrightarrow), 100 nM (\blackleftarrow) or 500 nM (\blackrightarrow) S1P. Data from three experiments (mean \pm SEM) are expressed as (A) delta TEER over time for 30 hours in 2 hour intervals and (B) as relative changes after S1P (100 nM or 500 nM) treatment. Significance was calculated with 2-way ANOVA with Bonferroni correction for multiple comparison. *P<0.05, **P<0.01, ***P<0.00162

Figure 11: S1P regulates tight junction protein mRNA expression in CaCo2 cells. Fully differentiated FCS-depleted CaCo2 cells were stimulated basolaterally (A, C, E, G, I) with vehicle control and 100 nM for 30 min, 2 or 4 hours and (B, D, F, H, J) with 500 nM (back bar) or 1 μ M JTE prior to 500 nM S1P (white bar) for 30 min or 4h. Data represents changes in relative mRNA expression of, claudin-1 (A, B), claudin-4 (C, D), occludin (E, F) zonula occludens-1 (G, H) and zonula occludens-2 (I, J) of four experiments (mean \pm SEM). Significance was calculated with one-way ANOVA as well as two-way ANOVA with Bonferroni correction for multiple comparison. *P<0.05.....63

Figure 12: Effect of allergen loaded targeted microparticle stimulation on IL-8 mRNA expression. Fully differentiated CaCo2 cells were stimulated with (A, C, E, G) AAL (\blacksquare), NA (\blacksquare), WGA (\blacksquare) or OVA (\blacksquare) for 0,1,2,3 or 6 hours or (B, D, F, H) allergen loaded MPs, Plain-MP (\blacksquare), coated with AAL-MP (\blacksquare), NA-MP (\blacksquare) or WGA-MP (\blacksquare) for 0,1,2,3 or 6 hours. Data represent fold change of relative IL-8 mRNA expression of four experiments (mean \pm SEM) compared to unstimulated control cells. Significance was calculated with two-way ANOVA with Bonferroni correction for multiple comparison. *P<0.05, **P<0.01, ***P<0.001.65

Figure 13: Influence of microparticle stimulation on CCL20 mRNA expression. CaCo2 monolayers cultivated for 21 days were either stimulated with (A, C, E, G) AAL (\blacksquare), NA (\blacksquare), WGA (\blacksquare) or OVA (\blacksquare) for 0,1,2,3 or 6 hours or (B, D, F, H) allergen loaded MPs, Plain-MP (\blacksquare), targeted with AAL-MP (\blacksquare), NA-MP (\blacksquare) or WGA-MP (\blacksquare) for 0,1,2,3 or 6 hours. Data represent fold change of relative CCL20 mRNA expression of four experiments (mean \pm SEM) compared to unstimulated control cells. Significance was calculated with two-way ANOVA with Bonferroni correction for multiple comparison. *P<0.05, **P<0.01, ***P<0.001.67

Figure 14: Changes in RANTES mRNA expression after microparticle treatment. Fully differentiated CaCo2 cells were either stimulated with (A, C, E, G) AAL (■), NA (■) WGA (□) or OVA (▨) for 0,1,2,3 or 6 hours or (B, D, F, H) allergen loaded MPs, Plain-MP (■), targeted with AAL-MP (■), NA-MP (■) or WGA-MP (□) for 0,1,2,3 or 6 hours. Data represent fold change of relative RANTES mRNA expression of four experiments (mean±SEM) compared to unstimulated control cells. Significance was calculated with two-way ANOVA with Bonferroni correction for multiple comparison. *P<0.05, **P<0.01, ***P<0.001.78

Figure 15: Influence of microparticle treatment on mRNA expression levels of TSLP. CaCo2 monolayers were stimulated with (A, C, E, G) AAL (■), NA (■), WGA (□) or OVA (▨) for 0,1,2,3 or (B, D, F, H) 6 hours or allergen loaded MPs, Plain-MP (■), targeted with AAL-MP (■), NA-MP (■) or WGA-MP (□) for 0,1,2,3 or 6 hours. Data represent fold change of relative TSLP mRNA expression of four experiments (mean±SEM) compared to unstimulated control cells. Significance was calculated with two-way ANOVA with Bonferroni correction for multiple comparison. *P<0.05, **P<0.01. 70

Figure 16: Changes in claudin-1 mRNA expression after particle stimulation. CaCo2 cells, cultured for 21 days were stimulated on the apical side with either (A, C, E, G) targeting substances, AAL (■), NA (■), WGA (□), OVA (▨) or (B, D, F, H) with allergen loaded MPs: Plain-MP (■), AAL-MP (■), NA-MP (■) or WGA-MP (□) for 0,1,2,3, and 6 hours. Data represent fold change of relative claudin-1 mRNA expression of four experiments (mean±SEM) compared to unstimulated control cells. Significance was calculated with two-way ANOVA with Bonferroni correction for multiple comparison. *P<0.05, **P<0.01, ***P<0.001.72

Figure 17: Effect of particle stimulation on mRNA expression of claudin-4. Fully differentiated CaCo2 monolayers were stimulated on the apical side with either (A, C, E, G) AAL (■), NA (■), WGA (□) or OVA (▨) or (B, D, F, H) with allergen loaded MPs: Plain-MP (■), AAL-MP (■), NA-MP (■) or WGA-MP (□) for 0,1,2,3 and 6 hours. Data represent fold change of relative claudin-4 mRNA expression of four experiments (mean±SEM) compared to unstimulated control cells. Significance was calculated with two-way ANOVA with Bonferroni correction for multiple comparison. *P<0.05, **P<0.01, ***P<0.001.....73

Figure 18: Influence of microparticle stimulation on occludin expression. CaCo2 monolayers cultivated for 21 days were either stimulated with (A, C, E, G) AAL (■), NA (■) WGA (□) or OVA (▨) for 0,1,2,3 or 6 hours or (B, D, F, H) allergen loaded MPs: Plain-MP (■), AAL-MP (■), NA-MP (■) or WGA-MP (□) for 0,1,2,3 or 6 hours. Data represent fold change of relative occludin mRNA expression of four experiments (mean±SEM) compared to unstimulated control cells. Significance was calculated with two-way ANOVA with Bonferroni correction for multiple comparison. *P<0.05, **P<0.01, ***P<0.00174

Figure 19: Changes in zonula occludens-1 mRNA expression after microparticle stimulation. Fully differentiated CaCo2 monolayers were stimulated for 0,1,2,3 or 6 hours with (A, C, E, G): AAL (■), NA (■), WGA (□), OVA (▨) or (B, D, F, H) with allergen loaded MPs: Plain-MP (■), AAL-MP (■), NA-MP (■) or WGA-MP (□). Data represent fold change of relative ZO-1 mRNA expression of four experiments (mean±SEM) compared to unstimulated control cells. Significance was calculated with two-way ANOVA with Bonferroni correction for multiple comparison.....75

Figure 20: Changes in zonula occludens-2 protein expression after microparticle stimulation. Fully differentiated CaCo2 monolayers were stimulated for 0,1,2,3 or 6 hours with (A, C, E, G): AAL (■), NA (■), WGA (□), OVA (▨) or (B, D, F, H) with allergen loaded MPs: Plain-MP (■), AAL-MP (■), NA-MP (■) or WGA-MP (□). Data represent fold change of relative ZO-2 mRNA expression of four experiments (mean±SEM) compared to unstimulated control cells. Significance was calculated with two-way ANOVA with Bonferroni correction for multiple comparison. *P<0.0576

7.3 Zusammenfassung

Der Darm ist eines der wichtigsten menschlichen Organe. Seine Hauptaufgabe, welche durch die semipermeable Darmwand reguliert wird, ist die ausreichende Aufnahme von Nährstoffen, Elektrolyten und Wasser.

In Menschen mit einer Lebensmittelallergie ist die Darmwand durchlässiger und erlaubt die verstärkte Aufnahme von Allergenen. Dies resultiert in der Produktion von IgE produzierenden B-Zellen sowie der Rekrutierung von anderen Effektorzellen wie Mastzellen. Diese produzieren nach ihrer Aktivierung große Mengen an Botenstoffen, welche die allergischen Reaktionen, Erweiterung der Blutgefäße, erhöhte Durchlässigkeit der Blutgefäße, Kontraktion der Atemmuskulatur bis hin zum anaphylaktischen Schock, verursachen.

Einer dieser Faktoren ist Sphingosine-1-Phosphat. Dieses bioaktive Lipid spielt eine wichtige Rolle in verschiedenen immunologischen Funktionen. So ist es etwa verantwortlich für die Rekrutierung von Lymphozyten und zur Freisetzung der Mediatoren von Mastzellen. Erhöhte S1P Spiegel führen in allergischen Menschen zur erhöhten Durchlässigkeit von Gefäßen und zur Kontraktion von glatten Muskeln. In dieser Studie erforschten wir die Interaktion von S1P mit dem intestinalen Epithel. Dabei entdeckten wir, dass die Epithelzellen in der Lage sind S1P zu produzieren und abzubauen, da sie Enzyme exprimieren, die dafür verantwortlich sind. Die Zellen haben die Fähigkeit durch die spezifischen Rezeptoren S1P2 und S1P3 auf S1P zu reagieren. Stimulation mit S1P hatte zur Folge, dass die Dichte der Epithelzellen zunahm und inflammatorische Zytokine, die nicht mit allergischen Reaktionen assoziiert sind, produziert wurden. Daraus schließen wir, dass S1P das intestinale Epithel gegen Schädigungen schützt.

Die meist verwendete Methode um Nahrungsmittelallergien zu behandeln ist die orale Verabreichung von stetig steigenden Allergen Dosen. Dabei wird eine immunologische Toleranz aufgebaut. Eine Methode zur Verabreichung ist das Einschließen des Allergens in Lektin gebundene Mikropartikel. Diese transportieren den Stoff direkt zu spezifischen Zellen des intestinalen Epithels. Der zweite Teil der Arbeit bestand darin herauszufinden ob Mikropartikel, gebunden an verschiedene Lektine, die Barriere des Epithels beeinflussen. Die Ergebnisse zeigen, dass Mikropartikel gebunden an die Neuraminidase von *Vibrio Cholerae* die besten Effekte erzielen, jedoch keine der getesteten Partikel die Barriere stören und zur Induktion von inflammatorischen Zytokinen führen. Daher schließen wir, dass die Mikropartikel eine gute Möglichkeit für die Behandlung von Nahrungsmittelallergien sind.